

國立交通大學

機械工程學系

碩士論文

Ge-Ku-Mathieu 系統及 Sprott 19, 22 系統的

渾沌與渾沌同步

Chaos and Chaos Synchronization of Ge-Ku-Mathieu
System and Sprott 19, 22 Systems



研究生：王翔平

指導教授：戈正銘 教授

中華民國九十九年六月

**Ge-Ku-Mathieu 系統及 Sprott 19, 22 系統的
渾沌與渾沌同步**

**Chaos and Chaos Synchronization of Ge-Ku-Mathieu
System and Sprott 19, 22 Systems**

研究生：王翔平

Student: Xiang-Ping Wang

指導教授：戈正銘

Advisor: Zheng-Ming Ge



A Thesis

Submitted to Department of Mechanical Engineering

College of Engineering

National Chiao Tung University

In Partial Fulfillment of the Requirement

For the Degree of master of science

In

Mechanical Engineering

June 2010

Hsinchu, Taiwan, Republic of China

中華民國九十九年六月

Ge-Ku-Mathieu 系統及 Sprott 19, 22 系統的 渾沌與渾沌同步

學生：王翔平

指導教授：戈正銘

國立交通大學

機械工程學系



本篇論文以相圖、龐卡萊映射圖、李亞普洛夫指數以及分歧圖等數值方法研究新 Ge-Ku-Mathieu 系統的渾沌現象。對此系統應用部分區域穩定性理論和實用漸進穩定理論來達成廣義同步；應用主動控制獲得雙重及多重渾沌交織同步。更進一步使用新模糊模型來研究 Sprott 19, 22 系統的模糊模型化和渾沌同步。此外，將探討新模糊邏輯常數控制器應用在投影同步及含有不確定性的渾沌系統。在以上研究中，皆可由相圖和時間歷程圖得到驗證。


Chaos and Chaos Synchronization of Ge-Ku-Mathieu System and Sprott 19, 22 Systems

Student : Xiang- Ping Wang

Advisor : Zheng-Ming Ge

Department of Mechanical Engineering, National Chiao Tung
University

Abstract



In this thesis, the chaotic behavior in new Ge-Ku-Mathieu system is studied by phase portraits, time history, Poincaré maps, Lyapunov exponent and bifurcation diagrams. A new kind of chaotic generalized synchronization, *different translation pragmatical generalized synchronization*, is obtained by pragmatical asymptotical stability theorem and partial region stability theory. Second new type for chaotic synchronization, *double and multiple symplectic synchronization*, are obtained by active control. A new method, using new fuzzy model, is studied for fuzzy modeling and synchronization of Sprott 19, 22 systems. Moreover, the new fuzzy logic constant controller is studied for projective synchronization and chaotic system with uncertainty. Numerical analyses, such as phase portraits and time histories can be provided to verify the effectiveness in all above studies.

誌謝

本篇碩士論文能夠順利的完成，首先要感謝的人，便是不斷給予耐心指導及諄諄教誨，我的指導教授戈正銘老師。老師在我求學的過程中，在研究上，給予我研究方向及專業領域的知識，遇到困難時，讓我學習如何克服及解決難題。感謝老師不厭其煩的修改論文，才讓本篇論文得以完整。私底下，與老師的相處，藉由老師深厚的文學素養，了解古今中外文史的發展，頓時對過去的史事有更深一層的領悟。從老師的詩詞創作裡，感受到對詩詞欣賞的意境，對文學上有進一步的認知。最後，誠摯感謝老師過去兩年辛苦的教導，對於未來的路，讓我有新的啟發及目標。

兩年的碩士研究生涯中，感謝博士班張晉銘、李仕宇學長細心指導，碩士班陳聰文、徐瑜韓、張育銘、陳志銘學長，在研究的過程中，給予我珍貴的意見及鼓勵。同時要感謝同學尚恩、振賓、泳厚在課業上的幫忙以及過去的兩年中互相扶持成長，留下許多記憶猶新的記憶。此外還要謝謝一些默默支持我的好朋友們，無法一一列名，沒有你們就沒有我精彩的人生，在此一併感謝。

最終感謝我父親及母親對我的養育及付出，讓我得以一路順利求學，可以不必擔心課業以外的事物，感謝弟弟們的支持。最後，感謝你們的支持，謹以此論文獻給你們，我會勇敢堅持下去，朝理想邁進。

Contents

Chinese Abstract.....	i
Abstract.....	ii
Acknowledgment.....	iii
Contents.....	iv
List of Figures.....	vi
Chapter 1 Introduction.....	1
Chapter 2 Chaos for a Ge-Ku-Mathieu System.....	6
2.1 Preliminary.....	6
2.2 Description of Ge-Ku-Mathieu System.....	6
2.3 Computational Analysis of Ge-Ku-Mathieu System.....	6
Chapter 3 Double Symplectic Synchronization for Ge-Ku-Mathieu System.....	10
3.1 Preliminary.....	10
3.2 Double Symplectic Synchronization Scheme.....	10
3.3 Synchronization of Two Different New Chaotic Systems.....	12
3.4 Summary.....	18
Chapter 4 Different Translation Pragmatical Generalized Synchronization by Stability Theory of Partial Region for Ge-Ku-Mathieu System.....	25
4.1 Preliminary.....	25
4.2 The Scheme of Different Translation Pragmatic Generalized Synchronization by Stability Theory of Partial Region Theory.....	25
4.3 Different Translation Pragmatical Synchronization of New Ge-Ku-Mathieu Chaotic System.....	28
4.4 Summary.....	37
Chapter 5 Multiple Symplectic Synchronization for Ge-Ku-Mathieu System.....	47
5.1 Preliminary.....	47
5.2 Multiple Symplectic Synchronization Scheme.....	47
5.3 Synchronization of Three Different Chaotic Systems.....	48
5.4 Summary.....	53
Chapter 6 Robust Projective Anti-Synchronization of Nonautonomous Chaotic Systems with Stochastic Disturbance by Fuzzy Logic Constant Controller.....	61
6.1 Preliminary.....	61
6.2 Projective Chaos Anti-Synchronization by FLCC Scheme.....	61
6.3 Simulation Results.....	65
6.4 Summary.....	78
Chapter 7 Fuzzy Modeling and Synchronization of Chaotic Systems by a New	

Fuzzy Model.....	92
7.1 Preliminary.....	92
7.2 New Fuzzy Model Theory.....	92
7.3 New Fuzzy Model of Chaotic Systems.....	94
7.4 Fuzzy Synchronization Scheme.....	103
7.5 Simulation Result.....	105
7.6 Summary.....	108
Chapter 8 Conclusions.....	115
Appendix A GYC Partial Region Stability Theory.....	117
Appendix B Pragmatical Asymptotical Stability Theory.....	125
References.....	128



List of Figures

Fig. 2.1. The pendulum on rotating arm.	7
Fig. 2.2 The bifurcation diagram for new Ge-Ku-Mathieu system.	8
Fig. 2.3 The Lyapunov exponents for new Ge-Ku-Mathieu system.	8
Fig. 2.4 Phase portrait, Poincaré maps, and time histories for new Ge-Ku-Mathieu system.	9
Fig. 3.1 The chaotic attractor of a new Double Ge-Ku system.	19
Fig. 3.2 The phase portrait of the controlled GKM system for Case1.	19
Fig. 3.3 Time histories of $x_i + y_i$ and $x_i \cos y_i$ for Case1.	20
Fig. 3.4 Time histories of the state errors for Case1.	20
Fig. 3.5 The chaotic attractor of a new Ge-Ku-van der Pol system.	21
Fig. 3.6 The phase portrait of the controlled GKM system for Case2.	21
Fig. 3.7 Time histories of $x_i + y_i$ and $x_i \cos y_i$ for Case2.	22
Fig. 3.8 Time histories of the state errors for Case2.	22
Fig. 3.9 The chaotic attractor of the Ge-Ku-Duffing system.	23
Fig. 3.10 The phase portrait of the controlled GKM system for Case3.	23
Fig. 3.11 Time histories of $x_i + y_i$ and $x_i \cos y_i$ for Case3.	24
Fig. 3.12 Time histories of the state errors for Case3.	24
Fig. 4.1 Coordinate translation.	38
Fig. 4.2 Coordinate translation.	38
Fig. 4.3 Phase portrait of the error dynamic for Case 1.	39
Fig. 4.4 Time histories of x_i, y_i for Case 1.	39

Fig. 4.5 Time histories of errors for Case 1.	40
Fig. 4.6 Time histories of parameter errors for Case 1.	40
Fig. 4.7 Time histories of parameter errors for Case 1.	41
Fig. 4.8 Phase portrait of the error dynamic for Case 2.	41
Fig. 4.9 Time histories of x_i, y_i for Case 2.	42
Fig. 4.10 Time histories of errors for Case 2.	42
Fig. 4.11 Time histories of parameter errors for Case 2.	43
Fig. 4.12 Time histories of parameter errors for Case 2.	43
Fig. 4.13 Phase portrait of the error dynamic for Case 3.	44
Fig. 4.14 Time histories of x_i, y_i for Case 3.	44
Fig. 4.15 Time histories of errors for Case 3.	45
Fig. 4.16 Time histories of parameter errors for Case 3.	45
Fig. 4.17 Time histories of parameter errors for Case 3.	46
Fig. 5.1 The chaotic attractor of the Chen system.	54
Fig. 5.2 The chaotic attractor of the Lorenz system.	54
Fig. 5.3 Phase portrait of a controlled new Ge-Ku-Mathieu system for Case 1.	55
Fig. 5.4 Time histories of $G(\mathbf{x}, \mathbf{y}, z, t)$ and $\mathbf{F}(\mathbf{x}, \mathbf{y}, z, t)$ for Case 1.	55
Fig. 5.5 Time histories of the state errors for Case 1.	56
Fig. 5.6 The chaotic attractor of the <i>Rössler</i> system.	56
Fig. 5.7 Phase portrait of the controlled Ge-Ku-Mathieu system for Case 2.	57
Fig. 5.8 Time histories of $G(\mathbf{x}, \mathbf{y}, z, t)$ and $\mathbf{F}(\mathbf{x}, \mathbf{y}, z, t)$ for Case 2.	57
Fig. 5.9 Time histories of the state errors for Case 2.	58
Fig. 5.10 The chaotic attractor of the spratt system.	58
Fig. 5.11 Phase portrait of the controlled Ge-Ku-Mathieu system for Case 3.	59

Fig. 5.12 Time histories of $G(\mathbf{x}, \mathbf{y}, z, t)$ and $\mathbf{F}(\mathbf{x}, \mathbf{y}, z, t)$ for Case 3.	59
Fig. 5.13 Time histories of the state errors for Case 3.	60
Fig. 6.1. The configuration of fuzzy logic controller.	79
Fig. 6.2. Membership function.	79
Fig. 6.3. Projections of phase portrait of chaotic Sprott No.19 system with $a=-0.6$, $b=2.75$.	80
Fig. 6.4. Δ_1 is pulse generator.	80
Fig. 6.5. Projections of phase portrait of nonautonomous chaotic Sprott 19 system and $a=-0.6$, $b=2.75$.	81
Fig. 6.6. Projections of phase portrait of chaotic Sprott 22 system with controllers.	81
Fig.6.7. Time histories of error derivatives for master and slave Sprott nonautonomous chaotic systems without controllers.	82
Fig. 6.8. Time histories of errors for Case1 (nonautonomous system) the FLCC is added after 30s.	82
Fig. 6.9. Time histories of states for Case1 (nonautonomous system) the FLCC is added after 30s.	83
Fig. 6.10. The stochastic signal of Δ_2 is band-limited white noise(PSD=0.1).	83
Fig. 6.11. Projections of phase portrait of nonautonomous chaotic Sprott 19 system with stochastic disturbance Δ_2 , $a=-0.6$ and $b=2.75$.	84
Fig. 6.12. Time histories of error derivatives for master and slave Sprott chaotic systems without controllers.	84
Fig. 6.13. Time histories of errors for subsection 3.1.2, the FLCC is applied after 30s.	85
Fig. 6.14. Time histories of states for subsection 3.1.2, the FLCC is applied after 30s.	85
Fig. 6.15. Time histories of errors for subsection 3.1.3 the traditional nonlinear	

controller is applied after 30s.	86
Fig. 6.16. Time histories of states for subsection 3.1.3 the traditional nonlinear controller is applied after 30s.	86
Fig. 6.17. Projections of phase portrait of nonautonomous chaotic Sprott 19 system with stochastic disturbance where $a=-0.6, b=2.75$.	87
Fig. 6.18. Time histories of error derivatives for subsection 3.2.1.	87
Fig. 6.19. Time histories of errors for section 3.2 where FLCC is added after 30s.	88
Fig. 6.20. Time histories of states for subsection 2-3.2 the FLCC is coming into after 30s.	88
Fig. 6.21. Projections of phase portrait of nonautonomous chaotic Sprott 19 system with stochastic disturbance where $a=-0.6, b=2.75$.	89
Fig. 6.22. Time histories of error derivatives for Sprott chaotic systems without controllers.	89
Fig. 6.23. Time histories of errors for subsection 3.2.2 where FLCC are added after 30s.	90
Fig. 6.24. Time histories of states for subsection 3.2.2 where the FLCC are added after 30s.	90
Fig. 6.25. Time histories of errors for subsection 3.2.3 where the traditional controllers are added into after 30s.	91
Fig. 6.26. Time histories of states for subsection 3.2.3 where the traditional controllers are added into after 30s.	91
Fig. 7.1 Chaotic behavior of Sprott 19 system.	109
Fig. 7.2 The uncertainty signal of Δ_1 is band-limited white noise(PSD=0.001).	109
Fig. 7.3 Δ_2 is pulse generator.	110
Fig. 7.4 Chaotic behavior of Sprott 19 system with uncertainty.	110
Fig. 7.5 Chaotic behavior of new fuzzy Sprott 19 system with uncertainty.	111
Fig. 7.6. Chaotic behavior of Sprott 22 system.	111

Fig. 7.7 Chaotic behavior of Sprott 22 system with uncertainty.	112
Fig. 7.8 Chaotic behavior of new fuzzy Sprott 22 system with uncertainty.	112
Fig. 7.9 Chaotic behavior of Lorenz system.	113
Fig. 7.10 Chaotic behavior of new fuzzy Lorenz system.	113
Fig. 7.11. Time histories of errors for Example 1.	114
Fig. 7.12. Time histories of errors for Example 2.	114



Chapter 1

Introduction

Chaos is very interesting nonlinear phenomenon, exhibiting sensitive dependence on initial conditions. Because of this property, chaotic behavior is beneficial and desirable in many applications such as mixing processes, heat transfer, biological systems[1,2] , etc. Chaos synchronization is beneficial and desirable in secure communication[3,4]. Many methods of synchronization have been proposed, such as linear and nonlinear feedback control[5-11].

Generally speaking, designing a system to mimic the behavior of another chaotic system is called synchronization. Synchronization of chaotic systems has received a significant attention, since Pecora and Carroll presented the chaos synchronization method to synchronize two identical chaotic systems with different initial values in 1990 [12].

The various types of synchronization, such as complete synchronization[13], phase synchronization[14], lag synchronization[15], and generalized synchronization [16-20], are investigated extensively in the past years. Among many kinds of synchronizations, the generalized synchronization is investigated. It means there exists a functional relationship between the states of the master and those of the slave. A special kind of generalized synchronizations $y = x + F(t)$ is studied[21], where x , y are the state vectors of the master and the slave respectively, $F(t)$ is a given vector function of time, which may take various form, either regular or chaotic functions of time. When $F(t)=0$, it reduces to a generalized synchronization. A new synchronization $y = H(x, y, t) + F(t)$ is studied, where x , y are the state vectors of the master and of the slave, respectively, $F(t)$ is a given function of time in different form, such as a regular or a chaotic function. The final desired state y of the slave

system not only depends upon the master system state x but also depends upon the slave system state y itself. Therefore the slave system is not a traditional pure slave obeying the master system completely but plays a role to determine the final desired state of the slave system. In other words, it plays an intertwined role, so we call this kind of synchronization is symplectic synchronization, and call the master system partner A, the slave system partner B[22].

In the current scheme of adaptive synchronization [23-27], the traditional Lyapunov stability theorem and Babalat lemma are used to prove that the error vector approaches zero, as time approaches infinity. But the question of that why the estimated parameters also approach uncertain parameters remains unanswered. By the pragmatism asymptotical stability theorem, the question can be answered strictly.

Furthermore, in chaos synchronization, most publications often assume that the synchronization system is without external disturbances. However, in practical applications, it is hard to avoid external disturbances due to uncontrollable environmental conditions. The implementation of control inputs of practical systems is frequently subject to uncertainties as a result of physical limitations. Thus, the derivation of a robust synchronization controller to resist the disturbance is studied.

In recent years, some chaos synchronizations based on fuzzy systems have been proposed since the fuzzy set theory was initiated by Zadeh [28], such as fuzzy control [29], fuzzy sliding mode controlling technique [30-31], LMI-based synchronization [32] and extended backstepping sliding mode controlling technique [33]. The fuzzy logic control (FLC) scheme has been widely developed and has been successful in many applications [34]. Recently Yau and Shieh [35] proposed a new idea in designing fuzzy logic controllers—constructing fuzzy rules subject to a common Lyapunov function such that the master-slave chaos systems satisfy stability in the Lyapunov sense. In [35], there are two main controllers in their slave system. One is

used in elimination of nonlinear terms and the other is built by fuzzy rules subject to a common Lyapunov function. Therefore the resulting controllers are in nonlinear form. In this paper, the regular form is necessary. In order to carry out the new method, the original system must be transformed into their regular form. Li and Ge [36] propose a new strategy which remains constructing fuzzy rules subject to Lyapunov direct method. The values of error derivatives are used to be the upper and lower bounds of FLCC. Through this new approach, a simplest constant controller can be obtained and the difficulty in realization of complicated controllers in chaos synchronization by Lyapunov direct method can be eliminated.

In recent years, fuzzy logic proposed by L. A. Zadeh [37] has received much attention as a powerful tool for the nonlinear control. Among various kinds of fuzzy methods, Takagi-Sugeno fuzzy (T-S fuzzy) system is widely accepted as a useful tool for design and analysis of fuzzy control system [38-43]. Currently, some chaos control and synchronization based on T-S fuzzy systems have been proposed, such as fuzzy sliding mode controlling technique [44-46], LMI-based synchronization [47-49] and robust control [50]. These researches are all focus on two identical nonlinear systems. Furthermore, two different nonlinear systems may have different numbers of nonlinear terms. It causes different numbers of linear subsystems. For synchronization of two different nonlinear systems, the traditional method using the idea of PDC to design the fuzzy control law for stabilization of the error dynamics can not be used here, since the number of subsystems becomes very large.

In this thesis, scheme of study is as follows. In Chapter 2, the chaos for a Ge-Ku-Mathieu (GKM) system is studied.

In Chapter 3, symplectic synchronization is defined as $y = H(x, y, t)$, where x, y are the state vectors of the “master” and of the “slave”, respectively. The final desired state y of the “slave” not only depends upon the “master” state x but also depends

upon the “slave” state y itself. Therefore the “slave” is not a traditional pure slave obeying the “master” completely but plays a role to determine the final desired state of the “slave” system. In other words, it plays an intertwined role, so we call this kind of synchronization, “symplectic synchronization”, and call the “master” system Partner A, the “slave” system Partner B. A new type of synchronization, double symplectic synchronization, $G(x, y, t) = F(x, y, t)$ is studied, where x, y are Partner A and Partner B, respectively. Due to the complexity of the form of the double symplectic synchronization, it may be applied to increase the security of secret communication.

In Chapter 4, a new chaos synchronization strategy by different shift pragmatic synchronization by stability theory of partial region [51-52] is proposed. By using the different shift pragmatic synchronization by stability theory of partial region, the Lyapunov function is a simple linear homogeneous function of error states and the controllers are more simple and have less simulation error because they are in lower degree than that of traditional controllers, for which the Lyapunov function is a quadratic form of error states, and the question of that why the estimated parameters also approach uncertain parameters can be answered strictly.

In Chapter 5, a new type of synchronization, multiple symplectic synchronization is studied. When the double symplectic functions is extended to a more general form, $\mathbf{G}(\mathbf{x}, \mathbf{y}, z, \dots, w, t) = \mathbf{F}(\mathbf{x}, \mathbf{y}, z, \dots, w, t)$, it is called “multiple symplectic synchronization”. Symplectic synchronization and double symplectic synchronization are special cases of the multiple symplectic synchronization.

In Chapter 6, the values of error derivatives are used to be the upper and lower bounds of FLCC. Through this new approach, a simplest constant controller can be obtained and the difficulty in realization of complicated controllers in chaos synchronization by Lyapunov direct method can be eliminated.

In Chapter 7, the new fuzzy model is proposed. It gives a new way to linearize complicated nonlinear system and only two subsystems are concluded.

In Chapter 8, conclusions are given.



Chapter 2

Chaos for a Ge-Ku-Mathieu System

2.1 Preliminary

In this Chapter, the chaotic behaviors of a new Ge-Ku Mathieu system is studied numerically by phase portraits, time histories, Poincaré maps, Lyapunov exponents, and bifurcation diagrams.

2.2 Description of Ge-Ku-Mathieu System

Ge and Ku [53] gave a chaotic system formed by a simple pendulum with its pivot rotating about a fixed axis as Fig. 2.1. This chaotic system is

$$\begin{aligned}\dot{x}_1 &= x_2, \\ \dot{x}_2 &= -ax_2 - \sin x_1 [b(c + \cos x_1) + d \sin wt],\end{aligned}\tag{2.1}$$

where a, b, c, d are parameters. After simplification $\sin x_1 = x_1$, $\cos x_1 = 1 - \frac{x_1^2}{2}$ and addition of coupling terms, combining with Mathieu equation

$$\begin{aligned}\dot{x}_3 &= x_4, \\ \dot{x}_4 &= -(g + hx_3)x_4 - (g + hx_3)nx_4^3 - lx_4 + px_3,\end{aligned}\tag{2.2}$$

where g, h, l, n, p are parameters, we get the Ge-Ku-Mathieu system

$$\begin{aligned}\dot{x}_1 &= x_2, \\ \dot{x}_2 &= -ax_2 - x_1 [b(c - x_1^2) + dx_2x_3], \\ \dot{x}_3 &= -(g + hx_1)x_3 + lx_2 + px_1x_3,\end{aligned}\tag{2.3}$$

where a, b, c, d, g, h, l, p are parameters.

2.3 Computational Analysis of Ge-Ku-Mathieu System

For numerical analysis of computation, this system exhibits chaos when the parameters of system are $a=-0.6$, $b=5$, $c=11$, $d=0.3$, $g=8$, $h=10$, $l=0.5$, $p=0.2$ and the initial states of system are $(0.01, 0.01, 0.01)$. The bifurcation diagram by changing damping parameter a is shown in Fig. 2.2. Its corresponding Lyapunov exponents are

shown in Fig. 2.3. The phase portraits, time histories, and Poincaré maps of the systems is showed in Fig. 2.4.

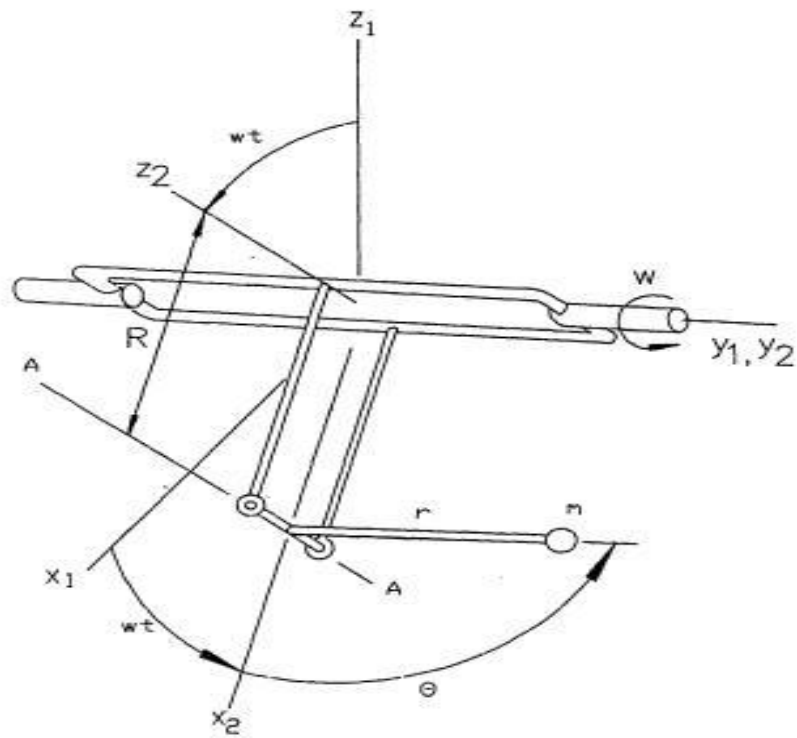


Fig. 2.1. The pendulum on rotating arm.

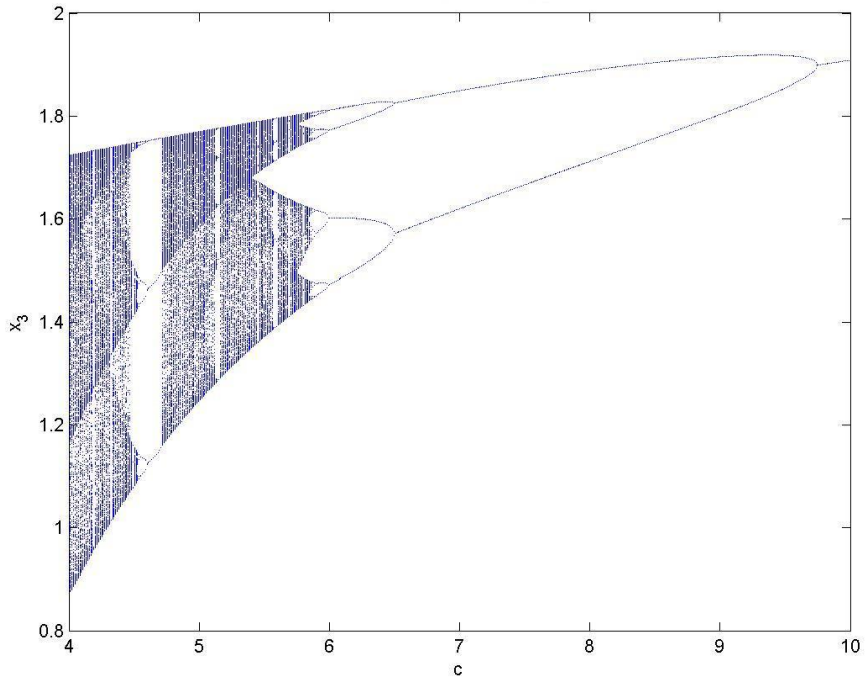


Fig. 2.2 The bifurcation diagram for new Ge-Ku-Mathieu system.

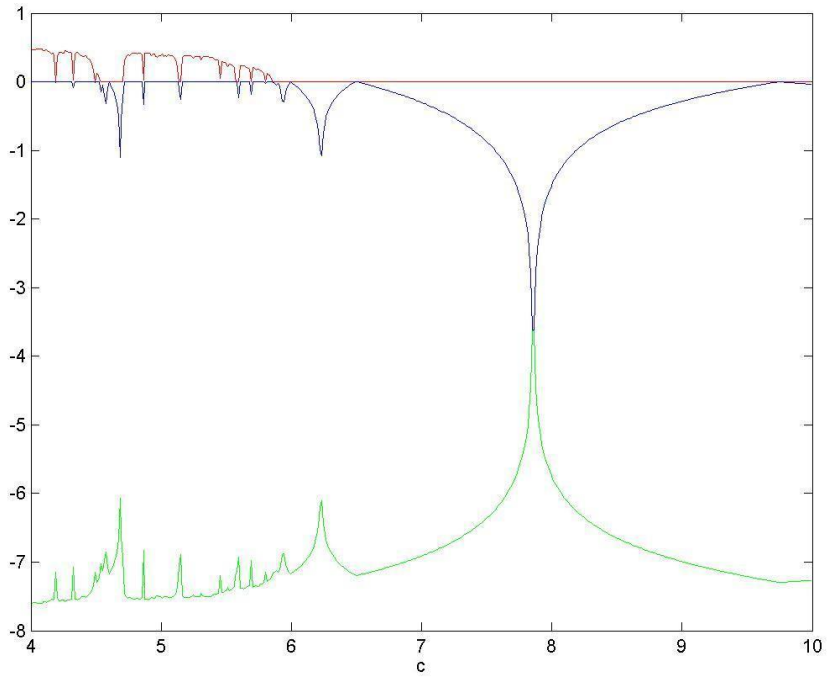


Fig. 2.3 The Lyapunov exponents for new Ge-Ku-Mathieu system.

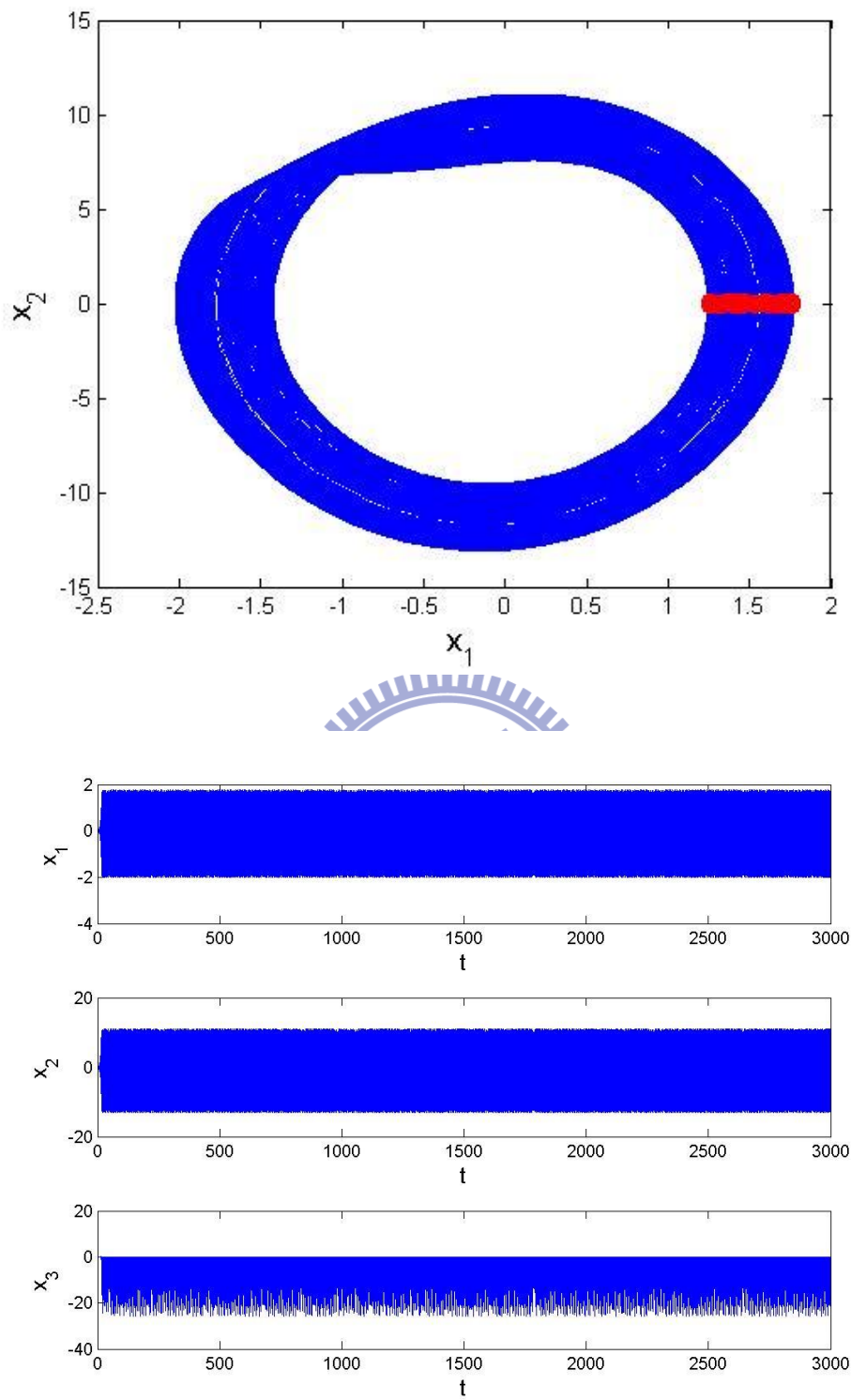


Fig. 2.4 Phase portrait, Poincaré maps, and time histories for new Ge-Ku-Mathieu system.

Chapter 3

Double Symplectic Synchronization for Ge-Ku-Mathieu System

3.1 Preliminary

In this Chapter, a new type of synchronization, double symplectic synchronization, $G(x, y, t) = F(x, y, t)$, for two new chaotic systems is proposed. It is an extension of symplectic synchronization, $y = F(x, y, t)$. Since the symplectic functions are presented on both sides of the equality, it is called double symplectic synchronization. Simulations present the chaotic behaviors of two new chaotic systems. The double symplectic synchronization can be applied to the design of secure communication with more security. Finally, simulations are provided to show the effectiveness of the proposed synchronization scheme.

3.2 Double Symplectic Synchronization Scheme

Consider two different nonlinear chaotic systems, Partner A and Partner B, described by

$$\dot{\mathbf{x}} = \mathbf{f}(\mathbf{x}, t), \quad (3.1)$$

$$\dot{\mathbf{y}} = \mathbf{C}(t)\mathbf{y} + \mathbf{g}(\mathbf{y}, t) + \mathbf{u}, \quad (3.2)$$

where $\mathbf{x} = [x_1, x_2, \dots, x_n]^T \in R^n$ and $\mathbf{y} = [y_1, y_2, \dots, y_n]^T \in R^n$ are the state vectors of Partner A and Partner B, $\mathbf{C} \in R^{n \times n}$ is a given matrix, \mathbf{f} and \mathbf{g} are continuous nonlinear vector functions, and \mathbf{u} is the controller. Our goal is to design the controller \mathbf{u} such that $\mathbf{G}(\mathbf{x}, \mathbf{y}, t)$ asymptotically approaches $\mathbf{F}(\mathbf{x}, \mathbf{y}, t)$, where $\mathbf{G}(\mathbf{x}, \mathbf{y}, t)$ and $\mathbf{F}(\mathbf{x}, \mathbf{y}, t)$ are two given functions. For simplicity we take $\mathbf{G}(\mathbf{x}, \mathbf{y}, t) = \mathbf{x} + \mathbf{y}$ and \mathbf{F} is a continuous nonlinear vector function.

Property 1 [54]: An $m \times n$ matrix A of real elements defines a linear mapping $y = Ax$ from R^n into R^m , and the induced p -norm of A for $p=1, 2$, and ∞ is given by

$$\|A\|_1 = \max_j \sum_{i=1}^m |a_{ij}|, \quad \|A\|_2 = [\lambda_{\max}(A^T A)]^{1/2}, \quad \|A\|_\infty = \max_i \sum_{j=1}^n |a_{ij}|. \quad (3.3)$$

The useful property of induced matrix norms for real matrix A is as follow:

$$\|A\|_2 \leq \sqrt{\|A\|_1 \|A\|_\infty}. \quad (3.4)$$

Theorem: For chaotic systems “Partner A” (1) and “Partner B” (2), if the controller \mathbf{u} is designed as

$$\mathbf{u} = (\mathbf{I} - \mathbf{D}_y \mathbf{F})^{-1} [\mathbf{D}_x \mathbf{F} \mathbf{f}(\mathbf{x}, t) + \mathbf{D}_y \mathbf{F} (\mathbf{C}(t) \mathbf{y} + \mathbf{g}(\mathbf{y}, t)) + \mathbf{D}_t \mathbf{F} - \mathbf{f}(\mathbf{x}, t) - \mathbf{g}(\mathbf{y}, t) + \mathbf{C}(t)(\mathbf{x} - \mathbf{F}) - \mathbf{K}(\mathbf{x} + \mathbf{y} - \mathbf{F})], \quad (3.5)$$

where $\mathbf{D}_x \mathbf{F}$, $\mathbf{D}_y \mathbf{F}$, $\mathbf{D}_t \mathbf{F}$ are the Jacobian matrices of $\mathbf{F}(\mathbf{x}, \mathbf{y}, t)$, $\mathbf{K} = \text{diag}(k_1, k_2, \dots, k_m)$, and satisfies

$$\frac{\min(k_i)}{\|\mathbf{C}(t)\|} > 1, \quad (3.6)$$

then the double symplectic synchronization will be achieved.

Proof: Define the error vectors as

$$\mathbf{e} = \mathbf{x} + \mathbf{y} - \mathbf{F}(\mathbf{x}, \mathbf{y}, t), \quad (3.7)$$

then the following error dynamics can be obtained by introducing the designed controller

$$\begin{aligned} \frac{d\mathbf{e}}{dt} &= \dot{\mathbf{e}} = \dot{\mathbf{x}} + \dot{\mathbf{y}} - \mathbf{D}_x \mathbf{F} \dot{\mathbf{x}} - \mathbf{D}_y \mathbf{F} \dot{\mathbf{y}} - \mathbf{D}_t \mathbf{F} \\ &= \mathbf{f}(\mathbf{x}, t) + \mathbf{C}(t) \mathbf{y} + \mathbf{g}(\mathbf{y}, t) - \mathbf{D}_x \mathbf{F} \mathbf{f}(\mathbf{x}, t) - \mathbf{D}_y \mathbf{F} (\mathbf{C}(t) \mathbf{y} + \mathbf{g}(\mathbf{y}, t)) - \mathbf{D}_t \mathbf{F} \\ &\quad + (\mathbf{I} - \mathbf{D}_y \mathbf{F}) \mathbf{u} \\ &= (\mathbf{C}(t) - \mathbf{K}) \mathbf{e}. \end{aligned} \quad (3.8)$$

Choose a positive definite Lyapunov function of the form

$$V(t) = \frac{1}{2} \mathbf{e}^T \mathbf{e}. \quad (3.9)$$

Taking the time derivative of $V(t)$ along the trajectory of Eq. (3.8), we have

$$\begin{aligned} \dot{V}(t) &= \mathbf{e}^T \dot{\mathbf{e}} \\ &= \mathbf{e}^T \mathbf{C}(t) \mathbf{e} - \mathbf{e}^T \mathbf{K} \mathbf{e} \\ &\leq \|\mathbf{C}(t)\| \|\mathbf{e}\|^2 - \min(k_i) \|\mathbf{e}\|^2 \\ &= (\|\mathbf{C}(t)\| - \min(k_i)) \|\mathbf{e}\|^2. \end{aligned} \quad (3.10)$$

Let $(\|\mathbf{C}(t)\| - \min(k_i)) \|\mathbf{e}\|^2 = M$, then $\dot{V}(t) \leq -M \|\mathbf{e}\|^2 = -2MV(t)$. Therefore, it can be obtained that

$$V(t) \leq V(0) e^{-2Mt} \quad (3.11)$$

and $\lim_{t \rightarrow \infty} \int_0^t |V(\xi)| d\xi$ is bounded. Besides, $V(t)$ is uniformly continuous.

According to Barbalat's lemma [55], the conclusion can be drawn that $\lim_{t \rightarrow \infty} V(t) = 0$,

i.e. $\lim_{t \rightarrow \infty} \|\mathbf{e}(t)\| = 0$. Thus, the double symplectic synchronization can be achieved asymptotically.

3.3 Synchronization of Two Different New Chaotic Systems

Case 1.

Consider a new Double Ge-Ku system as Partner A described by

$$\begin{aligned} \dot{x}_1 &= x_2, \\ \dot{x}_2 &= -mx_2 - x_1 \left[n(q - x_1^2) + wx_3 \right], \\ \dot{x}_3 &= -mx_3 - x_3 \left[n(q - x_3^2) + rx_1 \right], \end{aligned} \quad (3.12)$$

where $m = -0.5, n = -1.4, q = 1.9, w = 54, r = 6.2$ and the initial conditions are

$x_1(0) = 0.01, x_2(0) = 0.01, x_3(0) = 0.01$. Eq. (3.12) can be rewritten in the form of Eq.

(3.1), where $\mathbf{f}(\mathbf{x}, t) = \begin{bmatrix} x_2 \\ -mx_2 - x_1 \left[n(q - x_1^2) + wx_3 \right] \\ -mx_3 - x_3 \left[n(q - x_3^2) + rx_1 \right] \end{bmatrix}$. The chaotic attractor of the

Double Ge-Ku (DGK) system is shown in Fig. 3.1.

Ge-Ku-Mathieu (GKM) system is considered as Partner B. The controlled GKM system is

$$\begin{aligned} \dot{y}_1 &= y_2 + u_1, \\ \dot{y}_2 &= -ay_2 - y_1 \left[b(c - y_1^2) + dy_2y_3 \right] + u_2, \\ \dot{y}_3 &= -(g + hy_1)y_3 + ly_2 + py_1y_3 + u_3, \end{aligned} \quad (3.13)$$

where $a = -0.6, b = 5, c = 11, d = 0.3, g = 8, h = 10, l = 0.5, p = 0.2$, $\mathbf{u} = [u_1, u_2, u_3]^T$ is

the controller, and the initial conditions are $y_1(0) = 0.01, y_2(0) = 0.01, y_3(0) = 0.01$.

Eq. (3.13) can be rewritten in the form of Eq. (3.2), where $\mathbf{C}(t) = \begin{bmatrix} 0 & 1 & 0 \\ -bc & -a & 0 \\ 0 & l & -g \end{bmatrix}$

and $\mathbf{g}(\mathbf{y}, t) = \begin{bmatrix} 0 \\ by_1^3 - dy_1y_2y_3 \\ -hy_1y_3 + py_1y_3 \end{bmatrix}$. By applying *Property 1*, it is derived that

$$\|\mathbf{C}(t)\|_1 = bc, \quad \|\mathbf{C}(t)\|_\infty = -a + bc, \quad \text{and} \quad \|\mathbf{C}(t)\|_2 \leq \sqrt{bc(-a + bc)} = \sqrt{3058}. \quad \text{Then}$$

$$\|\mathbf{C}(t)\| = 55 \quad \text{is estimated.}$$

Define $\mathbf{F}(\mathbf{x}, \mathbf{y}, t) = \begin{bmatrix} x_1 \cos y_1 \\ x_2 \cos y_2 \\ x_3 \cos y_3 \end{bmatrix}$, and our goal is to achieve the double simplectic

synchronization $\mathbf{x} + \mathbf{y} = \mathbf{F}(\mathbf{x}, \mathbf{y}, t)$. According to Theorem, the inequality

$$\frac{\min(k_i)}{\|\mathbf{C}(t)\|} > 1 \quad \text{has to be satisfied. It can be obtained that} \quad \min(k_i) > 55. \quad \text{Thus we choose}$$

$$\mathbf{K} = \begin{bmatrix} k_1 & 0 & 0 \\ 0 & k_2 & 0 \\ 0 & 0 & k_3 \end{bmatrix} = \begin{bmatrix} 56 & 0 & 0 \\ 0 & 57 & 0 \\ 0 & 0 & 58 \end{bmatrix} \text{ and design the controller as}$$

$$u_1 = x_2 \cos y_1 - x_1 y_2 \sin y_1 - x_2 - y_2 + x_1 \cos y_1 - x_1 - y_1, \quad ,$$

$$u_2 = \left\{ -mx_2 - x_1 \left[n(q - x_1^2) + wx_3 \right] \right\} \cos y_2 - x_2 \left\{ -ay_2 - y_1 \left[b(c - y_1^2) + dy_2 y_3 \right] \right\} \sin y_2 \\ - \left\{ -mx_2 - x_1 \left[n(q - x_1^2) + wx_3 \right] \right\} - \left\{ -ay_2 - y_1 \left[b(c - y_1^2) + dy_2 y_3 \right] \right\} + x_2 \cos y_2 - x_2 - y_2,$$

$$u_3 = \left\{ -mx_3 - x_3 \left[n(q - x_3^2) + rx_1 \right] \right\} \cos y_3 - x_3 \left[-(g + hy_1) y_3 + ly_2 + py_1 y_3 \right] \sin y_3 \\ - \left\{ -mx_3 - x_3 \left[n(q - x_3^2) + rx_1 \right] \right\} - \left[-(g + hy_1) y_3 + ly_2 + py_1 y_3 \right] + x_3 \cos y_3 - x_3 - y_3,$$

The **Theorem** is satisfied and the double symplectic synchronization is achieved, the phase portrait of the controlled GKM system is shown in Fig. 3.2. The time histories of $x_i + y_i$, of $x_i \cos y_i$ and of the state errors are shown in Fig. 3.3 and Fig. 3.4, respectively.

Case 2.

Consider a new Ge-Ku-van der Pol (GKv) system as Partner A described by

$$\begin{aligned} \dot{x}_1 &= x_2, \\ \dot{x}_2 &= -mx_2 - x_3 \left[n(q - x_1^2) + wx_3 \right], \\ \dot{x}_3 &= -sx_3 - f(1 - x_3^2)x_2 + rx_1, \end{aligned} \quad (3.14)$$

where $m = 0.08, n = -0.35, q = 100.56, w = -1000.02, s = 0.61, f = 0.08, r = 0.01$ and

the initial conditions are $x_1(0) = 0.01, x_2(0) = 0.01, x_3(0) = 0.01$. Eq. (3.14) can be

rewritten in the form of Eq. (3.1), where $\mathbf{f}(\mathbf{x}, t) = \begin{bmatrix} x_2 \\ -mx_2 - x_3 \left[n(q - x_1^2) + wx_3 \right] \\ -sx_3 - f(1 - x_3^2)x_2 + rx_1 \end{bmatrix}$.

The chaotic attractor of a new GKv system is shown in Fig. 3.5.

A new Ge-Ku-Mathieu (GKM) system is considered as Partner B. The controlled GKM system is

$$\begin{aligned} \dot{y}_1 &= y_2 + u_1, \\ \dot{y}_2 &= -ay_2 - y_1 \left[b(c - y_1^2) + dy_2y_3 \right] + u_2, \\ \dot{y}_3 &= -(g + hy_1)y_3 + ly_2 + py_1y_3 + u_3, \end{aligned} \quad (3.15)$$

where $a = -0.6, b = 5, c = 11, d = 0.3, g = 8, h = 10, l = 0.5, p = 0.2$, $\mathbf{u} = [u_1, u_2, u_3]^T$ is the controller, and the initial conditions are $y_1(0) = 0.01$, $y_2(0) = 0.01$, $y_3(0) = 0.01$. Eq. (3.15) can be rewritten in the form of Eq. (3.2), where

$$\mathbf{C}(t) = \begin{bmatrix} 0 & 1 & 0 \\ -bc & -a & 0 \\ 0 & l & -g \end{bmatrix} \text{ and } \mathbf{g}(\mathbf{y}, t) = \begin{bmatrix} 0 \\ by_1^3 - dy_1y_2y_3 \\ -hy_1y_3 + py_1y_3 \end{bmatrix}. \text{ By applying } \mathbf{Property 1}, \text{ it}$$

can be derived that $\|\mathbf{C}(t)\| = bc$, $\|\mathbf{C}(t)\|_\infty = -a + bc$, and

$$\|\mathbf{C}(t)\|_2 \leq \sqrt{bc(-a + bc)} = \sqrt{3058}. \text{ Then } \|\mathbf{C}(t)\| = 55 \text{ is}$$

estimated.

$$\text{Define } \mathbf{F}(\mathbf{x}, \mathbf{y}, t) = \begin{bmatrix} x_1 \cos y_1 \\ x_2 \cos y_2 \\ x_3 \cos y_3 \end{bmatrix}, \text{ and our goal is to achieve the double simplectic}$$

synchronization $\mathbf{x} + \mathbf{y} = \mathbf{F}(\mathbf{x}, \mathbf{y}, t)$. According to Theorem, the inequality

$\frac{\min(k_i)}{\|\mathbf{C}(t)\|} > 1$ must be satisfied. It can be obtained that $\min(k_i) > 55$. Thus we choose

$$\mathbf{K} = \begin{bmatrix} k_1 & 0 & 0 \\ 0 & k_2 & 0 \\ 0 & 0 & k_3 \end{bmatrix} = \begin{bmatrix} 56 & 0 & 0 \\ 0 & 57 & 0 \\ 0 & 0 & 58 \end{bmatrix} \text{ and design the controller as}$$

$$u_1 = x_2 \cos y_1 - x_1 y_2 \sin y_1 - x_2 - y_2 + x_1 \cos y_1 - x_1 - y_1,$$

$$u_2 = \left\{ -mx_2 - x_3 \left[n(q - x_1^2) + wx_3 \right] \right\} \cos y_2 - x_2 \left\{ -ay_2 - y_1 \left[b(c - y_1^2) + dy_2y_3 \right] \right\} \sin y_2 \\ - \left\{ -mx_2 - x_3 \left[n(q - x_1^2) + wx_3 \right] \right\} - \left\{ -ay_2 - y_1 \left[b(c - y_1^2) + dy_2y_3 \right] \right\} + x_2 \cos y_2 - x_2 - y_2,$$

$$u_3 = \left\{ -sx_3 + f(1 - x_3^2)x_2 + rx_1 \right\} \cos y_3 - x_3 \left[-(g + hy_1)y_3 + ly_2 + py_1y_3 \right] \sin y_3 \\ - \left\{ -sx_3 + f(1 - x_3^2)x_2 + rx_1 \right\} - \left[-(g + hy_1)y_3 + ly_2 + py_1y_3 \right] + x_3 \cos y_3 - x_3 - y_3,$$

The **Theorem** is satisfied and the double symplectic synchronization is achieved, the phase portrait of the controlled GKM system and the time histories of $x_i + y_i$, of $x_i \cos y_i$ and of the state errors are shown in Fig. 3.6 and Fig. 3.7 and Fig. 3.8, respectively.

Case 3.

Consider a new GKD system as Partner A described by

$$\begin{aligned} \dot{x}_1 &= x_2, \\ \dot{x}_2 &= -mx_2 - x_1 \left[n(q - x_1^2) + wx_3 \right], \\ \dot{x}_3 &= -x_3 - x_3^3 - fx_2 + rx_1, \end{aligned} \quad (3.16)$$

where $m = 0.1, n = 11, q = 40, w = 54, f = 6, r = 30$ and the initial conditions are $x_1(0) = 2, x_2(0) = 2.4, x_3(0) = 5$. Eq. (3.16) can be rewritten in the form of Eq. (3.1),

$$\text{where } \mathbf{f}(\mathbf{x}, t) = \begin{bmatrix} x_2 \\ -mx_2 - x_1 \left[n(q - x_1^2) + wx_3 \right] \\ -x_3 - x_3^3 - fx_2 + rx_1 \end{bmatrix}. \text{ The chaotic attractor of the new}$$

GKD system is shown in Fig. 3.9.

Ge-Ku-Mathieu (GKM) system is considered as Partner B. The controlled GKM system is

$$\begin{aligned}
\dot{y}_1 &= y_2 + u_1, \\
\dot{y}_2 &= -ay_2 - y_1 \left[b(c - y_1^2) + dy_2 y_3 \right] + u_2, \\
\dot{y}_3 &= -(g + hy_1)y_3 + ly_2 + py_1 y_3 + u_3,
\end{aligned} \tag{3.17}$$

where $a = -0.6, b = 5, c = 11, d = 0.3, g = 8, h = 10, l = 0.5, p = 0.2$, $\mathbf{u} = [u_1, u_2, u_3]^T$ is

the controller, and the initial conditions are $y_1(0) = 0.01, y_2(0) = 0.01, y_3(0) = 0.01$.

Eq. (3.17) can be rewritten in the form of Eq. (3.2), where $\mathbf{C}(t) = \begin{bmatrix} 0 & 1 & 0 \\ -bc & -a & 0 \\ 0 & l & -g \end{bmatrix}$

and $\mathbf{g}(\mathbf{y}, t) = \begin{bmatrix} 0 \\ by_1^3 - dy_1 y_2 y_3 \\ -hy_1 y_3 + py_1 y_3 \end{bmatrix}$. By applying *Property 1*, it can be derived that

$\|\mathbf{C}(t)\|_1 = bc$, $\|\mathbf{C}(t)\|_\infty = -a + bc$, and $\|\mathbf{C}(t)\|_2 \leq \sqrt{bc(-a + bc)} = \sqrt{3058}$. Then

$\|\mathbf{C}(t)\| = 55$ is estimated.

Define $\mathbf{F}(\mathbf{x}, \mathbf{y}, t) = \begin{bmatrix} x_1 \cos y_1 \\ x_2 \cos y_2 \\ x_3 \cos y_3 \end{bmatrix}$, and our goal is to achieve the double simplectic

synchronization $\mathbf{x} + \mathbf{y} = \mathbf{F}(\mathbf{x}, \mathbf{y}, t)$. According to Theorem, the inequality

$\frac{\min(k_i)}{\|\mathbf{C}(t)\|} > 1$ must be satisfied. It can be obtained that $\min(k_i) > 55$. Thus we choose

$\mathbf{K} = \begin{bmatrix} k_1 & 0 & 0 \\ 0 & k_2 & 0 \\ 0 & 0 & k_3 \end{bmatrix} = \begin{bmatrix} 56 & 0 & 0 \\ 0 & 57 & 0 \\ 0 & 0 & 58 \end{bmatrix}$ and design the controller as

$$u_1 = x_2 \cos y_1 - x_1 y_2 \sin y_1 - x_2 - y_2 + x_1 \cos y_1 - x_1 - y_1,$$

$$\begin{aligned}
u_2 &= \left\{ -mx_2 - x_1 \left[n(q - x_1^2) + wx_3 \right] \right\} \cos y_2 - x_2 \left\{ -ay_2 - y_1 \left[b(c - y_1^2) + dy_2 y_3 \right] \right\} \sin y_2 \\
&\quad - \left\{ -mx_2 - x_1 \left[n(q - x_1^2) + wx_3 \right] \right\} - \left\{ -ay_2 - y_1 \left[b(c - y_1^2) + dy_2 y_3 \right] \right\} + x_2 \cos y_2 - x_2 - y_2,
\end{aligned}$$

$$u_3 = \left\{ -x_3 - x_3^3 - fx_2 + rx_1 \right\} \cos y_3 - x_3 \left[-(g + hy_1) y_3 + ly_2 + py_1 y_3 \right] \sin y_3 \\ - \left\{ -x_3 - x_3^3 - fx_2 + rx_1 \right\} - \left[-(g + hy_1) y_3 + ly_2 + py_1 y_3 \right] + x_3 \cos y_3 - x_3 - y_3,$$

The **Theorem** is satisfied and the double symplectic synchronization is achieved, the phase portrait of the controlled GKM system and the time histories of $x_i + y_i$, of $x_i \cos y_i$ and of the state errors are shown in Fig. 3.10 and Fig. 3.11 and Fig. 3.12, respectively.

3.4 Summary

In this Chapter, a new double symplectic synchronization of chaotic systems are investigated based on Barbalat's Lemma. Traditional generalized synchronization and symplectic synchronization are special cases for the double symplectic synchronization. By applying active control, the double symplectic synchronization is achieved. The simulation results show that the proposed scheme is effective and feasible for all chaotic systems. Furthermore, the double symplectic synchronization could be applied to the design of secret communication with more security than either generalized, or symplectic synchronization due to the complexity of its synchronization form.

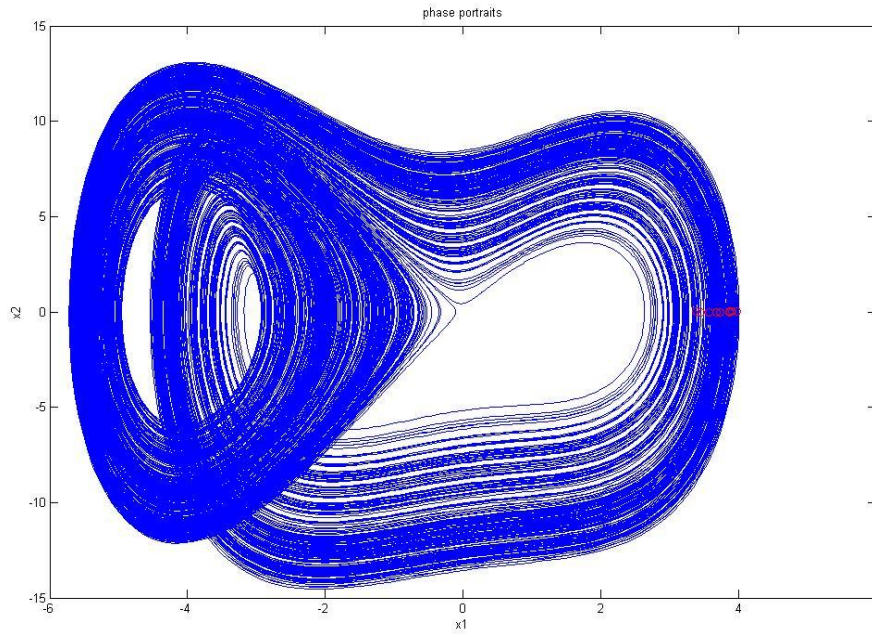


Fig. 3.1 The chaotic attractor of a new Double Ge-Ku system.

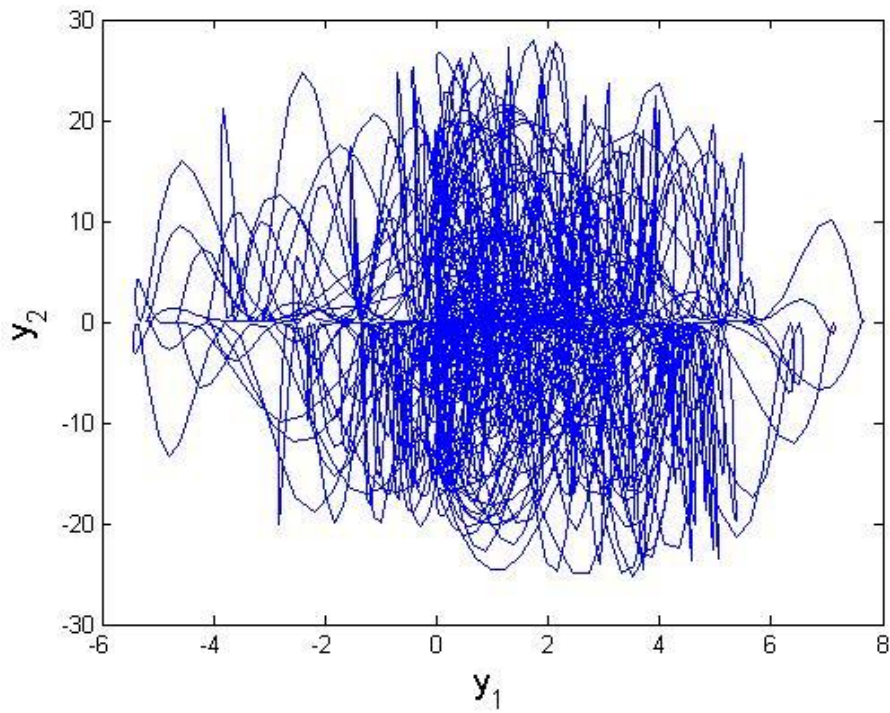


Fig. 3.2 The phase portrait of the controlled GKM system for Case1.

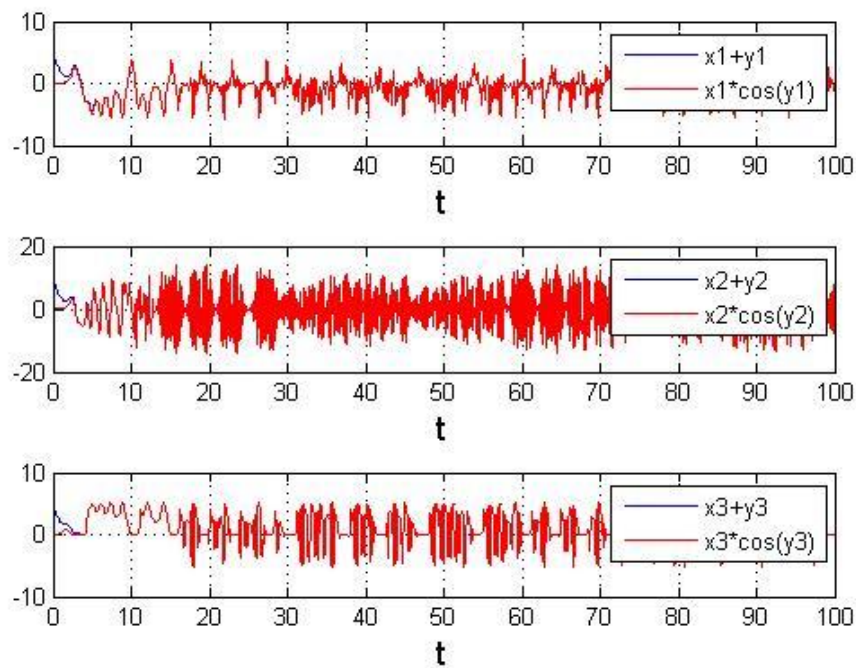


Fig. 3.3 Time histories of $x_i + y_i$ and $x_i \cos y_i$ for Case1.

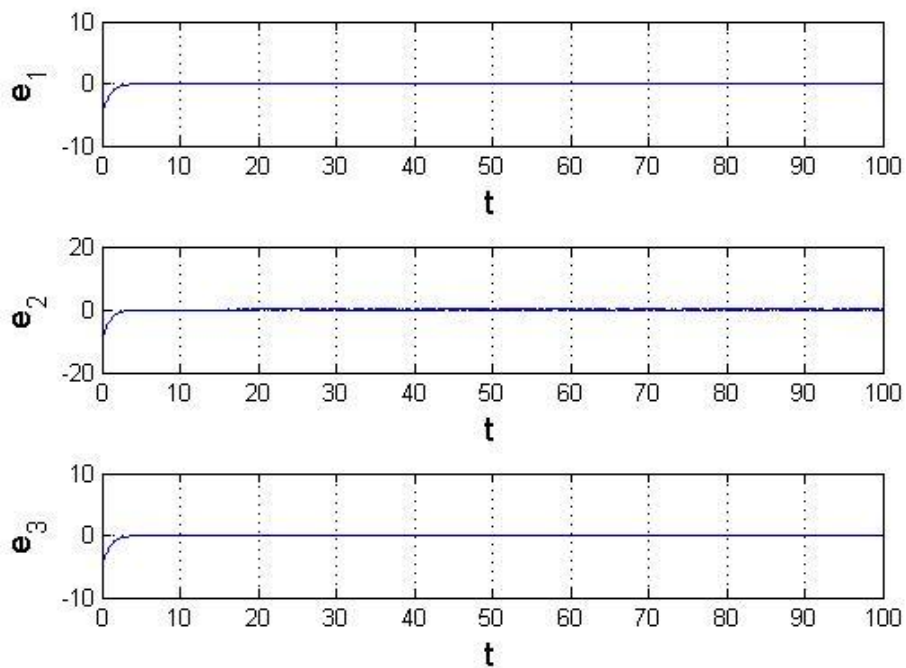


Fig. 3.4 Time histories of the state errors for Case1.

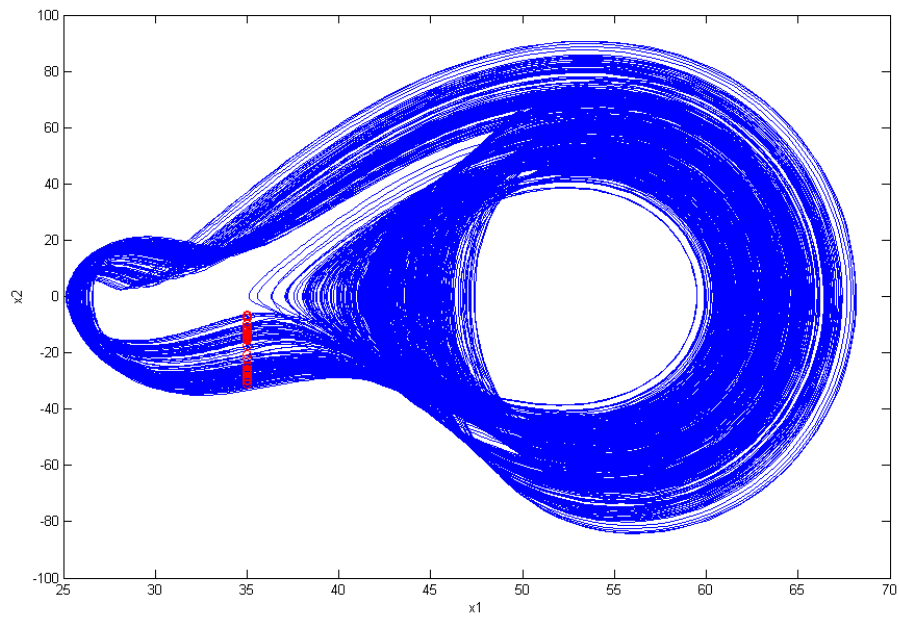


Fig. 3.5 The chaotic attractor of a new Ge-Ku-van der Pol system.

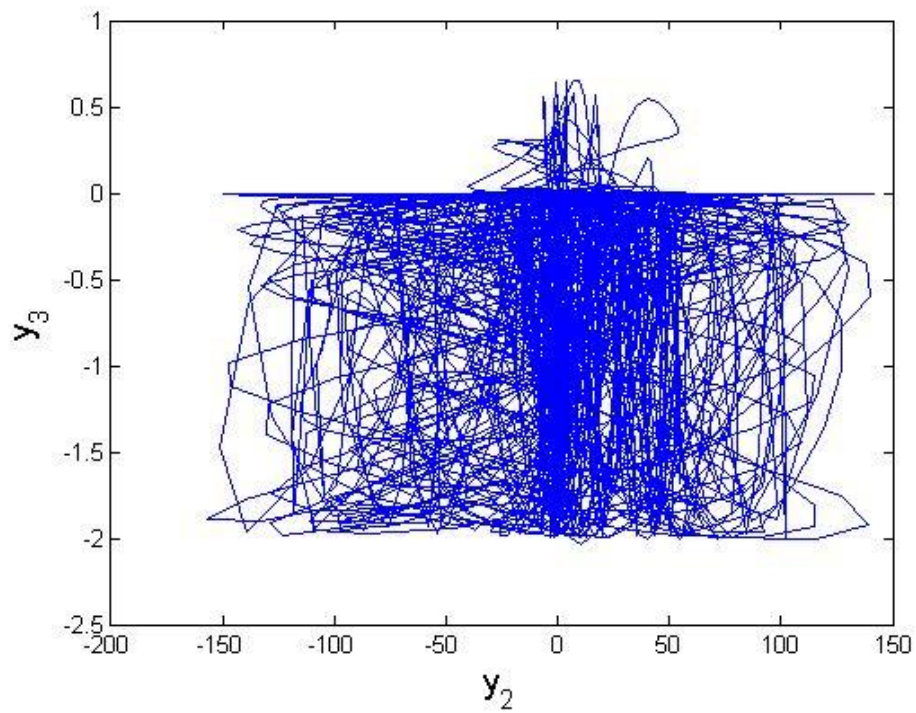


Fig. 3.6 The phase portrait of the controlled GKM system for Case2.

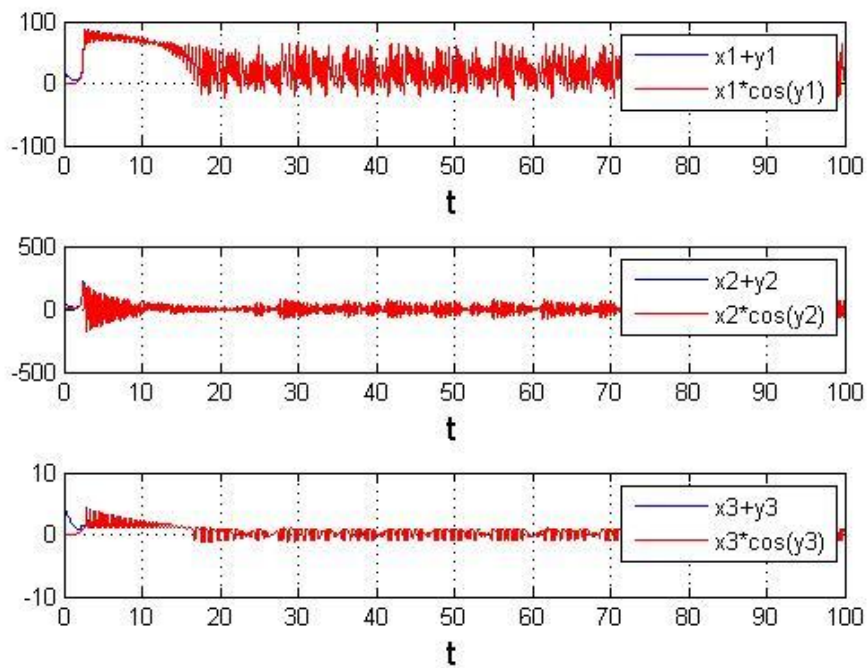


Fig. 3.7 Time histories of $x_i + y_i$ and $x_i \cos y_i$ for Case2.

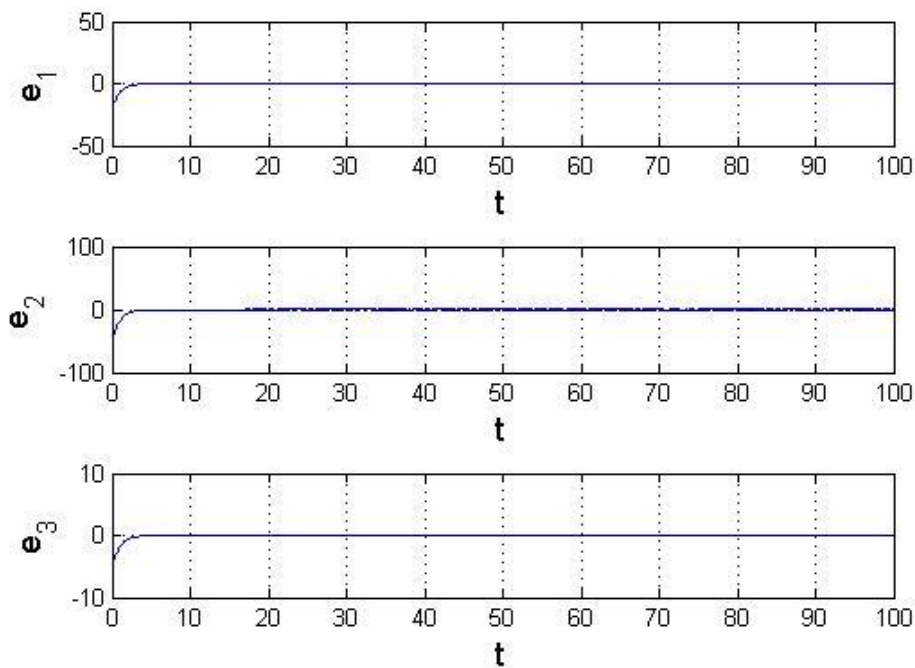


Fig. 3.8 Time histories of the state errors for Case2.

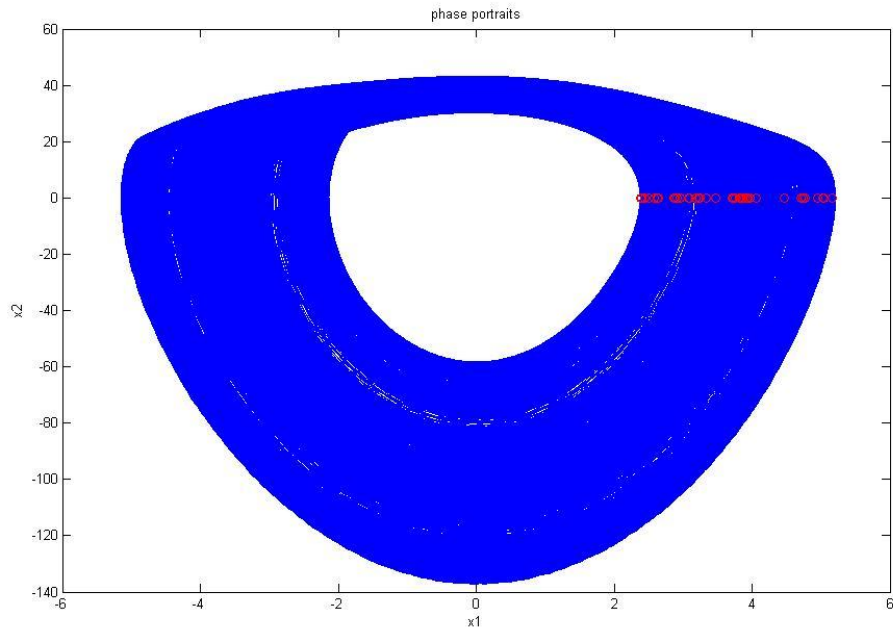


Fig. 3.9 The chaotic attractor of the Ge-Ku-Duffing system.

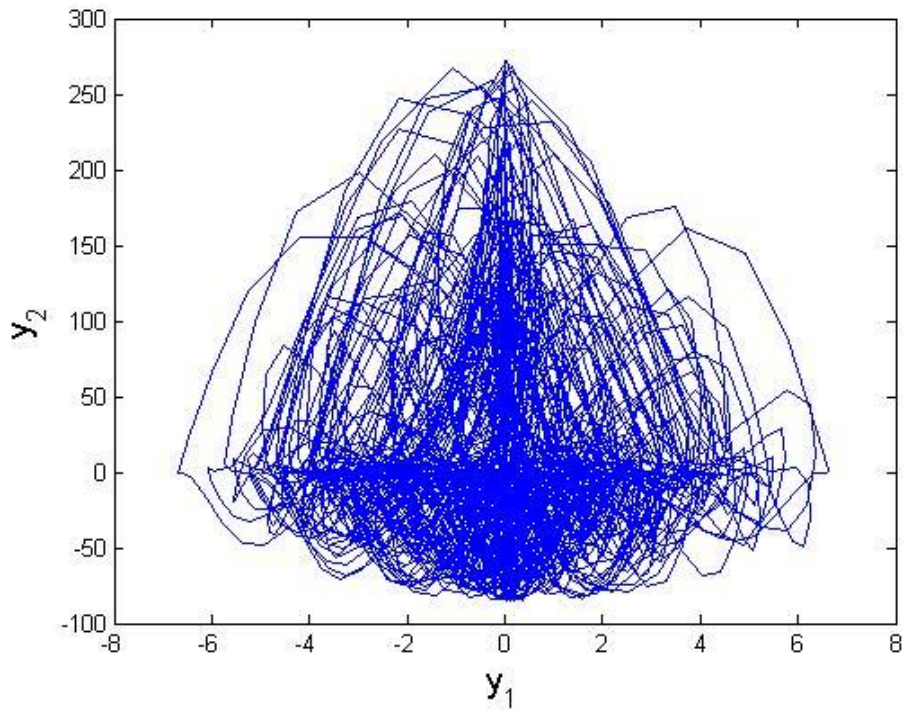


Fig. 3.10 The phase portrait of the controlled GKM system for Case3.

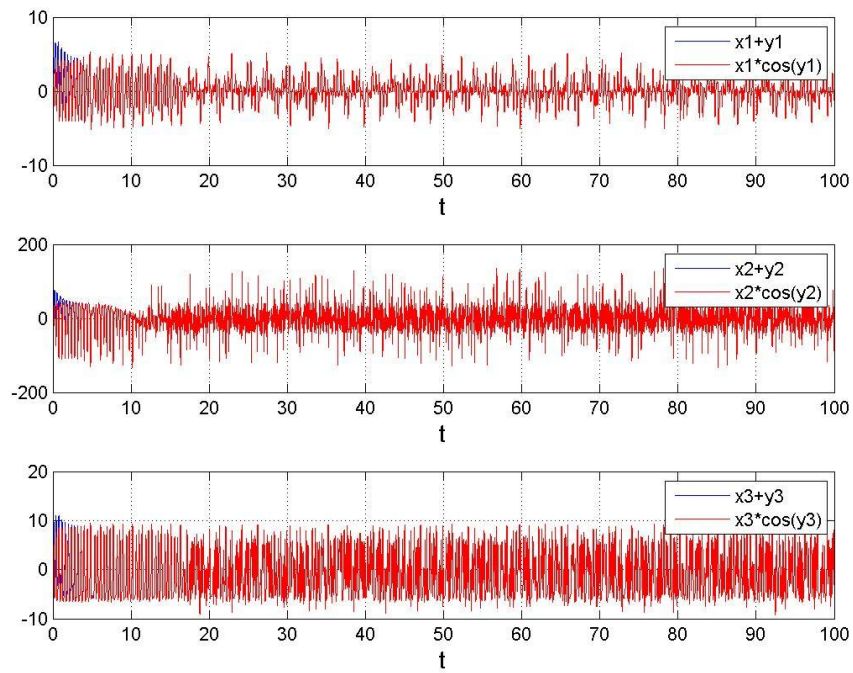


Fig. 3.11 Time histories of $x_i + y_i$ and $x_i \cos y_i$ for Case3.

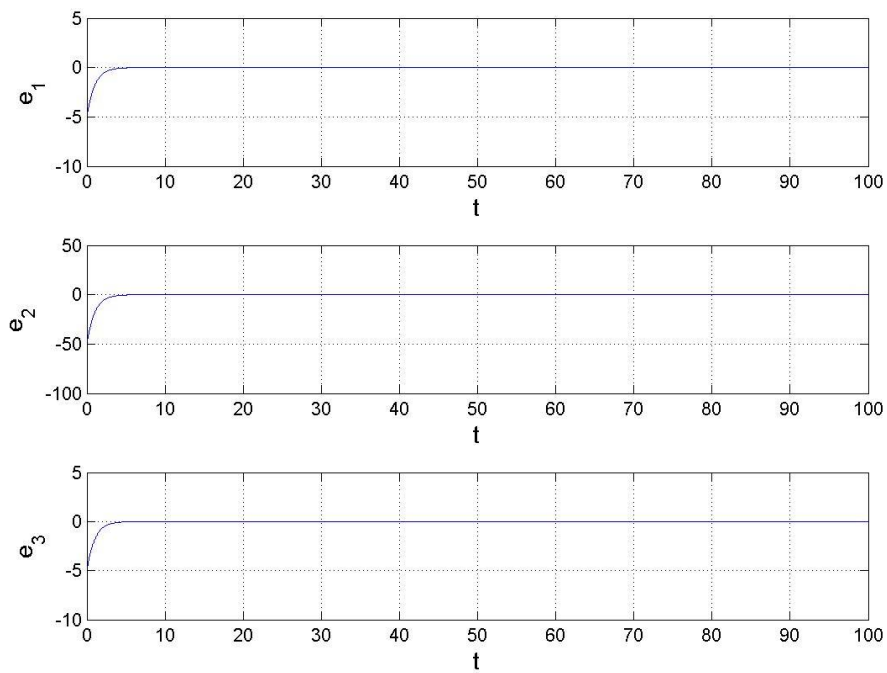


Fig. 3.12 Time histories of the state errors for Case3.

Chapter 4

Different Translation Pragmatical Generalized Synchronization by Stability Theory of Partial Region for Ge-Ku-Mathieu System

4.1 Preliminary

In this Chapter, a new strategy to achieve different translation generalized synchronization by partial region stability theory and pragmatical stability theory is proposed, by which the Lyapunov function is a simple linear homogeneous function of error states, the controllers are more simple since they are in lower degree than that of traditional controllers.

4.2 The Scheme of Different Translation Pragmatical Generalized Synchronization by Stability Theory of Partial Region Theory

There are two identical nonlinear dynamical systems, and the master system synchronizes the slave system. The master system is given by

$$\dot{x} = Ax + f(x, B) \quad (4.1)$$

The master system after the origin of x -coordinate system is translated to $[K_1, K_1, \dots, K_1]$ is

$$\dot{x}' = Ax' + f(x', B) \quad (4.1')$$

where $x' = [x'_1, x'_2, \dots, x'_n]^T = [x_1 - K_1, x_2 - K_1, \dots, x_n - K_1]^T \in R^n$ denotes a state vector,

where $K_1 = [K_1, K_1, \dots, K_1]$ is a constant vector with positive element K_1 as shown

in Fig. 4.1. A is an $n \times n$ uncertain constant coefficients matrix, f is a nonlinear vector function, and B is a vector of uncertain constant coefficients in f .

The slave system is given by

$$\dot{y} = Ay + f(y, B) + u(t) \quad (4.2)$$

A is an $n \times n$ estimated coefficient matrix, B is a vector of estimated coefficients in f , and $u(t) = [u_1(t), u_2(t), \dots, u_n(t)]^T \in R^n$ is a control input vector.

The slave system after the origin of y -coordinate system is translated to $[K_2, K_2, \dots, K_2]$ is

$$\dot{y}' = Ay' + f(y', B) + u(t) \quad (4.2')$$

where $y' = [y'_1, y'_2, \dots, y'_n]^T = y = [y_1 - K_2, y_2 - K_2, \dots, y_n - K_2] \in R^n$ denotes a state vector, where K_2 is a constant vector with positive element K_2 as shown in Fig.

4.2.

Our goal is to design a controller $u(t)$ so that the state vector of the translated slave system (4.2') asymptotically approaches the state vector of the translated master system (3.1') plus a given nonchaotic or chaotic vector function

$$F(t) = [F_1(t), F_2(t), \dots, F_n(t)]^T :$$

$$\dot{y}' = G(x') = \dot{x}' + F(t) . \quad (4.3)$$

The synchronization can be accomplished when $t \rightarrow \infty$, the limit of the error vector

$e(t) = [e_1, e_2, \dots, e_n]^T$ approaches zero:

$$\lim_{t \rightarrow \infty} e = 0 \quad (4.4)$$

where

$$e = x' - y' + F(t) . \quad (4.5)$$

From Eq. (4.5) we have

$$\dot{e} = \dot{x}' - \dot{y}' + \dot{F}(t) \quad (4.6)$$

$$\dot{e} = Ax' - Ay' + f(x', B) - f(y', B) + \dot{F}(t) - u(t). \quad (4.7)$$

where K_1 and K_2 are chosen to guarantee that the error dynamics always occurs in the first quadrant of e coordinate system.

A Lyapunov function $V(e, A, B)$ is chosen as a positive definite function in first quadrant of e coordinate system by stability theory in partial region as shown in Appendix A:

$$V(e, A, B) = e + A + B \quad (4.8)$$

where $A = A - A$, $B = B - B$, A and B are two column matrices whose elements are all the elements of matrix A and of column matrix B , respectively.

Its derivative along any solution of the differential equation system consisting of Eq. (4.7) and update parameter differential equations for A and B is

$$\dot{V}(e, A, B) = Ax' - Ay' + f(x', B) - f(y', B) + \dot{F}(t) - u(t) + \dot{\tilde{A}} + \dot{\tilde{B}} \quad (4.9)$$

where $u(t)$, $\dot{\tilde{A}}$, and $\dot{\tilde{B}}$ are chosen so that $\dot{V} = Ce$, C is a diagonal negative definite matrix, and \dot{V} is a negative semi-definite function of e and parameter differences \tilde{A} and \tilde{B} . By pragmatcal asymptotically stability theorem in Appendix B, the Lyapunov function used is a simple linear homogeneous function of states and the controllers are simpler because they in lower order than the that of traditional controllers. Traditional Lyapunov stability theorem and Babalat lemma are used to prove the error vector approaches zero, as time approaches infinity[56-58]. But the question, why the estimated parameters also approach to the uncertain parameters, remains unanswered. By pragmatcal asymptotical stability theorem, the question can be answered strictly.

4.3 Different Translation Pragmatical Synchronization of New Ge-Ku-Mathieu Chaotic System

Case 1.

The following chaotic systems are two translated master and slave Ge-Ku-Mathieu (GKM) systems of which the old origin is translated to $(x_1, x_2, x_3) = (100, 100, 100)$, $(y_1, y_2, y_3) = (50, 50, 50)$ to guarantee the error dynamics always happens in the first quadrant of e coordinate system.

$$\begin{cases} \dot{x}_1 = x_2 - 100 \\ \dot{x}_2 = -a(x_2 - 100) - (x_1 - 100)\{b[c - (x_1 - 100)^2] + d(x_2 - 150)(x_3 - 100)\} \\ \dot{x}_3 = -[g + h(x_1 - 100)](x_3 - 100) + l(x_2 - 100) + p(x_1 - 100)(x_3 - 100) \end{cases} \quad (4.10)$$

$$\begin{cases} \dot{y}_1 = y_2 - 50 + u_1 \\ \dot{y}_2 = -a(y_2 - 50) - (y_1 - 50)\{\hat{b}[\hat{c} - (y_1 - 50)^2] + d(y_2 - 50)(y_3 - 50)\} + u_2 \\ \dot{y}_3 = -[g + h(y_1 - 50)](y_3 - 50) + \hat{l}(y_2 - 50) + p(y_1 - 50)(y_3 - 50) + u_3 \end{cases} \quad (4.11)$$

Let initial states be $(x_1, x_2, x_3) = (100.01, 100.01, 100.01)$, $(y_1, y_2, y_3) = (50.01, 50.01, 50.01)$, $a_0 = -1$, $\hat{b}_0 = -2$, $\hat{c}_0 = -4$, $d_0 = -1$, $g_0 = -3$,

$h_0 = -6$, $\hat{l}_0 = -4$, $p_0 = -5$ and system parameters $a = -0.6, b = 5, c = 11, d = 0.3$, $g = 8, h = 10, l = 0.5, p = 0.2$.

$$\text{The state error is } e = x' - y' + F(t) = x' - y' + \sin t \quad (4.12)$$

where $F(t) = \sin t$ is a nonchaotic given function of time. We find that the error dynamic without controller always exists in first quadrant as shown in Fig. 4.3.

$$\lim_{t \rightarrow \infty} e_i = \lim_{t \rightarrow \infty} (x'_i - y'_i + \sin t) = 0, \quad i = 1, 2, 3 \quad (4.13)$$

Our aim is $\lim_{t \rightarrow \infty} e = 0$. We obtain the error dynamics:

$$\begin{cases} \dot{e}_1 = x_2 - 100 - y_2 + 50 - u_1 + \cos t \\ \dot{e}_2 = -a(x_2 - 100) - (x_1 - 100)\{b[c - (x_1 - 100)^2] + d(x_2 - 100)(x_3 - 100)\} \\ + a(y_2 - 50) + (y_1 - 50)\{\hat{b}[\hat{c} - (y_1 - 50)^2] + d(y_2 - 50)(y_3 - 50)\} - u_2 + \cos t \\ \dot{e}_3 = -[g + h(x_1 - 100)](x_3 - 100) + l(x_2 - 100) + p(x_1 - 100)(x_3 - 100) \\ + [g + h(y_1 - 50)](y_3 - 50) - \hat{l}(y_2 - 50) - \widehat{p}(y_1 - 50)(y_3 - 50) - u_3 + \cos t \end{cases} \quad (4.14)$$

where $\tilde{a} = a - \hat{a}$, $\tilde{b} = b - \hat{b}$, $\tilde{c} = c - \hat{c}$, $\tilde{d} = d - \hat{d}$, $\tilde{g} = g - \hat{g}$, $\tilde{h} = h - \hat{h}$, $\tilde{l} = l - \hat{l}$,

$\tilde{p} = p - \hat{p}$, and a , \hat{b} , \hat{c} , d , g , h , \hat{l} , p are estimates of uncertain parameters a , b , c , d , g , h , l and p respectively.

Using different translation pragmatismal synchronization by stability theory of partial region, we can choose a Lyapunov function in the form of a positive definite function in first quadrant:

$$V = e_1 + e_2 + e_3 + a + \tilde{b} + \tilde{c} + d + g + h + \tilde{l} + p \quad (4.15)$$

Its time derivative is

$$\begin{aligned} \dot{V} &= \dot{e}_1 + \dot{e}_2 + \dot{e}_3 + \dot{\tilde{a}} + \dot{\tilde{b}} + \dot{\tilde{c}} + \dot{\tilde{d}} + \dot{\tilde{g}} + \dot{\tilde{h}} + \dot{\tilde{l}} + \dot{\tilde{p}} \\ &= (x_2 - 100 - y_2 + 50 - u_1 + \cos t) \\ &\quad - a(x_2 - 100) - (x_1 - 100)\{b[c - (x_1 - 100)^2] + d(x_2 - 100)(x_3 - 100)\} \\ &\quad + a(y_2 - 50) + (y_1 - 50)\{\hat{b}[\hat{c} - (y_1 - 50)^2] + d(y_2 - 50)(y_3 - 50)\} - u_2 + \cos t \\ &\quad + \{-[g + h(x_1 - 100)](x_3 - 100) + l(x_2 - 100) + p(x_1 - 100)(x_3 - 100) \\ &\quad + [\widehat{g} + \widehat{h}(y_1 - 50)](y_3 - 50) - \hat{l}(y_2 - 50) - \widehat{p}(y_1 - 50)(y_3 - 50) - u_3 + \cos t\} \\ &\quad + \dot{\tilde{a}} + \dot{\tilde{b}} + \dot{\tilde{c}} + \dot{\tilde{d}} + \dot{\tilde{g}} + \dot{\tilde{h}} + \dot{\tilde{l}} + \dot{\tilde{p}} \end{aligned} \quad (4.16)$$

Choose

$$\begin{cases} \dot{\tilde{a}} = -\dot{\hat{a}} = -\tilde{a}e_2 \\ \dot{\tilde{b}} = -\dot{\hat{b}} = -\tilde{b}e_2 \\ \dot{\tilde{c}} = -\dot{\hat{c}} = -\tilde{c}e_2 \\ \dot{\tilde{d}} = -\dot{\hat{d}} = -\tilde{d}e_2 \\ \dot{\tilde{g}} = -\dot{\hat{g}} = -\tilde{g}e_3 \\ \dot{\tilde{h}} = -\dot{\hat{h}} = -\tilde{h}e_3 \\ \dot{\tilde{l}} = -\dot{\hat{l}} = -\tilde{l}e_3 \\ \dot{\tilde{p}} = -\dot{\hat{p}} = -\tilde{p}e_3 \end{cases} \quad (4.17)$$

$$\begin{cases} u_1 = x_2 - 100 - y_2 + 50 + \cos t + e_1 \\ u_2 = -a(x_2 - 100) - (x_1 - 100)\{b[c - (x_1 - 100)^2] + d(x_2 - 100)(x_3 - 100)\} \\ + a(y_2 - 50) + (y_1 - 50)\{\hat{b}[\hat{c} - (y_1 - 50)^2] + d(y_2 - 50)(y_3 - 50)\} \\ + \cos t + e_2 - \tilde{a}e_2 - \tilde{b}e_2 - \tilde{c}e_2 - de_2 \\ u_3 = -[g + h(x_1 - 100)](x_3 - 100) + l(x_2 - 100) + p(x_1 - 100)(x_3 - 100) \\ + [\widehat{g} + \widehat{h}(y_1 - 50)](y_3 - 50) - \hat{l}(y_2 - 50) - \hat{p}(y_1 - 50)(y_3 - 50) \\ + \cos t + e_3 - \tilde{g}e_3 - \tilde{h}e_3 - \tilde{l}e_3 - \tilde{p}e_3 \end{cases} \quad (3.18)$$

We obtain

$$\dot{V} = -e_1 - e_2 - e_3 < 0 \quad (4.19)$$

which is a negative semi-definite function of $e_1, e_2, e_3, \tilde{a}, \tilde{b}, \tilde{c}, \tilde{d}, \tilde{g}, \tilde{h}, \tilde{l},$

\tilde{p} , in the first quadrant. The Lyapunov asymptotical stability theorem is not satisfied.

We can not obtain that common origin of error dynamics (4.14) and parameter dynamics (4.17) is asymptotically stable. By pragmatistical asymptotically stability

theorem, D is a 11-manifold, $n=11$ and the number of error state variables $p=3$. When

$e_1 = e_2 = e_3 = 0$ and $\tilde{a}, \tilde{b}, \tilde{c}, \tilde{d}, \tilde{g}, \tilde{h}, \tilde{l}, \tilde{p}$, take arbitrary values, $\dot{V} = 0$, so

X is of 3 dimensions i.e. $p=3, m=n-p=11-3=8, m+1 < n$ is satisfied. According to the

pragmatistical asymptotically stability theorem, error vector e approaches zero and the

estimated parameters also approach the uncertain parameters. The equilibrium point is

pragmatistically asymptotically stable. Under the assumption of equal probability, it is

actually asymptotically stable. The simulation results are shown in Figs. 4.4-4.7.

Case 2.

The following chaotic systems are two translated master and slave Ge-Ku-Mathieu (GKM) systems of which the old origin is translated to $(x_1, x_2, x_3) = (100, 100, 100)$, $(y_1, y_2, y_3) = (50, 50, 50)$ to guarantee that the error dynamics always happens in the first quadrant e coordinate system.

$$\begin{cases} \dot{x}_1 = x_2 - 100 \\ \dot{x}_2 = -a(x_2 - 100) - (x_1 - 100)\{b[c - (x_1 - 100)^2] + d(x_2 - 100)(x_3 - 100)\} \\ \dot{x}_3 = -[g + h(x_1 - 100)](x_3 - 100) + l(x_2 - 100) + p(x_1 - 100)(x_3 - 100) \end{cases} \quad (4.20)$$

$$\begin{cases} \dot{y}_1 = y_2 - 50 + u_1 \\ \dot{y}_2 = -a(y_2 - 50) - (y_1 - 50)\{\hat{b}[\hat{c} - (y_1 - 50)^2] + d(y_2 - 50)(y_3 - 50)\} + u_2 \\ \dot{y}_3 = -[g + h(y_1 - 50)](y_3 - 50) + \hat{l}(y_2 - 50) + p(y_1 - 50)(y_3 - 50) + u_3 \end{cases} \quad (4.21)$$

Let initial states be $(x_1, x_2, x_3) = (100.01, 100.01, 100.01)$, $(y_1, y_2, y_3) = (50.01, 50.01, 50.01)$, $a_0 = -1$, $\hat{b}_0 = 2$, $\hat{c}_0 = 4$, $d_0 = 0.1$, $g_0 = 3$, $h_0 = 6$, $\hat{l}_0 = 0.4$, $p_0 = 0.15$ and system parameters $a = -0.6, b = 5, c = 11, d = 0.3$, $g = 8, h = 10, l = 0.5, p = 0.2$.

The state error is $e = x' - y' + F(t)$, where $F(t) = \mathbf{z} = [z_1, z_2, z_3]$ is the chaotic state vector of Lorenz system:

$$\begin{cases} \dot{z}_1 = r(z_2 - z_1) \\ \dot{z}_2 = z_1(q - z_3) - z_2 \\ \dot{z}_3 = z_1 z_2 - m z_3 \end{cases} \quad (4.22)$$

Let initial states be $\mathbf{z} = [z_1, z_2, z_3] = [0.01, 0.01, 0.01]$ and system parameters $r = 10$, $q = 28$, $m = \frac{8}{3}$, the Lorenz system is chaotic. We find that the error dynamics without controller always exists in first quadrant as shown in Fig. 4.8.

Our aim is $\lim_{t \rightarrow \infty} e = 0$. We obtain the error dynamics.

$$\lim_{t \rightarrow \infty} e_i = \lim_{t \rightarrow \infty} [x_i' - y_i' + z] = 0, \quad i = 1, 2, 3 \quad (4.23)$$

$$\begin{cases} \dot{e}_1 = x_2 - 100 - y_2 + 50 - u_1 + r(z_2 - z_1) \\ \dot{e}_2 = -a(x_2 - 100) - (x_1 - 100)\{b[c - (x_1 - 100)^2] + d(x_2 - 100)(x_3 - 100)\} \\ + a(y_2 - 50) + (y_1 - 50)\{\hat{b}[\hat{c} - (y_1 - 50)^2] + d(y_2 - 50)(y_3 - 50)\} - u_2 \\ + z_1(q - z_3) - z_2 \\ \dot{e}_3 = -[g + h(x_1 - 100)](x_3 - 100) + l(x_2 - 100) + p(x_1 - 100)(x_3 - 100) \\ + [\widetilde{g} + \widetilde{h}(y_1 - 50)](y_3 - 50) - \hat{l}(y_2 - 50) - \widehat{p}(y_1 - 50)(y_3 - 50) - u_3 \\ + z_1 z_2 - m z_3 \end{cases} \quad (4.24)$$

where $\tilde{a} = a - \hat{a}$, $\tilde{b} = b - \hat{b}$, $\tilde{c} = c - \hat{c}$, $\tilde{d} = d - \hat{d}$, $\tilde{g} = g - \hat{g}$, $\tilde{h} = h - \hat{h}$, $\tilde{l} = l - \hat{l}$,

$\tilde{p} = p - \hat{p}$, and a , \hat{b} , \hat{c} , d , g , h , \hat{l} , p , are estimates of uncertain parameters a , b , c , d , g , h , l and p respectively.

Using different translation pragmatical synchronization by stability theory of partial region, we can choose a Lyapunov function in the form of a positive definite function in first quadrant:

$$V = e_1 + e_2 + e_3 + a + \tilde{b} + \tilde{c} + d + g + h + \tilde{l} + p \quad (4.25)$$

Its time derivative is

$$\begin{aligned} \dot{V} &= \dot{e}_1 + \dot{e}_2 + \dot{e}_3 + \dot{\tilde{a}} + \dot{\tilde{b}} + \dot{\tilde{c}} + \dot{\tilde{d}} + \dot{\tilde{g}} + \dot{\tilde{h}} + \dot{\tilde{l}} + \dot{\tilde{p}} \\ &= [x_2 - 100 - y_2 + 50 - u_1 + r(z_2 - z_1)] \\ &\quad - a(x_2 - 100) - (x_1 - 100)\{b[c - (x_1 - 100)^2] + d(x_2 - 100)(x_3 - 100)\} \\ &\quad + a(y_2 - 50) + (y_1 - 50)\{\hat{b}[\hat{c} - (y_1 - 50)^2] + d(y_2 - 50)(y_3 - 50)\} - u_2 \\ &\quad + z_1(q - z_3) - z_2 \\ &\quad + \{-[g + h(x_1 - 100)](x_3 - 100) + l(x_2 - 100) + p(x_1 - 100)(x_3 - 100) \\ &\quad + [\widetilde{g} + \widetilde{h}(y_1 - 50)](y_3 - 50) - \hat{l}(y_2 - 50) - \widehat{p}(y_1 - 50)(y_3 - 50) - u_3\} \\ &\quad + z_1 z_2 - m z_3 + \dot{\tilde{a}} + \dot{\tilde{b}} + \dot{\tilde{c}} + \dot{\tilde{d}} + \dot{\tilde{g}} + \dot{\tilde{h}} + \dot{\tilde{l}} + \dot{\tilde{p}} \end{aligned} \quad (4.26)$$

Choose

$$\begin{cases} \dot{\tilde{a}} = -\dot{\hat{a}} = -\tilde{a}e_2 \\ \dot{\tilde{b}} = -\dot{\hat{b}} = -\tilde{b}e_2 \\ \dot{\tilde{c}} = -\dot{\hat{c}} = -\tilde{c}e_2 \\ \dot{\tilde{d}} = -\dot{\hat{d}} = -\tilde{d}e_2 \\ \dot{\tilde{g}} = -\dot{\hat{g}} = -\tilde{g}e_3 \\ \dot{\tilde{h}} = -\dot{\hat{h}} = -\tilde{h}e_3 \\ \dot{\tilde{l}} = -\dot{\hat{l}} = -\tilde{l}e_3 \\ \dot{\tilde{p}} = -\dot{\hat{p}} = -\tilde{p}e_3 \end{cases} \quad (4.27)$$

$$\begin{cases} u_1 = x_2 - 100 - y_2 + 50 + r(z_2 - z_1) + e_1 \\ u_2 = -a(x_2 - 100) - (x_1 - 100)\{b[c - (x_1 - 100)]^2 + d(x_2 - 100)(x_3 - 100)\} \\ + a(y_2 - 50) + (y_1 - 50)\{\hat{b}[\hat{c} - (y_1 - 50)]^2 + d(y_2 - 50)(y_3 - 50)\} \\ + z_1(q - z_3) - z_2 + e_2 - ae_2 - \tilde{b}e_2 - \tilde{c}e_2 - de_2 \\ u_3 = -[g + h(x_1 - 100)](x_3 - 100) + l(x_2 - 100) + p(x_1 - 100)(x_3 - 100) \\ + [\widetilde{g + h}(y_1 - 50)](y_3 - 50) - \hat{l}(y_2 - 50) - \widetilde{p}(y_1 - 50)(y_3 - 50) \\ + z_1z_2 - mz_3 + e_3 - \widetilde{ge_3} - \widetilde{he_3} - \widetilde{le_3} - \widetilde{pe_3} \end{cases} \quad (4.28)$$

We obtain

$$\dot{V} = -e_1 - e_2 - e_3 < 0 \quad (4.29)$$

which is a negative semi-definite function of $e_1, e_2, e_3, \tilde{a}, \tilde{b}, \tilde{c}, \tilde{d}, \tilde{g}, \tilde{h}, \tilde{l}, \tilde{p}$, in the first quadrant. The Lyapunov asymptotical stability theorem is not satisfied. We can not obtain that common origin of error dynamics (4.24) and parameter dynamics (4.27) is asymptotically stable. By pragmatistical asymptotically stability theorem, D is a 11-manifold, $n=11$ and the number of error state variables $p=3$. When $e_1 = e_2 = e_3 = 0$ and $\tilde{a}, \tilde{b}, \tilde{c}, \tilde{d}, \tilde{g}, \tilde{h}, \tilde{l}, \tilde{p}$, take arbitrary values, $\dot{V} = 0$, so X is of 3 dimensions i.e. $p=3, m=n-p=11-3=8, m+1 < n$ is satisfied. According to the pragmatistical asymptotically stability theorem, error vector e approaches zero and the estimated parameters also approach the uncertain parameters. The equilibrium point is pragmatistically asymptotically stable. Under the assumption of equal probability, it is actually asymptotically stable. The simulation results are shown in Figs. 4.9-4.12.

Case 3.

The following chaotic systems are two translated master and slave Ge-Ku-Mathieu (GKM) systems of which the old origin is translated to $(x_1, x_2, x_3) = (350, 350, 350)$, $(y_1, y_2, y_3) = (50, 50, 50)$ to guarantee the error dynamics always happens in the first quadrant of e coordinate system.

$$\begin{cases} \dot{x}_1 = x_2 - 350 \\ \dot{x}_2 = -a(x_2 - 350) - (x_1 - 350)\{b[c - (x_1 - 350)^2] + d(x_2 - 350)(x_3 - 350)\} \\ \dot{x}_3 = -[g + h(x_1 - 350)](x_3 - 350) + l(x_2 - 350) + p(x_1 - 350)(x_3 - 350) \end{cases} \quad (4.30)$$

$$\begin{cases} \dot{y}_1 = y_2 - 50 + u_1 \\ \dot{y}_2 = -a(y_2 - 50) - (y_1 - 50)\{\hat{b}[\hat{c} - (y_1 - 50)^2] + d(y_2 - 50)(y_3 - 50)\} + u_2 \\ \dot{y}_3 = -[g + h(y_1 - 50)](y_3 - 50) + \hat{l}(y_2 - 50) + p(y_1 - 50)(y_3 - 50) + u_3 \end{cases} \quad (4.31)$$

Let initial states be $(x_1, x_2, x_3) = (350.01, 350.01, 350.01)$, $(y_1, y_2, y_3) = (50.01, 50.01, 50.01)$, $a_0 = -1$, $\hat{b}_0 = 2$, $\hat{c}_0 = 4$, $d_0 = 0.1$, $g_0 = 3$, $h_0 = 6$, $\hat{l}_0 = 0.4$, $p_0 = 0.15$ and system parameters $a = -0.6, b = 5, c = 11, d = 0.3$, $g = 8, h = 10, l = 0.5, p = 0.2$.

The state error is $e = x - y + F(t)$, where $F(t) = \mathbf{z} = [z_1, z_2, z_3]$ is state vector the new Ge-Ku-van der Pol system:

$$\begin{cases} \dot{z}_1 = z_2 \\ \dot{z}_2 = -mz_2 - z_3[n(q - z_1^2) + wz_3] \\ \dot{z}_3 = -sz_3 + f(1 - z_3^2)z_2 + rz_1 \end{cases} \quad (4.32)$$

Let initial states be $\mathbf{z} = [z_1, z_2, z_3] = (0.01, 0.01, 0.01)$ and system parameters $m = 0.08$, $n = -0.35$, $q = 100.56$, $w = -1000.02$, $s = 0.61$, $f = 0.08$, $r = 0.01$ the Ge-Ku-van der Pol system is a chaotic system.

We find that the error dynamic without controller always exists in first quadrant as shown in Fig. 4.13.

Our aim is $\lim_{t \rightarrow \infty} e = 0$. We obtain the error dynamics.

$$\lim_{t \rightarrow \infty} e_i = \lim_{t \rightarrow \infty} [x_i' - y_i' + z] = 0, \quad i = 1, 2, 3 \quad (4.33)$$

$$\begin{cases} \dot{e}_1 = x_2 - 350 - y_2 + 50 - u_1 + z_2 \\ \dot{e}_2 = -a(x_2 - 350) - (x_1 - 350)\{b[c - (x_1 - 350)^2] + d(x_2 - 350)(x_3 - 350)\} \\ + a(y_2 - 50) + (y_1 - 50)\{\hat{b}[\hat{c} - (y_1 - 50)^2] + d(y_2 - 50)(y_3 - 50)\} - u_2 \\ - mz_2 - z_3[n(q - z_1^2) + wz_3] \\ \dot{e}_3 = -[g + h(x_1 - 350)](x_3 - 350) + l(x_2 - 350) + p(x_1 - 350)(x_3 - 350) \\ + [\widetilde{g} + \widetilde{h}(y_1 - 50)](y_3 - 50) - \hat{l}(y_2 - 50) - \widehat{p}(y_1 - 50)(y_3 - 50) - u_3 \\ - sz_3 + f(1 - z_3^2)z_2 + rz_1 \end{cases} \quad (4.34)$$

where $\tilde{a} = a - \hat{a}$, $\tilde{b} = b - \hat{b}$, $\tilde{c} = c - \hat{c}$, $\tilde{d} = d - \hat{d}$, $\tilde{g} = g - \hat{g}$, $\tilde{h} = h - \hat{h}$, $\tilde{l} = l - \hat{l}$,

$\tilde{p} = p - \hat{p}$, and a , \hat{b} , \hat{c} , d , g , h , \hat{l} , p , are estimates of uncertain parameters a , b , c , d , g , h , l and p respectively.

Using different translation pragmatical synchronization by stability theory of partial region, we can choose a Lyapunov function in the form of a positive definite function in first quadrant:

$$V = e_1 + e_2 + e_3 + a + \tilde{b} + \tilde{c} + d + g + h + \tilde{l} + p \quad (4.35)$$

Its time derivative is

$$\begin{aligned} \dot{V} &= \dot{e}_1 + \dot{e}_2 + \dot{e}_3 + \dot{\tilde{a}} + \dot{\tilde{b}} + \dot{\tilde{c}} + \dot{\tilde{d}} + \dot{\tilde{g}} + \dot{\tilde{h}} + \dot{\tilde{l}} + \dot{\tilde{p}} \\ &= [x_2 - 350 - y_2 + 50 - u_1 + z_2] \\ &\quad - a(x_2 - 350) - (x_1 - 350)\{b[c - (x_1 - 350)^2] + d(x_2 - 350)(x_3 - 350)\} \\ &\quad + a(y_2 - 50) + (y_1 - 50)\{\hat{b}[\hat{c} - (y_1 - 50)^2] + d(y_2 - 50)(y_3 - 50)\} - u_2 \\ &\quad - mz_2 - z_3[n(q - z_1^2) + wz_3] \\ &\quad + \{-[g + h(x_1 - 350)](x_3 - 350) + l(x_2 - 350) + p(x_1 - 350)(x_3 - 350) \\ &\quad + [\widetilde{g} + \widetilde{h}(y_1 - 50)](y_3 - 50) - \hat{l}(y_2 - 50) - \widehat{p}(y_1 - 50)(y_3 - 50) - u_3 \\ &\quad - sz_3 + f(1 - z_3^2)z_2 + rz_1\} + \dot{\tilde{a}} + \dot{\tilde{b}} + \dot{\tilde{c}} + \dot{\tilde{d}} + \dot{\tilde{g}} + \dot{\tilde{h}} + \dot{\tilde{l}} + \dot{\tilde{p}} \end{aligned} \quad (4.36)$$

Choose

$$\begin{cases} \dot{\tilde{a}} = -\dot{\hat{a}} = -\tilde{a}e_2 \\ \dot{\tilde{b}} = -\dot{\hat{b}} = -\tilde{b}e_2 \\ \dot{\tilde{c}} = -\dot{\hat{c}} = -\tilde{c}e_2 \\ \dot{\tilde{d}} = -\dot{\hat{d}} = -\tilde{d}e_2 \\ \dot{\tilde{g}} = -\dot{\hat{g}} = -\tilde{g}e_3 \\ \dot{\tilde{h}} = -\dot{\hat{h}} = -\tilde{h}e_3 \\ \dot{\tilde{l}} = -\dot{\hat{l}} = -\tilde{l}e_3 \\ \dot{\tilde{p}} = -\dot{\hat{p}} = -\tilde{p}e_3 \end{cases} \quad (4.37)$$

$$\begin{cases} u_1 = x_2 - 350 - y_2 + 50 + z_2 + e_1 \\ u_2 = -a(x_2 - 350) - (x_1 - 350)\{b[c - (x_1 - 350)^2] + d(x_2 - 350)(x_3 - 350)\} \\ + a(y_2 - 50) + (y_1 - 50)\{\hat{b}[\hat{c} - (y_1 - 50)^2] + d(y_2 - 50)(y_3 - 50)\} \\ - mz_2 - z_3[n(q - z_1^2) + wz_3] + e_2 - ae_2 - \tilde{b}e_2 - \tilde{c}e_2 - de_2 \\ u_3 = -[g + h(x_1 - 350)](x_3 - 350) + l(x_2 - 350) + p(x_1 - 350)(x_3 - 350) \\ + [\widehat{g} + \widehat{h}(y_1 - 50)](y_3 - 50) - \hat{l}(y_2 - 50) - \hat{p}(y_1 - 50)(y_3 - 50) \\ - sz_3 + f(1 - z_3^2)z_2 + rz_1 + e_3 - \tilde{g}e_3 - \tilde{h}e_3 - \tilde{l}e_3 - \tilde{p}e_3 \end{cases} \quad (4.38)$$

We obtain

$$\dot{V} = -e_1 - e_2 - e_3 < 0 \quad (4.39)$$

which is a negative semi-definite function of $e_1, e_2, e_3, \tilde{a}, \tilde{b}, \tilde{c}, \tilde{d}, \tilde{g}, \tilde{h}, \tilde{l}, \tilde{p}$, in the first quadrant. The Lyapunov asymptotical stability theorem is not satisfied.

We can not obtain that common origin of error dynamics (4.34) and parameter dynamics (4.37) is asymptotically stable. By pragmatistical asymptotically stability theorem, D is a 11-manifold, $n=11$ and the number of error state variables $p=3$. When $e_1 = e_2 = e_3 = 0$ and $\tilde{a}, \tilde{b}, \tilde{c}, \tilde{d}, \tilde{g}, \tilde{h}, \tilde{l}, \tilde{p}$, take arbitrary values, $\dot{V} = 0$, so X is of 3 dimensions i.e. $p=3, m=n-p=11-3=8, m+1 < n$ is satisfied. According to the pragmatistical asymptotically stability theorem, error vector e approaches zero and the estimated parameters also approach the uncertain parameters. The equilibrium point is pragmatically asymptotically stable. Under the assumption of equal probability, it is actually asymptotically stable. The simulation results are shown in Figs. 4.14-4.17.

4.4 Summary

In this chapter, a new strategy to achieve chaos synchronization by the different translation pragmatical synchronization using stability theory of partial region is proposed. The pragmatical asymptotical stability theorem fills the vacancy between the actual asymptotical stability and mathematical asymptotical stability, the conditions of the Lyapunov function for pragmatical asymptotical stability are lower than that for traditional asymptotical stability. By using the different translation pragmatical synchronization by stability theory of partial region, with the same conditions for Lyapunov function, $V > 0$, $\dot{V} \leq 0$, as that in current scheme of adaptive synchronization, we not only obtain the generalized synchronization of chaotic systems but also prove strictly that the estimated parameters approach the uncertain values and the Lyapunov function is simple linear homogeneous function for error states, the controllers are more simple and have less simulation error because they are in lower degree than that of traditional controllers.

It is important to note that K_1 , K_2 are not arbitrary, two proper values must chosen to make that the error dynamics always in first quadrant, so give two more insurances for secret communication than other synchronization methods.

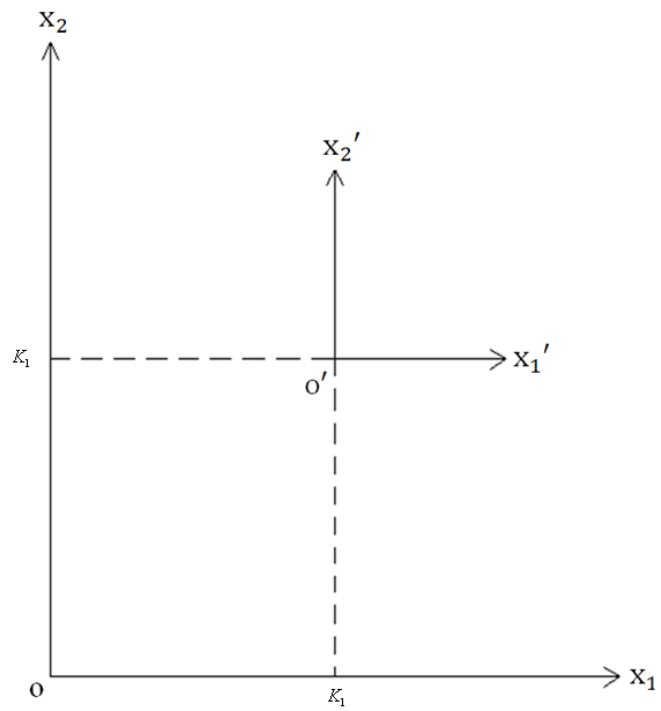


Fig. 4.1 Coordinate translation.

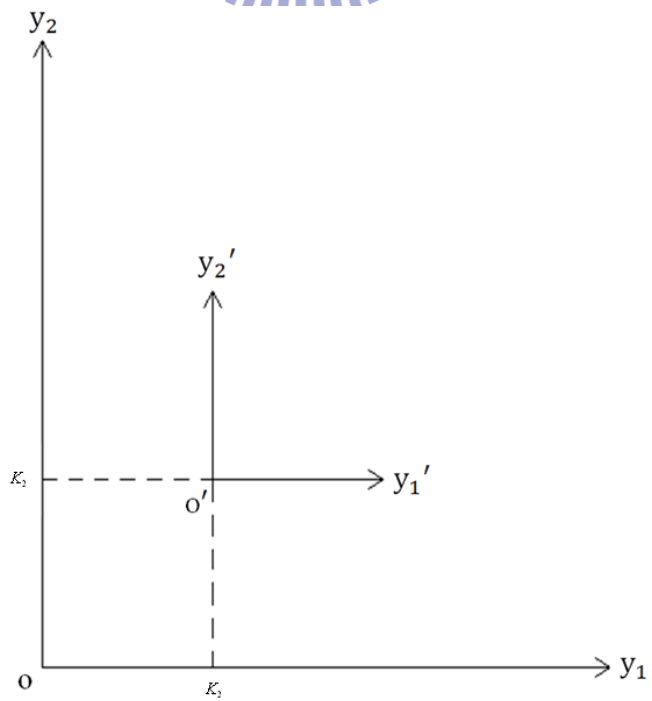


Fig. 4.2 Coordinate translation.

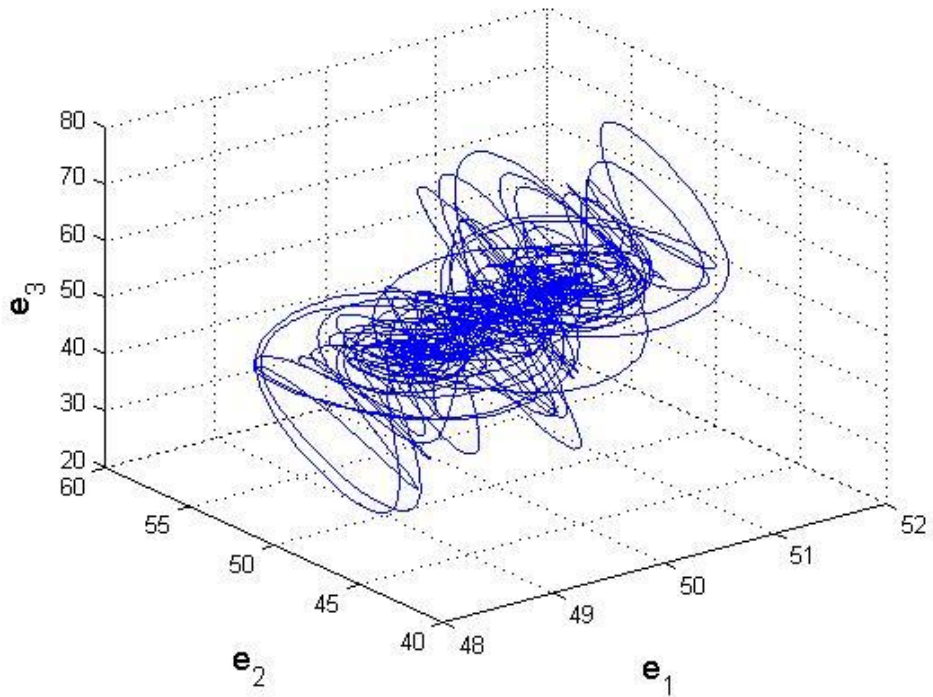


Fig. 4.3 Phase portrait of the error dynamic for Case 1.

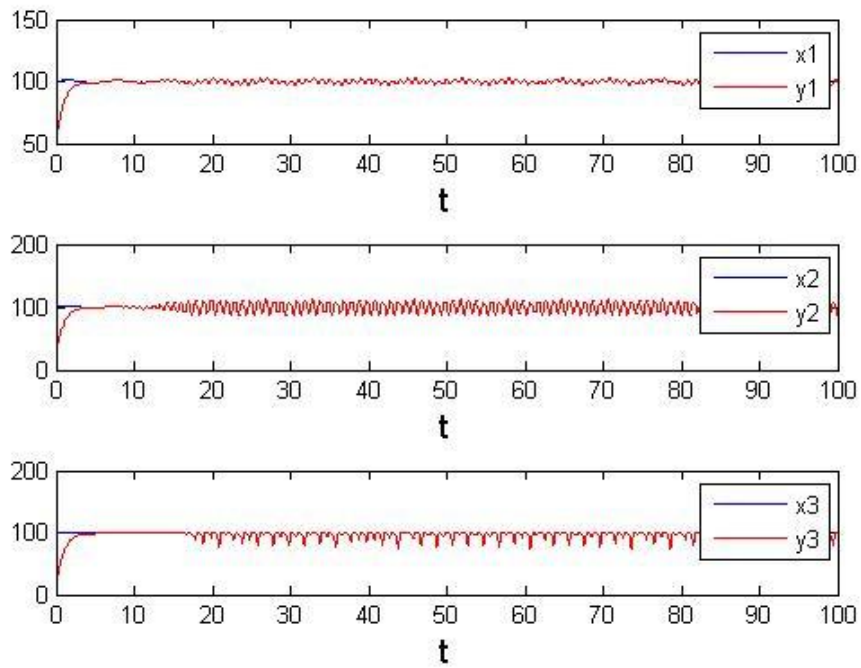


Fig. 4.4 Time histories of x_i, y_i for Case 1.

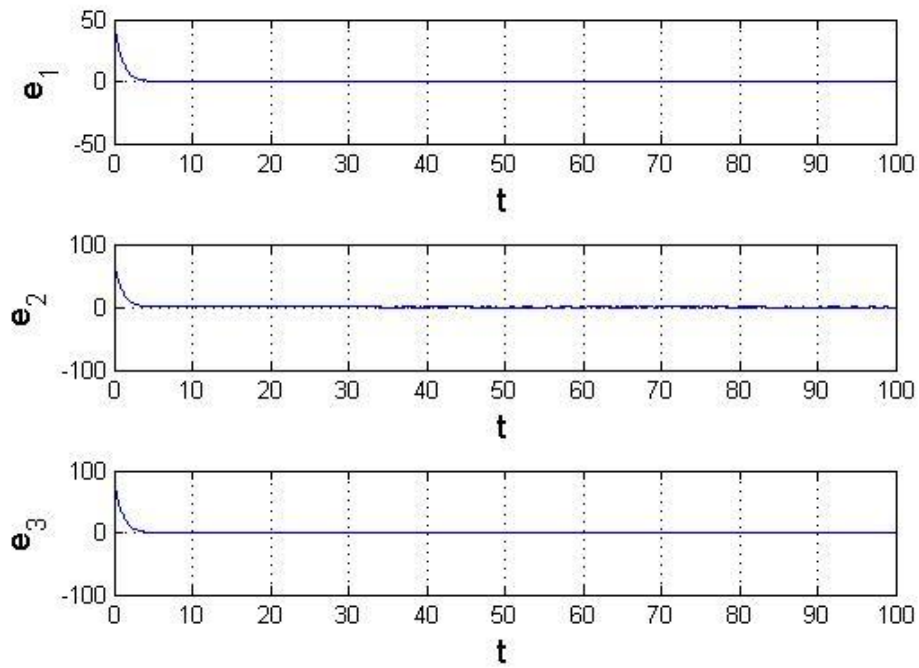


Fig. 4.5 Time histories of errors for Case 1.

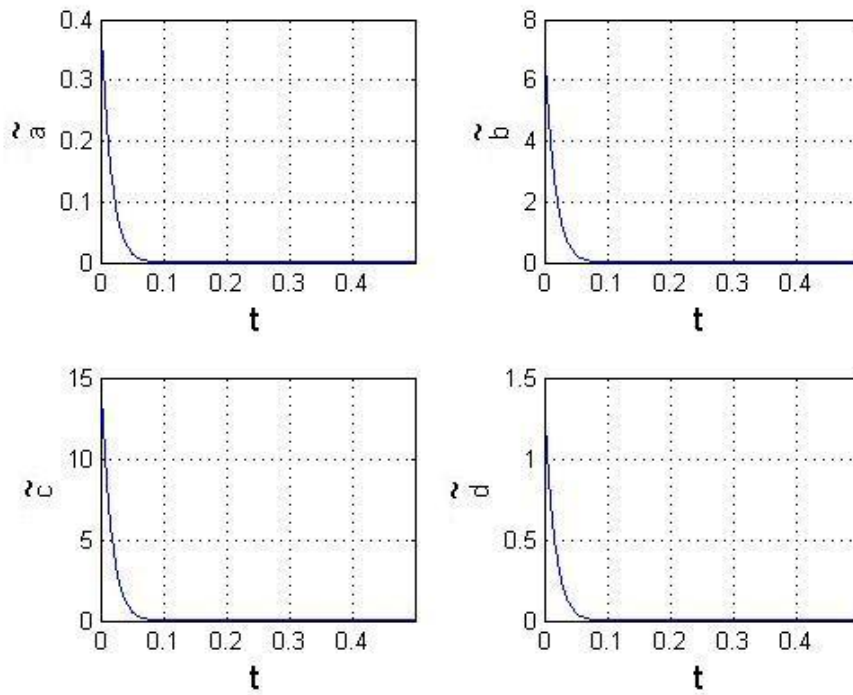


Fig. 4.6 Time histories of parameter errors for Case 1.

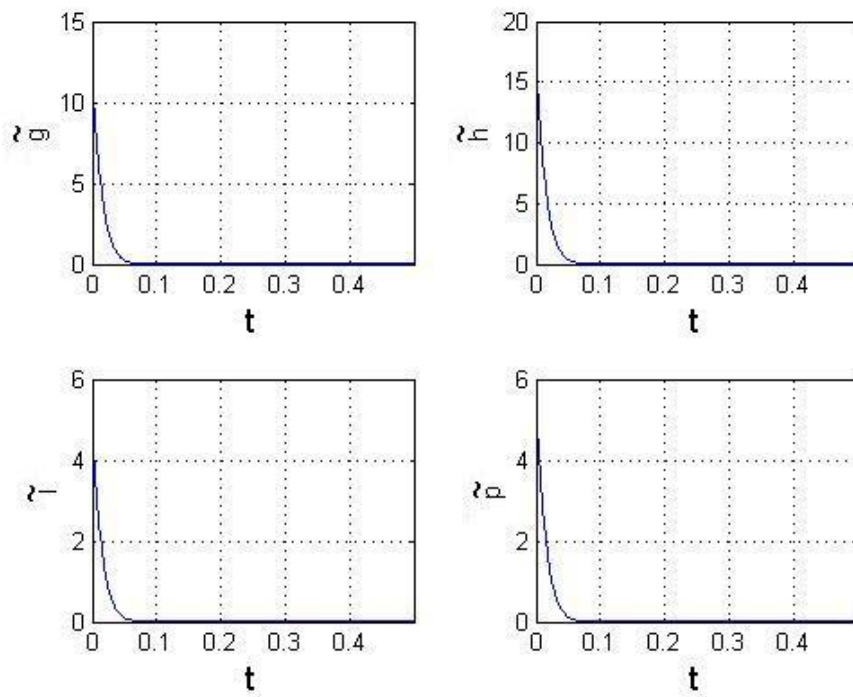


Fig. 4.7 Time histories of parameter errors for Case 1.

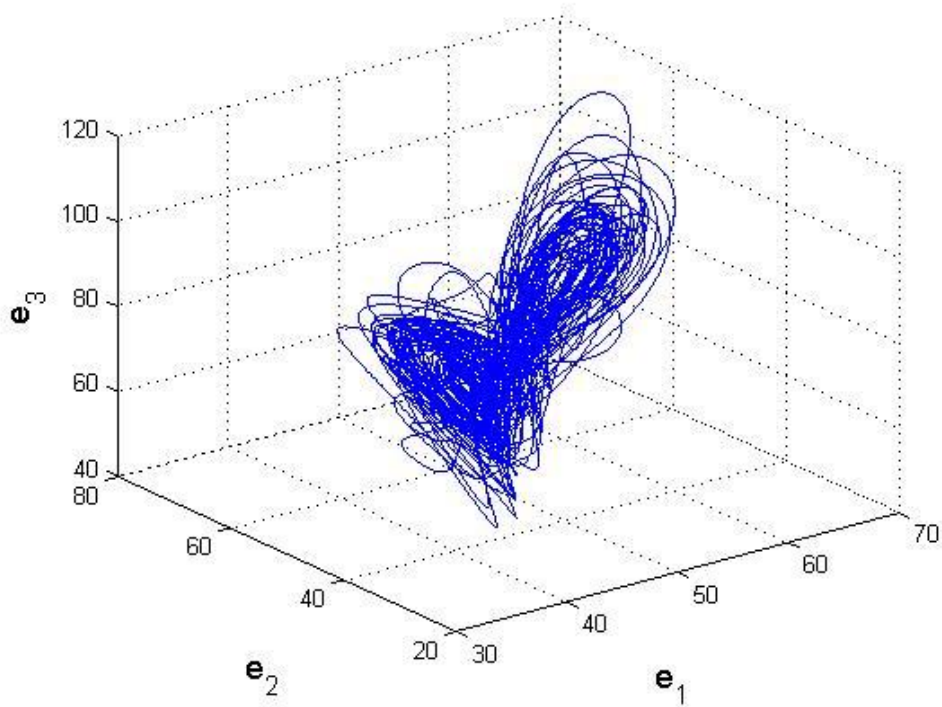


Fig. 4.8 Phase portrait of the error dynamic for Case 2.

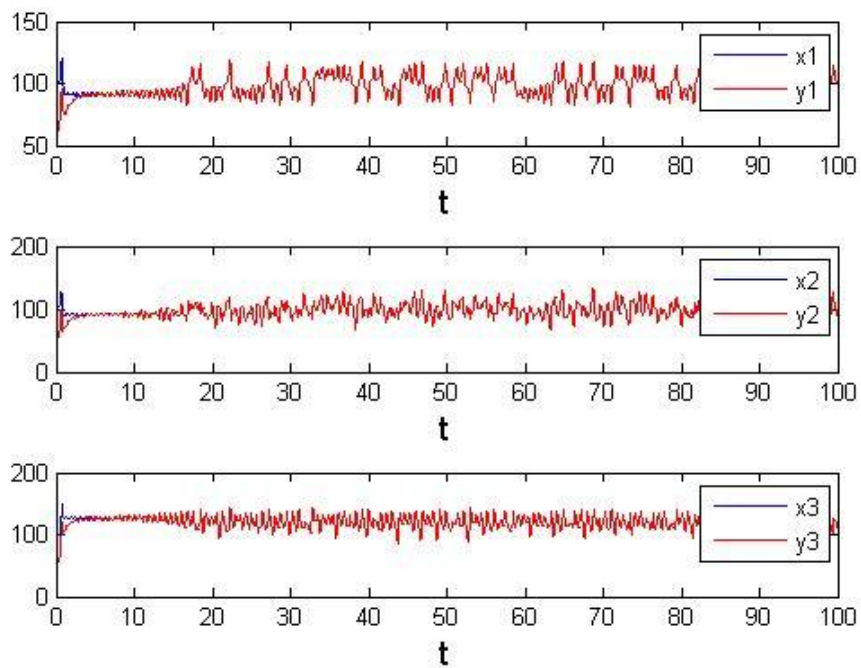


Fig. 4.9 Time histories of x_i, y_i for Case 2.

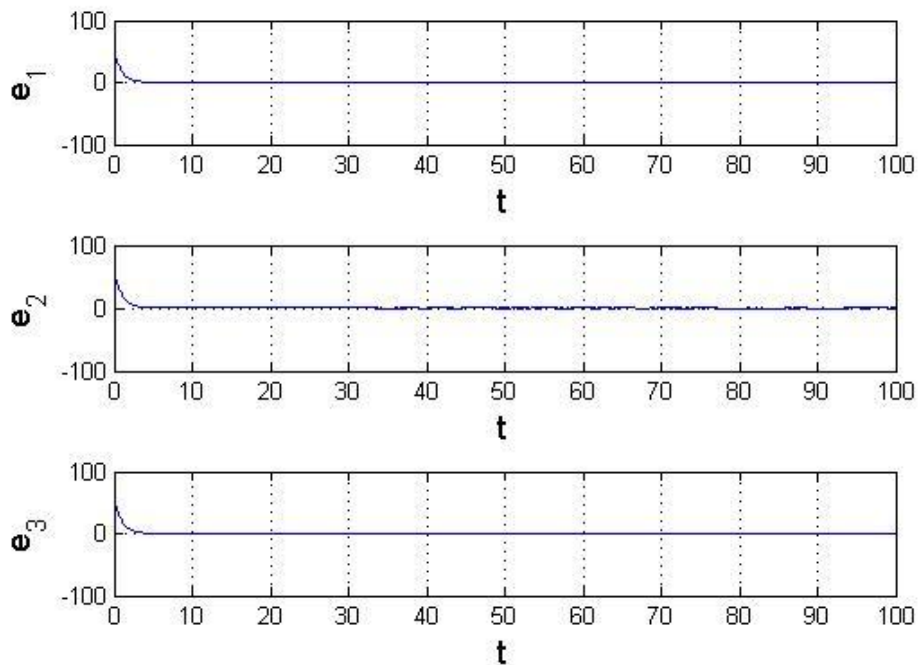


Fig. 4.10 Time histories of errors for Case 2.

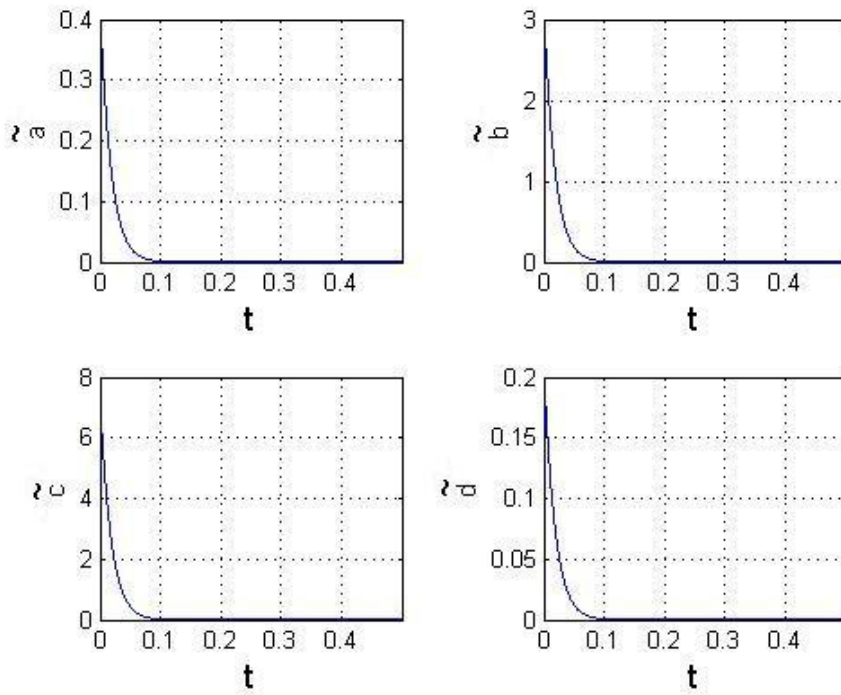


Fig. 4.11 Time histories of parameter errors for Case 2.

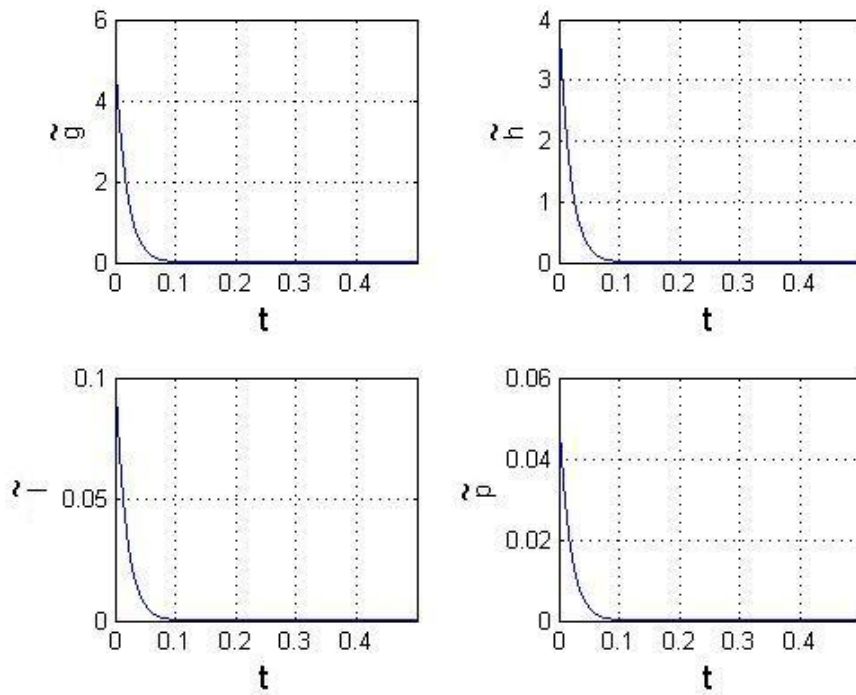


Fig. 4.12 Time histories of parameter errors for Case 2.

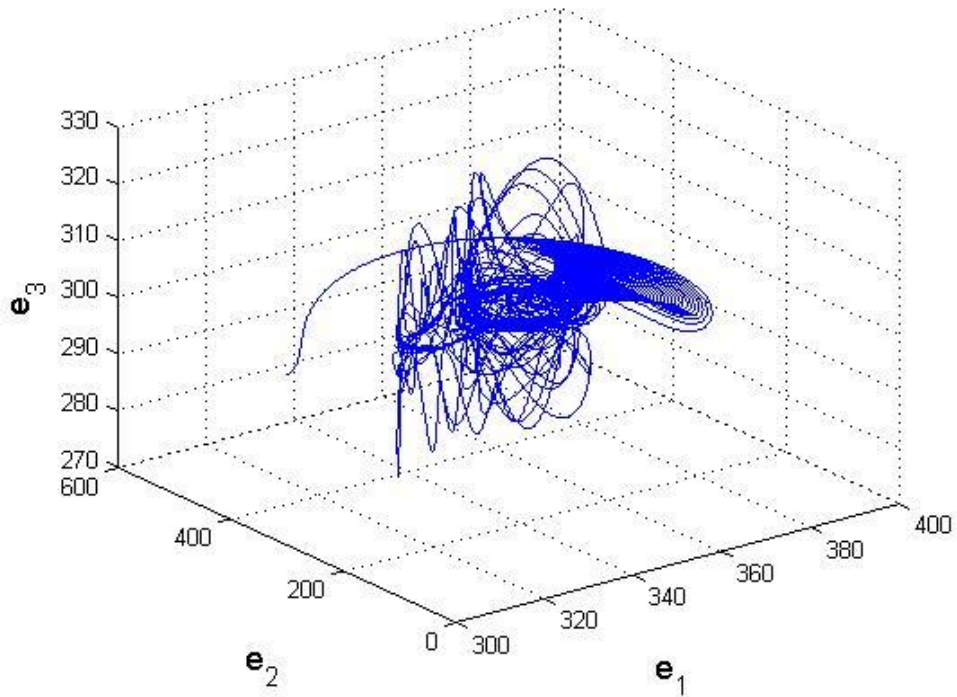


Fig. 4.13 Phase portrait of the error dynamic for Case 3.

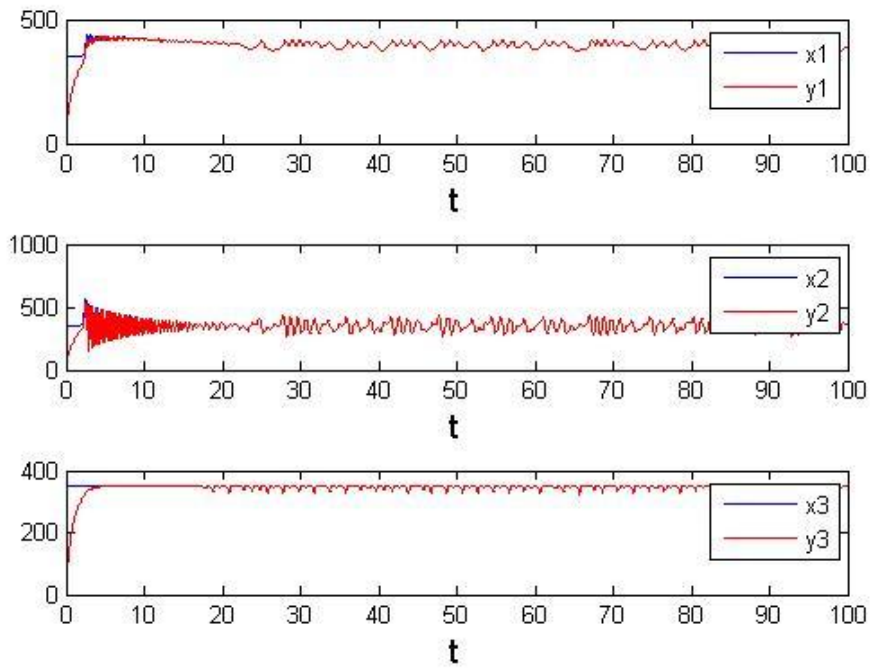


Fig. 4.14 Time histories of x_i , y_i for Case 3.

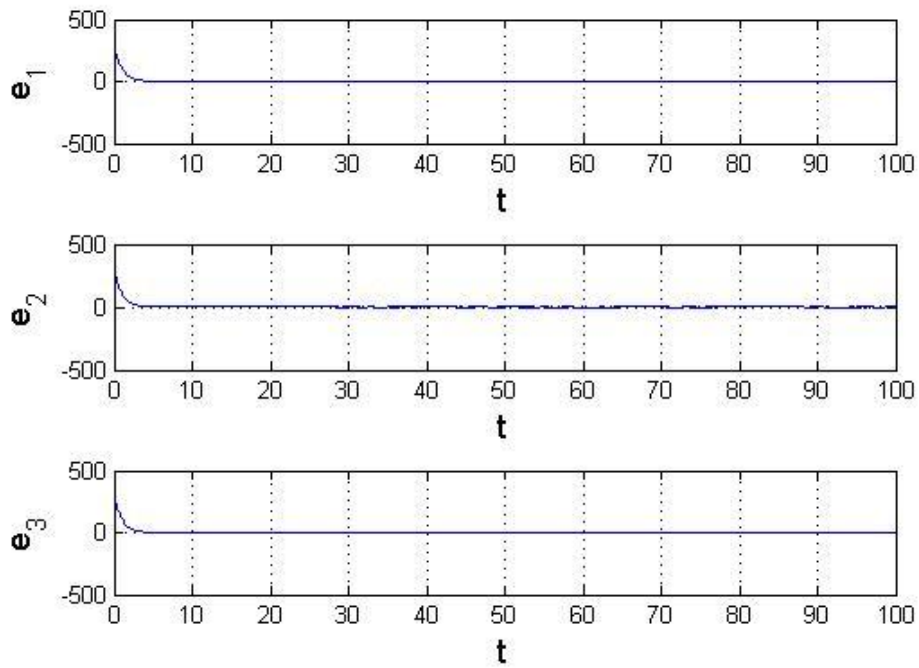


Fig. 4.15 Time histories of errors for Case 3.

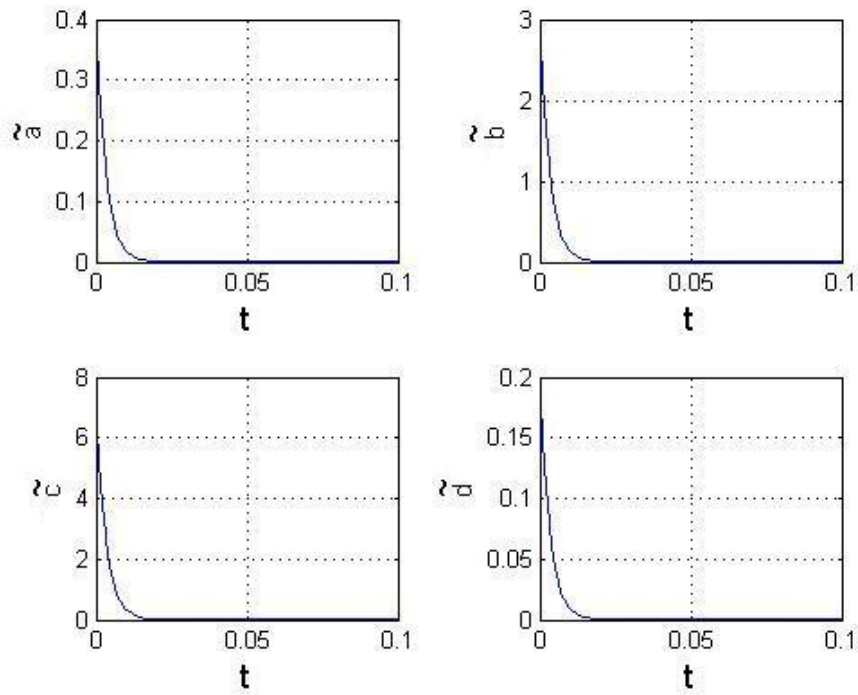


Fig. 4.16 Time histories of parameter errors for Case 3.

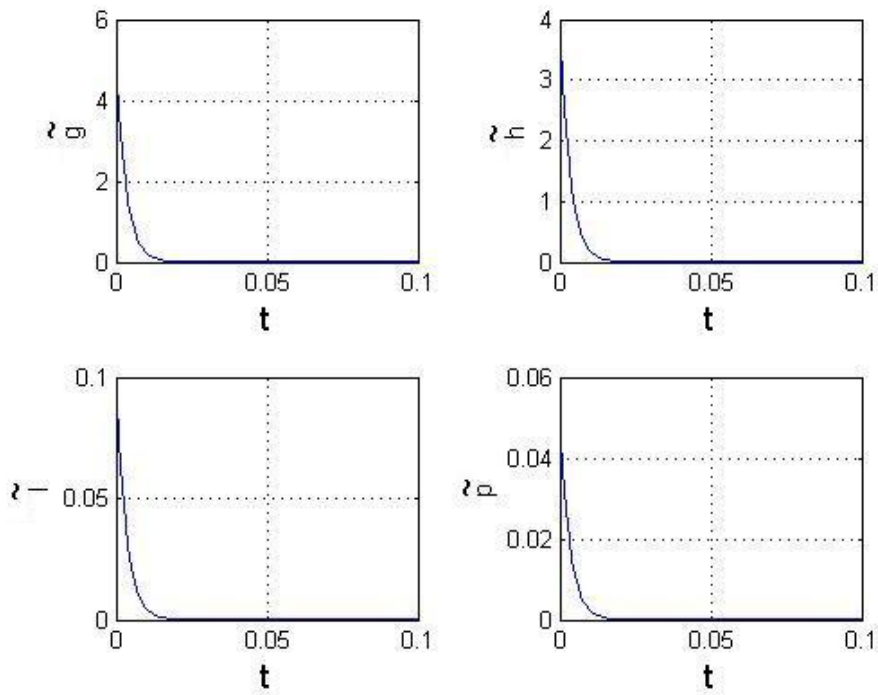


Fig. 4.17 Time histories of parameter errors for Case 3.



Chapter 5

Multiple Symplectic Synchronization for Ge-Ku-Mathieu System

5.1 Preliminary

In this Chapter, a new type of synchronization, multiple symplectic synchronization is studied. Symplectic synchronization and double symplectic synchronization are special cases of the multiple symplectic synchronization. When the double symplectic functions is extended to a more general form, $\mathbf{G}(\mathbf{x}, \mathbf{y}, z, \dots, w, t) = \mathbf{F}(\mathbf{x}, \mathbf{y}, z, \dots, w, t)$, it is called “multiple symplectic synchronization”. The multiple symplectic synchronization may be applied to increase the security of secret communication due to the complexity of its synchronization form.



5.2 Multiple Symplectic Synchronization Scheme

Generalized synchronization refers to a functional relation between the state vectors of master and of slave, i.e. $\mathbf{y} = \mathbf{F}(\mathbf{x}, t)$, where \mathbf{x} and \mathbf{y} are the state vectors of master and slave. Recently, generalized synchronization is extended to a more general form, $\mathbf{y} = \mathbf{F}(\mathbf{x}, \mathbf{y}, t)$. This means that the final desired state \mathbf{y} of the “slave” system not only depends upon the “master” system state \mathbf{x} but also depends upon the state \mathbf{y} itself. Therefore the “slave” system is not traditional pure slave obeying the master system completely but plays a role to determine the final desired state of the “slave” system. This kind of synchronization, is called “symplectic synchronization”, and the “master” system is called Partner A, the “slave” system is called Partner B.

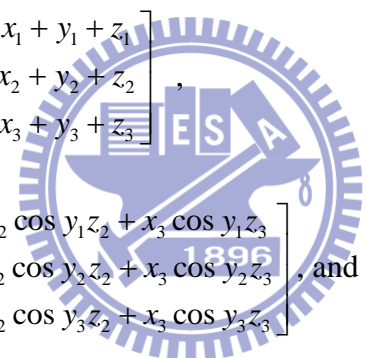
Since the symplectic functions are presented at both the right hand side and the left hand side of the equality, it is called double symplectic synchronization,

$\mathbf{G}(\mathbf{x}, \mathbf{y}, t) = \mathbf{F}(\mathbf{x}, \mathbf{y}, t)$. Where \mathbf{x}, \mathbf{y} are state vectors of Partner A and Partner B, respectively, $\mathbf{G}(\mathbf{x}, \mathbf{y}, t)$ and $\mathbf{F}(\mathbf{x}, \mathbf{y}, t)$ are given vector functions of \mathbf{x}, \mathbf{y} and time.

When the double symplectic functions is extended to a more general form, $\mathbf{G}(\mathbf{x}, \mathbf{y}, z, \dots, w, t) = \mathbf{F}(\mathbf{x}, \mathbf{y}, z, \dots, w, t)$, it is called “multiple symplectic synchronization”. Where $\mathbf{x}, \mathbf{y}, z, \dots, w$ are state vectors of Partner A and Partner B, respectively, $\mathbf{G}(\mathbf{x}, \mathbf{y}, z, \dots, w, t)$ and $\mathbf{F}(\mathbf{x}, \mathbf{y}, z, \dots, w, t)$ are given vector functions of $\mathbf{x}, \mathbf{y}, z, \dots, w$ and time.

5.3 Synchronization of Three Different Chaotic Systems

Case 1.



Define $G(\mathbf{x}, \mathbf{y}, z, t) = \begin{bmatrix} x_1 + y_1 + z_1 \\ x_2 + y_2 + z_2 \\ x_3 + y_3 + z_3 \end{bmatrix}$, and our goal is to achieve the

$\mathbf{F}(\mathbf{x}, \mathbf{y}, z, t) = \begin{bmatrix} x_1 \cos y_1 z_1 + x_2 \cos y_1 z_2 + x_3 \cos y_1 z_3 \\ x_1 \cos y_2 z_1 + x_2 \cos y_2 z_2 + x_3 \cos y_2 z_3 \\ x_1 \cos y_3 z_1 + x_2 \cos y_3 z_2 + x_3 \cos y_3 z_3 \end{bmatrix}$

multiple symplectic synchronization $G(\mathbf{x}, \mathbf{y}, z, t) = \mathbf{F}(\mathbf{x}, \mathbf{y}, z, t)$.

Consider the Chen system is described by

$$\begin{aligned} \dot{x}_1 &= m(x_2 - x_1), \\ \dot{x}_2 &= (w - m)x_1 - x_1 x_3 + wx_2, \\ \dot{x}_3 &= x_1 x_2 - nx_3, \end{aligned} \tag{5.1}$$

where $m = 35, n = 3, w = 27.2$ and the initial condition is

$x_1(0) = 0.5, x_2(0) = 0.26, x_3(0) = 0.35$. The chaotic attractor of the Chen system is

shown in Fig. 5.1.

The Lorenz system is described by

$$\begin{aligned} \dot{z}_1 &= r(z_2 - z_1), \\ \dot{z}_2 &= z_1(s - z_3) - z_2, \\ \dot{z}_3 &= z_1 z_2 - fz_3, \end{aligned} \tag{5.2}$$

where $r = 10, s = 28, f = \frac{8}{3}$ and the initial condition is

$z_1(0) = 0.01, z_2(0) = 0.01, z_3(0) = 0.01$. The chaotic attractor of the Lorenz system is

shown in Fig. 5.2.

The controlled Ge-Ku-Mathieu(GKM) system is described by

$$\begin{aligned}\dot{y}_1 &= y_2 + u_1, \\ \dot{y}_2 &= -ay_2 - y_1 \left[b(c - y_1^2) + dy_2 y_3 \right] + u_2, \\ \dot{y}_3 &= -(g + hy_1)y_3 + ly_2 + py_1 y_3 + u_3,\end{aligned}\tag{5.3}$$

where $a = -0.6, b = 5, c = 11, d = 0.3, g = 8, h = 10, l = 0.5, p = 0.2$, $\mathbf{u} = [u_1, u_2, u_3]^T$ is

the controller, and the initial condition is $y_1(0) = 0.01, y_2(0) = 0.01, y_3(0) = 0.01$.

Thus we design the controller as

$$\begin{aligned}u_1 &= m(x_2 - x_1)z_1 \cos y_1 + x_1 \cos y_1 r(z_2 - z_1) - x_1 z_1 y_2 \sin y_1 + z_2 \cos y_1 ((w - m)x_1 - x_1 x_3 + wx_2) \\ &\quad + x_2 \cos y_1 (z_1(s - z_3) - z_2) - x_2 z_2 y_2 \sin y_1 + (x_1 x_2 - nx_3)z_3 \cos y_1 + x_3 \cos y_1 (z_1 z_2 - fz_3) \\ &\quad - x_3 z_3 y_2 \sin y_1 - m(x_2 - x_1) - y_2 - r(z_2 - z_1) + e_1\end{aligned}$$

$$\begin{aligned}u_2 &= m(x_2 - x_1)z_1 \cos y_2 + x_1 \cos y_2 r(z_2 - z_1) - x_1 z_1 (-ay_2 - y_1(b(c - y_1^2) + dy_2 y_3)) \sin y_2 \\ &\quad + z_2 \cos y_2 ((w - m)x_1 - x_1 x_3 + wx_2) + x_2 \cos y_2 (z_1(s - z_3) - z_2) \\ &\quad - x_2 z_2 (-ay_2 - y_1(b(c - y_1^2) + dy_2 y_3)) \sin y_2 + (x_1 x_2 - nx_3)z_3 \cos y_2 + x_3 \cos y_2 (z_1 z_2 - fz_3) \\ &\quad - x_3 z_3 \sin y_2 (-ay_2 - y_1(b(c - y_1^2) + dy_2 y_3)) - ((w - m)x_1 - x_1 x_3 + wx_2) \\ &\quad - (-ay_2 - y_1(b(c - y_1^2) + dy_2 y_3)) - (z_1(s - z_3) - z_2) + e_2\end{aligned}$$

$$\begin{aligned}u_3 &= m(x_2 - x_1)z_1 \cos y_3 + x_1 \cos y_3 r(z_2 - z_1) - x_1 z_1 (-(g + hy_1)y_3 + ly_2 + py_1 y_3) \sin y_3 \\ &\quad + z_2 \cos y_3 ((w - m)x_1 - x_1 x_3 + wx_2) + x_2 \cos y_3 (z_1(s - z_3) - z_2) \\ &\quad - x_2 z_2 (-(g + hy_1)y_3 + ly_2 + py_1 y_3) \sin y_3 + (x_1 x_2 - nx_3)z_3 \cos y_3 + x_3 \cos y_3 (z_1 z_2 - fz_3) \\ &\quad - x_3 z_3 \sin y_3 (-(g + hy_1)y_3 + ly_2 + py_1 y_3) - (x_1 x_2 - nx_3) \\ &\quad - (-(g + hy_1)y_3 + ly_2 + py_1 y_3) - (z_1 z_2 - fz_3) + e_3\end{aligned}$$

The **Theorem** in Chapter 3 is satisfied and the multiple symplectic synchronization is achieved. The phase portrait of the controlled Ge-Ku-Mathieu

system and the time histories of $G(\mathbf{x}, \mathbf{y}, z, t)$ and $\mathbf{F}(\mathbf{x}, \mathbf{y}, z, t)$ and the time histories of the state errors are shown in Fig. 5.3 and Fig. 5.4 and Fig. 5.5, respectively.

Case 2.

$$\text{Define } G(\mathbf{x}, \mathbf{y}, z, t) = \begin{bmatrix} x_1 + y_1 + z_1 \\ x_2 + y_2 + z_2 \\ x_3 + y_3 + z_3 \end{bmatrix},$$

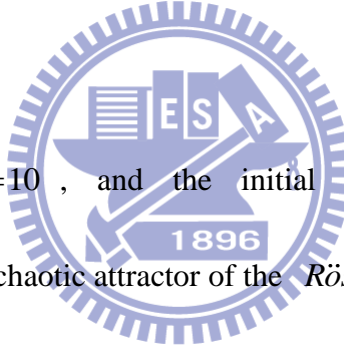
$$\mathbf{F}(\mathbf{x}, \mathbf{y}, z, t) = \begin{bmatrix} x_1 \sin y_1 z_1 + x_2 \sin y_1 z_2 + x_3 \sin y_1 z_3 \\ x_1 \sin y_2 z_1 + x_2 \sin y_2 z_2 + x_3 \sin y_2 z_3 \\ x_1 \sin y_3 z_1 + x_2 \sin y_3 z_2 + x_3 \sin y_3 z_3 \end{bmatrix}, \text{ and our goal is to achieve the}$$

multiple symplectic synchronization $G(\mathbf{x}, \mathbf{y}, z, t) = \mathbf{F}(\mathbf{x}, \mathbf{y}, z, t)$.

Consider the *Rössler* system is described by

$$\begin{aligned} \dot{x}_1 &= -(x_2 + x_3), \\ \dot{x}_2 &= x_1 + mx_2, \\ \dot{x}_3 &= n + x_1 x_3 - wx_3, \end{aligned} \tag{5.4}$$

where $m = 0.15, n = 0.2, w = 10$, and the initial conditions are $x_1(0) = 2$, $x_2(0) = 2.4$, $x_3(0) = 5$. The chaotic attractor of the *Rössler* system is shown in Fig. 5.6.



The Lorenz system is described by

$$\begin{aligned} \dot{z}_1 &= r(z_2 - z_1), \\ \dot{z}_2 &= z_1(s - z_3) - z_2, \\ \dot{z}_3 &= z_1 z_2 - fz_3, \end{aligned} \tag{5.5}$$

where $r = 10, s = 28, f = \frac{8}{3}$ and the initial condition is

$$z_1(0) = 0.01, z_2(0) = 0.01, z_3(0) = 0.01.$$

The controlled Ge-Ku-Mathieu(GKM) system is described by

$$\begin{aligned} \dot{y}_1 &= y_2 + u_1, \\ \dot{y}_2 &= -ay_2 - y_1 \left[b(c - y_1^2) + dy_2 y_3 \right] + u_2, \\ \dot{y}_3 &= -(g + hy_1) y_3 + ly_2 + py_1 y_3 + u_3, \end{aligned} \tag{5.6}$$

where $a = -0.6, b = 5, c = 11, d = 0.3, g = 8, h = 10, l = 0.5, p = 0.2$, $\mathbf{u} = [u_1, u_2, u_3]^T$ is

the controller, and the initial condition is $y_1(0) = 0.01, y_2(0) = 0.01, y_3(0) = 0.01$.

Thus we design the controller as

$$\begin{aligned} u_1 = & -(x_2 + x_3)z_1 \sin y_1 + x_1 \sin y_1 r(z_2 - z_1) + x_1 z_1 y_2 \cos y_1 + z_2 \sin y_1 (x_1 + mx_2) \\ & + x_2 \sin y_1 (z_1(s - z_3) - z_2) + x_2 z_2 y_2 \cos y_1 + (n + x_1 x_3 - wx_3)z_3 \sin y_1 + x_3 \sin y_1 (z_1 z_2 - fz_3) \\ & + x_3 z_3 y_2 \cos y_1 - (-(x_2 + x_3)) - y_2 - r(z_2 - z_1) + e_1 \end{aligned}$$

$$\begin{aligned} u_2 = & -(x_2 + x_3)z_1 \sin y_2 + x_1 \sin y_2 r(z_2 - z_1) + x_1 z_1 (-ay_2 - y_1(b(c - y_1^2) + dy_2 y_3)) \cos y_2 \\ & + z_2 \sin y_2 (x_1 + mx_2) + x_2 \sin y_2 (z_1(s - z_3) - z_2) \\ & + x_2 z_2 (-ay_2 - y_1(b(c - y_1^2) + dy_2 y_3)) \cos y_2 + (n + x_1 x_3 - wx_3)z_3 \sin y_2 + x_3 \sin y_2 (z_1 z_2 - fz_3) \\ & + x_3 z_3 \cos y_2 (-ay_2 - y_1(b(c - y_1^2) + dy_2 y_3)) - (x_1 + mx_2) \\ & - (-ay_2 - y_1(b(c - y_1^2) + dy_2 y_3)) - (z_1(s - z_3) - z_2) + e_2 \end{aligned}$$

$$\begin{aligned} u_3 = & -(x_2 + x_3)z_1 \sin y_3 + x_1 \sin y_3 r(z_2 - z_1) + x_1 z_1 (-(g + hy_1)y_3 + ly_2 + py_1 y_3) \cos y_3 \\ & + z_2 \sin y_3 (x_1 + mx_2) + x_2 \sin y_3 (z_1(s - z_3) - z_2) \\ & + x_2 z_2 (-(g + hy_1)y_3 + ly_2 + py_1 y_3) \cos y_3 + (n + x_1 x_3 - wx_3)z_3 \sin y_3 + x_3 \sin y_3 (z_1 z_2 - fz_3) \\ & + x_3 z_3 \cos y_3 (-(g + hy_1)y_3 + ly_2 + py_1 y_3) - (n + x_1 x_3 - wx_3) \\ & - (-(g + hy_1)y_3 + ly_2 + py_1 y_3) - (z_1 z_2 - fz_3) + e_3 \end{aligned}$$

The **Theorem** in Chapter 3 is satisfied and the multiple symplectic synchronization is achieved. The phase portrait of the controlled Ge-Ku-Mathieu system and the time histories of $G(\mathbf{x}, \mathbf{y}, z, t)$ and $\mathbf{F}(\mathbf{x}, \mathbf{y}, z, t)$ and the time histories of the state errors are shown in Fig. 5.7 and Fig. 5.8 and Fig. 5.9, respectively.

Case 3.

$$\text{Define } G(\mathbf{x}, \mathbf{y}, z, t) = \begin{bmatrix} x_1 + y_1 + z_1 \\ x_2 + y_2 + z_2 \\ x_3 + y_3 + z_3 \end{bmatrix}, \quad \mathbf{F}(\mathbf{x}, \mathbf{y}, z, t) = \begin{bmatrix} x_1 y_1 z_1 + x_2 y_1 z_2 + x_3 y_1 z_3 \\ x_1 y_2 z_1 + x_2 y_2 z_2 + x_3 y_2 z_3 \\ x_1 y_3 z_1 + x_2 y_3 z_2 + x_3 y_3 z_3 \end{bmatrix},$$

and our goal is to achieve the multiple symplectic synchronization

$$G(\mathbf{x}, \mathbf{y}, z, t) = \mathbf{F}(\mathbf{x}, \mathbf{y}, z, t).$$

Consider the spratt system is described by

$$\begin{aligned}\dot{x}_1 &= x_2 x_3, \\ \dot{x}_2 &= x_1^2 - x_2, \\ \dot{x}_3 &= 1 - mx_1,\end{aligned}\tag{5.7}$$

where $m = 4$ and the initial conditions are $x_1(0) = -1, x_2(0) = -1, x_3(0) = -1$. The

chaotic attractor of the spratt system is shown in Fig. 5.10.

The Lorenz system is described by

$$\begin{aligned}\dot{z}_1 &= r(z_2 - z_1), \\ \dot{z}_2 &= z_1(s - z_3) - z_2, \\ \dot{z}_3 &= z_1 z_2 - fz_3,\end{aligned}\tag{5.8}$$

where $r = 10, s = 28, f = \frac{8}{3}$ and the initial condition is

$$z_1(0) = 0.01, z_2(0) = 0.01, z_3(0) = 0.01.$$

The controlled Ge-Ku-Mathieu(GKM) system is described by

$$\begin{aligned}\dot{y}_1 &= y_2 + u_1, \\ \dot{y}_2 &= -ay_2 - y_1 \left[b(c - y_1^2) + dy_2 y_3 \right] + u_2, \\ \dot{y}_3 &= -(g + hy_1)y_3 + ly_2 + py_1 y_3 + u_3,\end{aligned}\tag{5.9}$$

where $a = -0.6, b = 5, c = 11, d = 0.3, g = 8, h = 10, l = 0.5, p = 0.2$, $\mathbf{u} = [u_1, u_2, u_3]^T$ is

the controller, and the initial condition is $y_1(0) = 0.01, y_2(0) = 0.01, y_3(0) = 0.01$.

Thus we design the controller as

$$\begin{aligned}u_1 &= x_2 x_3 z_1 y_1 + x_1 y_1 r(z_2 - z_1) + x_1 z_1 y_2 + z_2 y_1 (x_1^2 - x_2) \\ &\quad + x_2 y_1 (z_1 (s - z_3) - z_2) + x_2 z_2 y_2 + (1 - mx_1) z_3 y_1 + x_3 y_1 (z_1 z_2 - fz_3) \\ &\quad + x_3 z_3 y_2 - x_2 x_3 - y_2 - r(z_2 - z_1) + e_1,\end{aligned}$$

$$\begin{aligned}
u_2 = & x_2 x_3 z_1 y_2 + x_1 y_2 r(z_2 - z_1) + x_1 z_1 (-ay_2 - y_1(b(c - y_1^2) + dy_2 y_3)) \\
& + z_2 y_2 (x_1^2 - x_2) + x_2 y_2 (z_1(s - z_3) - z_2) \\
& + x_2 z_2 (-ay_2 - y_1(b(c - y_1^2) + dy_2 y_3)) + (1 - mx_1) z_3 y_2 + x_3 y_2 (z_1 z_2 - fz_3) \\
& + x_3 z_3 (-ay_2 - y_1(b(c - y_1^2) + dy_2 y_3)) - (x_1^2 - x_2) \\
& - (-ay_2 - y_1(b(c - y_1^2) + dy_2 y_3)) - (z_1(s - z_3) - z_2) + e_2
\end{aligned}$$

$$\begin{aligned}
u_3 = & x_2 x_3 z_1 y_3 + x_1 y_3 r(z_2 - z_1) + x_1 z_1 (-(g + hy_1)y_3 + ly_2 + py_1 y_3) \\
& + z_2 y_3 (x_1^2 - x_2) + x_2 y_3 (z_1(s - z_3) - z_2) \\
& + x_2 z_2 (-(g + hy_1)y_3 + ly_2 + py_1 y_3) + (1 - mx_1) z_3 y_3 + x_3 y_3 (z_1 z_2 - fz_3) \\
& + x_3 z_3 (-(g + hy_1)y_3 + ly_2 + py_1 y_3) - (1 - mx_1) \\
& - (-(g + hy_1)y_3 + ly_2 + py_1 y_3) - (z_1 z_2 - fz_3) + e_3
\end{aligned}$$

The **Theorem** in Chapter 3 is satisfied and the multiple symplectic synchronization is achieved. The phase portrait of the controlled Ge-Ku-Mathieu system and the time histories of $G(\mathbf{x}, \mathbf{y}, z, t)$ and $\mathbf{F}(\mathbf{x}, \mathbf{y}, z, t)$ and the time histories of the state errors are shown in Fig. 5.11 and Fig. 5.12 and Fig. 5.13, respectively.

5.4 Summary

A new type of synchronization, multiple symplectic synchronization, is studied in this Chapter. It is an extension of double symplectic synchronization. By applying active control, the multiple symplectic synchronization is achieved. The simulation results show that the proposed scheme is effective and feasible. Furthermore, the multiple symplectic synchronization of chaotic systems can be used to increase the security of secret communication.

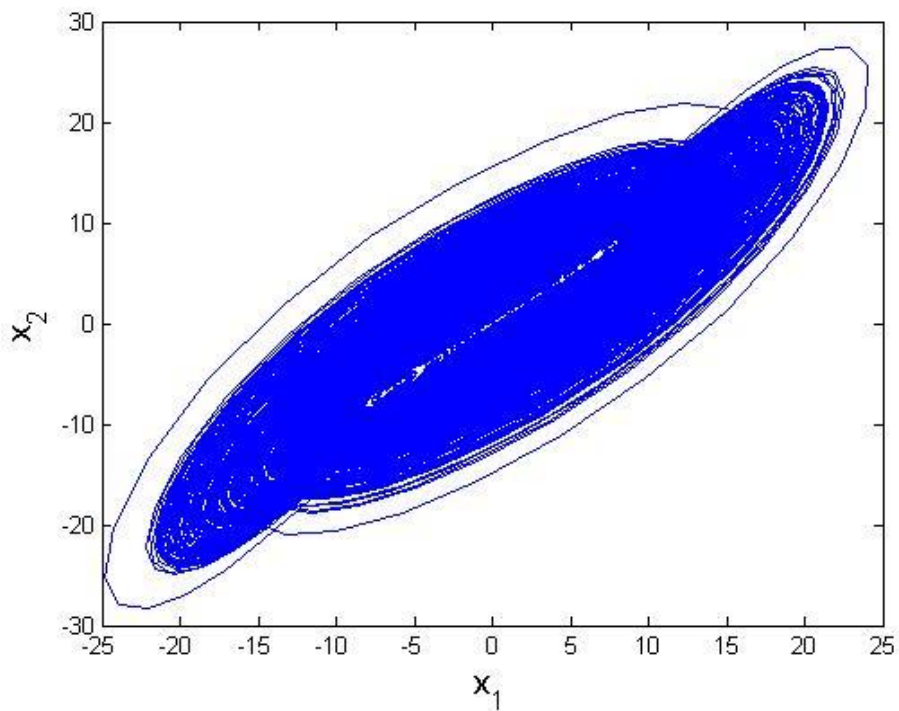


Fig. 5.1 The chaotic attractor of the Chen system.

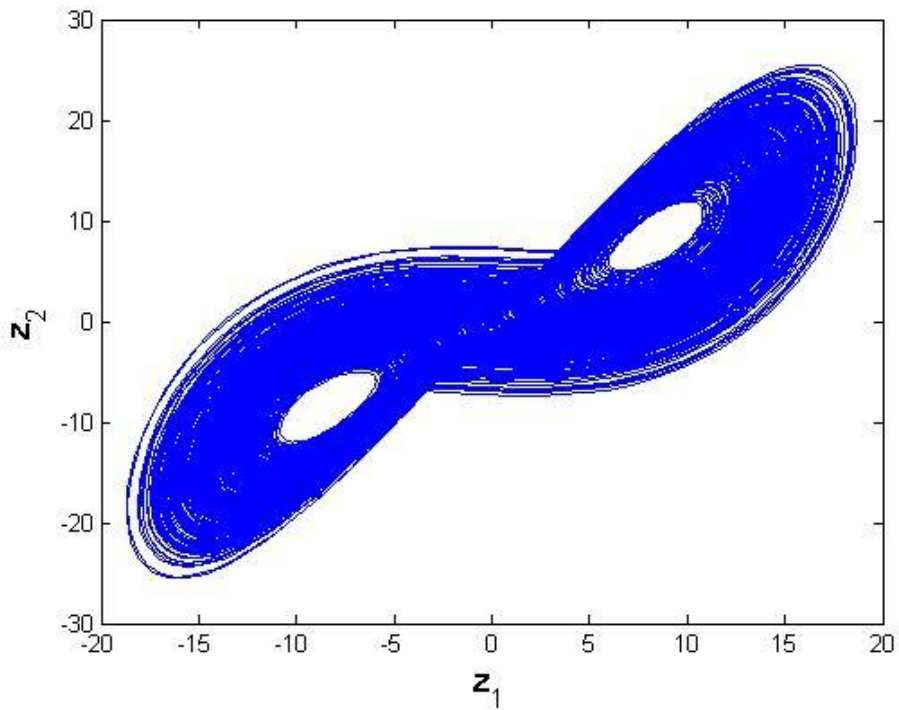


Fig. 5.2 The chaotic attractor of the Lorenz system.

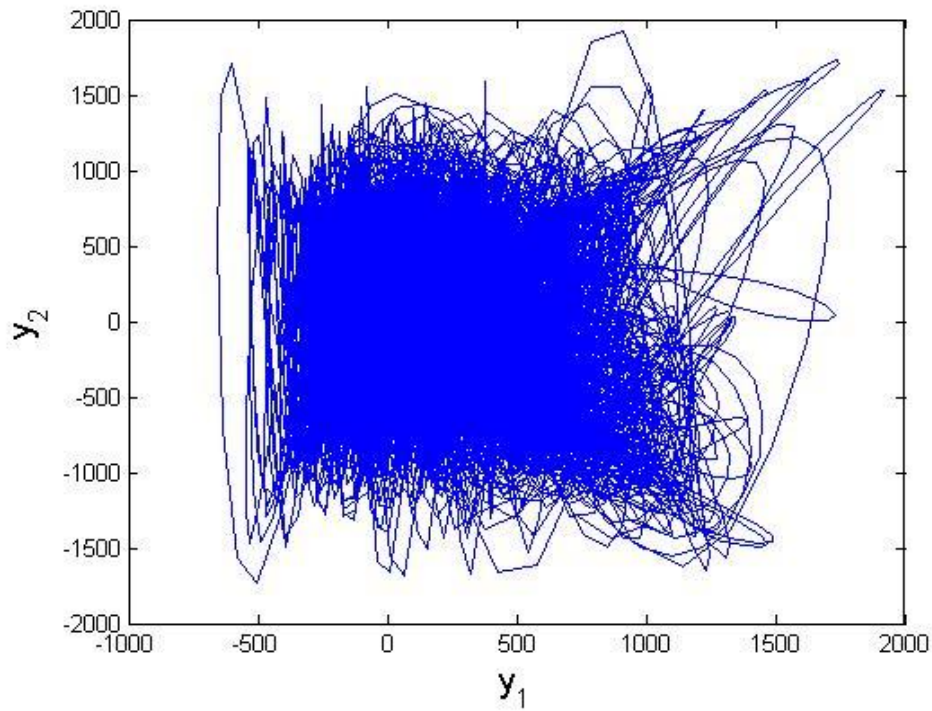


Fig. 5.3 Phase portrait of a controlled new Ge-Ku-Mathieu system for Case 1.

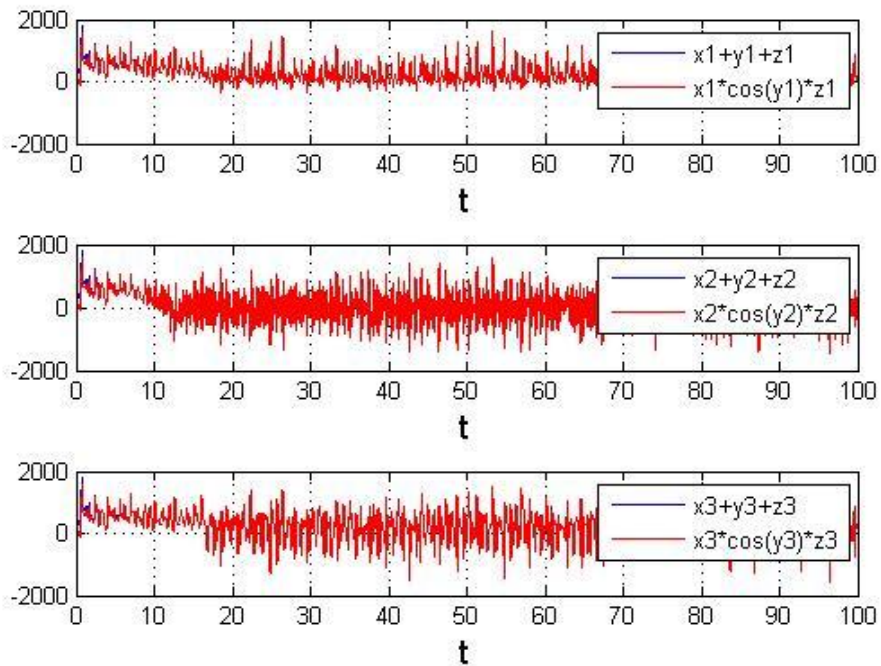


Fig. 5.4 Time histories of $G(\mathbf{x}, \mathbf{y}, \mathbf{z}, t)$ and $\mathbf{F}(\mathbf{x}, \mathbf{y}, \mathbf{z}, t)$ for Case 1.

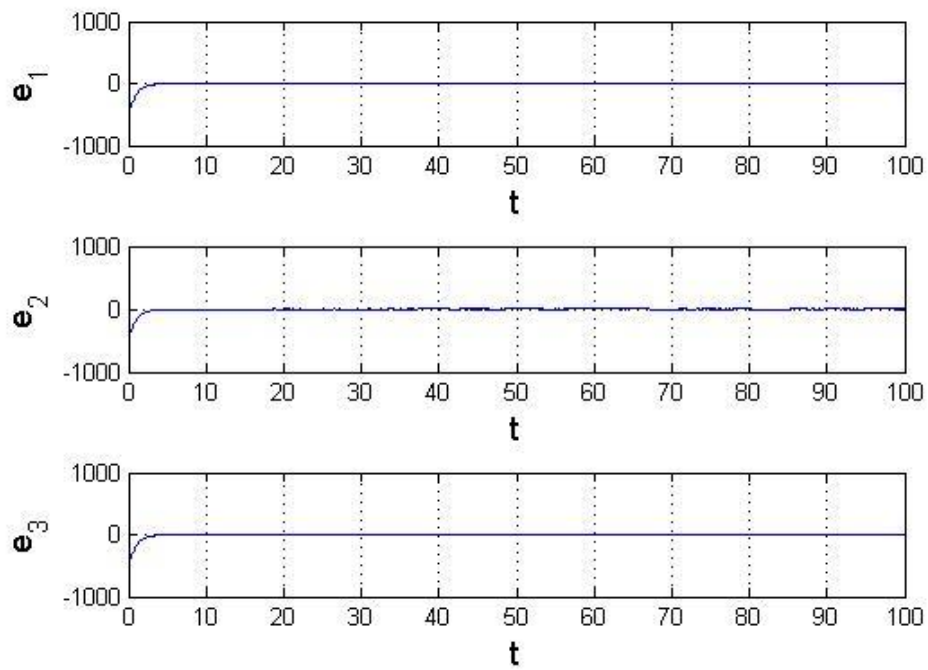


Fig. 5.5 Time histories of the state errors for Case 1.

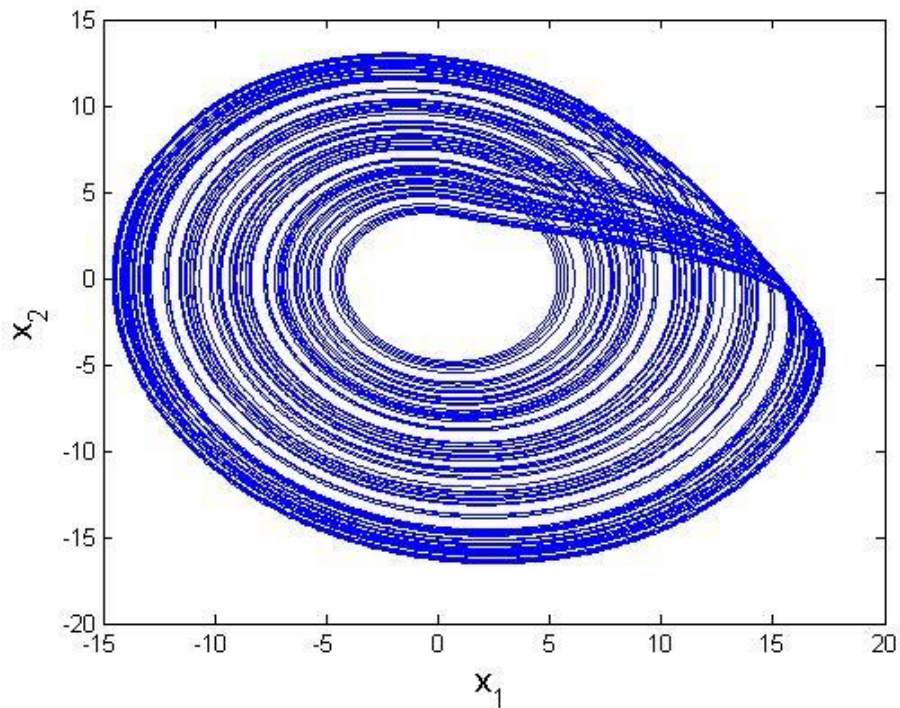
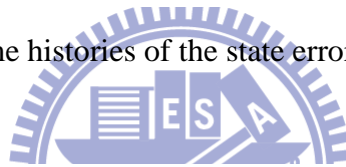


Fig. 5.6 The chaotic attractor of the *Rössler* system.

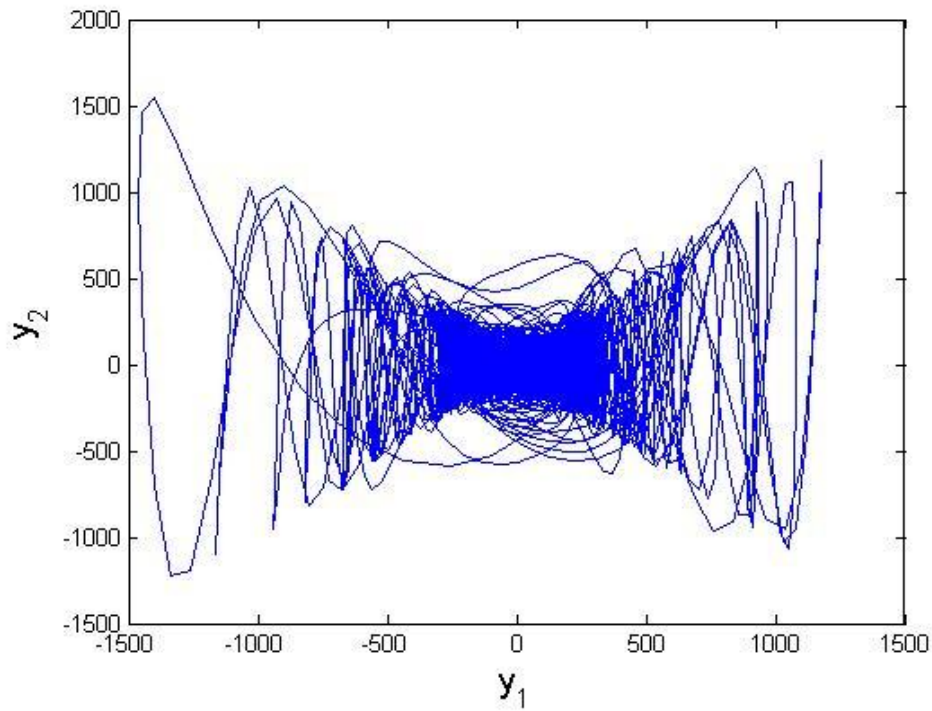


Fig. 5.7 Phase portrait of the controlled Ge-Ku-Mathieu system for Case 2.

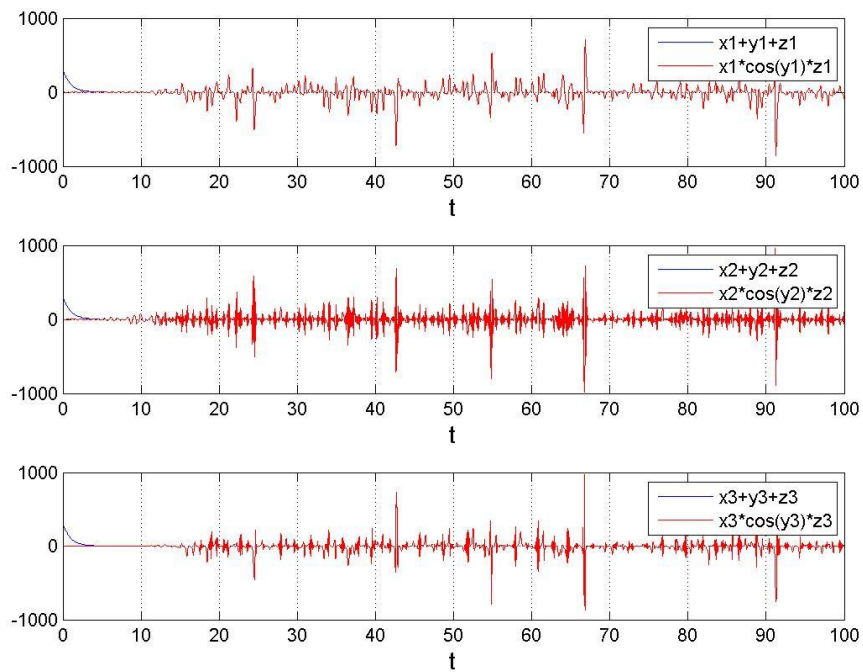


Fig. 5.8 Time histories of $G(\mathbf{x}, \mathbf{y}, \mathbf{z}, t)$ and $\mathbf{F}(\mathbf{x}, \mathbf{y}, \mathbf{z}, t)$ for Case 2.

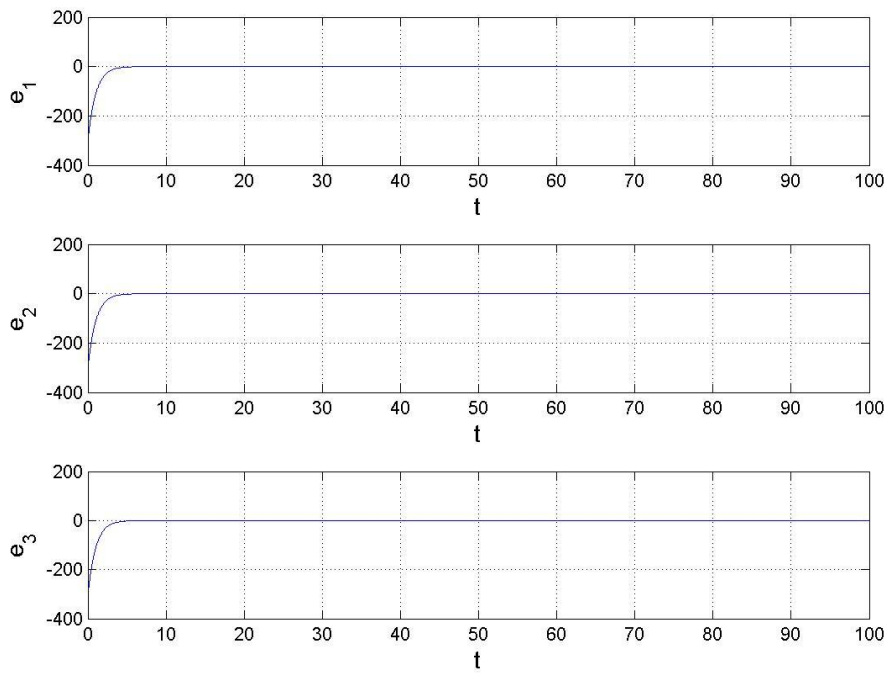


Fig. 5.9 Time histories of the state errors for Case 2.

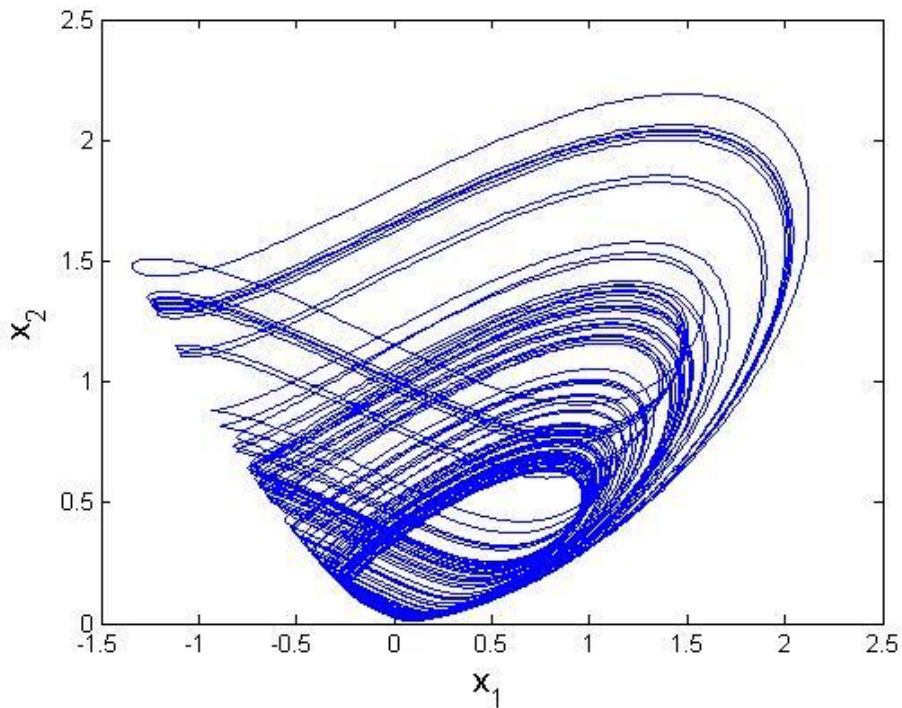
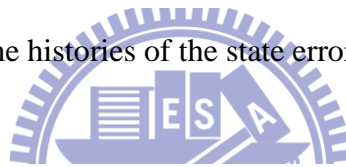


Fig. 5.10 The chaotic attractor of the spott system.

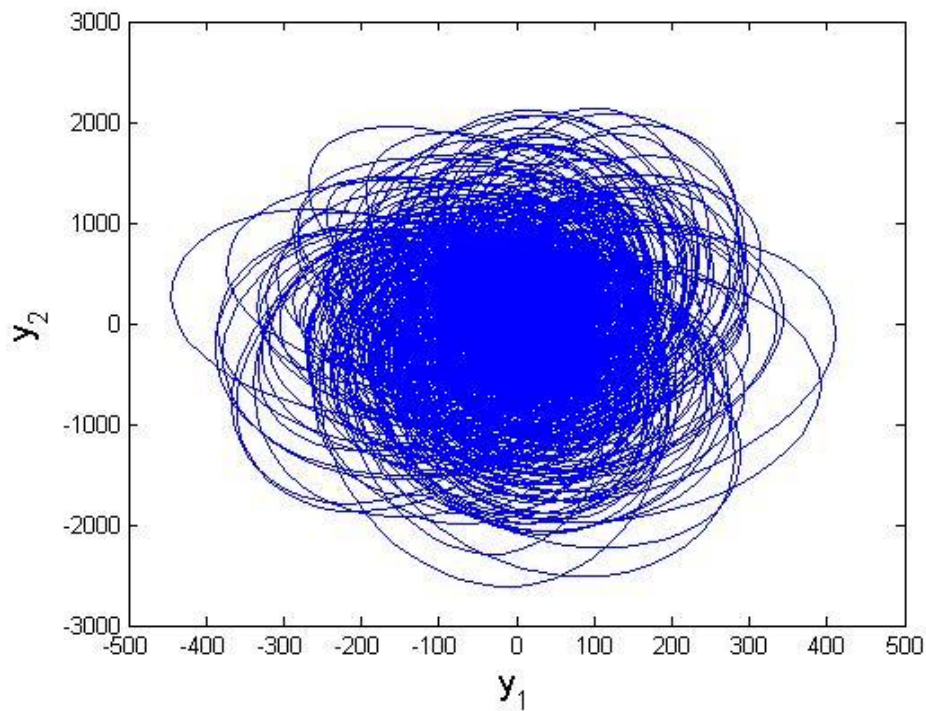


Fig. 5.11 Phase portrait of the controlled Ge-Ku-Mathieu system for Case 3.

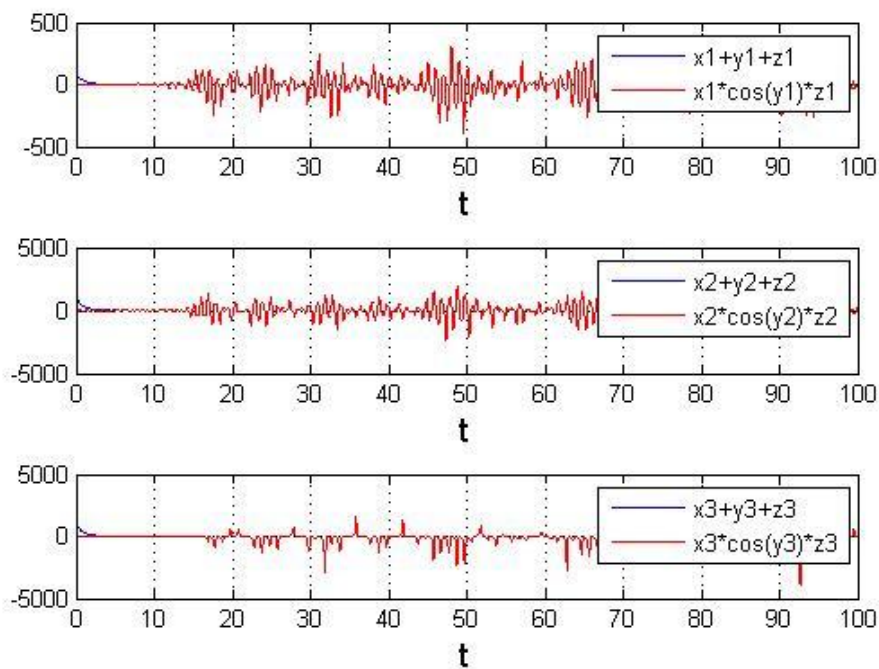


Fig. 5.12 Time histories of $G(\mathbf{x}, \mathbf{y}, \mathbf{z}, t)$ and $\mathbf{F}(\mathbf{x}, \mathbf{y}, \mathbf{z}, t)$ for Case 3.

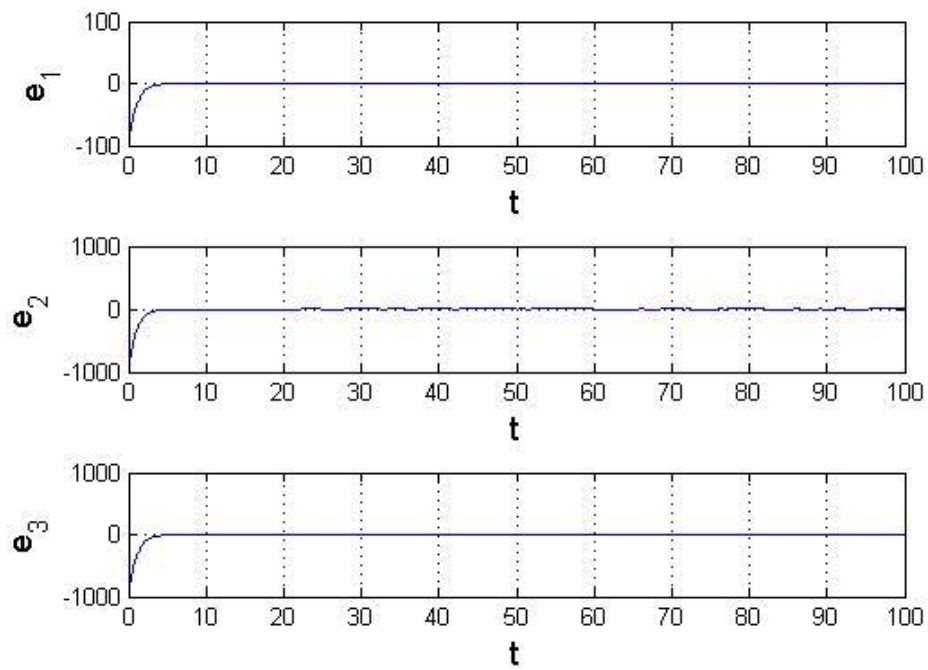
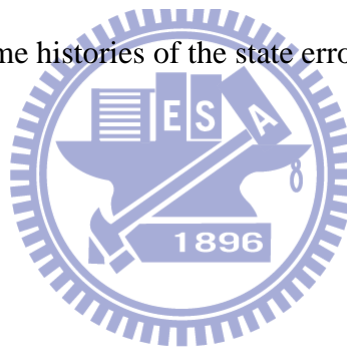


Fig. 5.13 Time histories of the state errors for Case 3.



Chapter 6

Robust Projective Anti-Synchronization of Nonautonomous Chaotic Systems with Stochastic Disturbance by Fuzzy Logic Constant Controller

6.1 Preliminary

In this paper, a simplest fuzzy logic constant controller (FLCC), which is derived via fuzzy logic design and Lyapunov direct method, is presented for projective anti-synchronization of nonautonomous chaotic systems with uncertain and stochastic signals. Controllers in traditional Lyapunov direct method are always nonlinear and complicated. However, FLCC proposed are such simple controllers which are constant numbers, decided via the values of the upper and lower bounds of the error derivatives. This new method is used in projective anti-synchronization of nonautonomous chaotic systems with stochastic disturbance to show the robustness and effectiveness of FLCC.

6.2 Projective Chaos Anti-Synchronization by FLCC Scheme

Consider the following master chaotic system

$$\dot{\mathbf{x}} = (A + \Delta)\mathbf{x} + f(\mathbf{x}) + \zeta \quad (6.1)$$

where $\mathbf{x} = [x_1, x_2, \dots, x_n]^T \in R^n$ denotes a state vector, A is an $n \times n$ constant coefficient matrix, f is a nonlinear vector function, Δ is nonautonomous term and ζ is stochastic disturbance.

The slave system which can be either identical or different from the master, is

$$\dot{\mathbf{y}} = B\mathbf{y} + g(\mathbf{y}) + \mathbf{u} \quad (6.2)$$

where $\mathbf{y} = [y_1, y_2, \dots, y_n]^T \in R^n$ denotes a state vector, B is an $n \times n$ constant

coefficient matrix, g is a nonlinear vector function, and $\mathbf{u} = [u_1, u_2, \dots, u_n]^T \in R^n$ is the fuzzy logic controller needed to be designed.

For projective anti-synchronization, in order to make the chaos state $-\mathbf{y}$ approaching the goal state $\alpha\mathbf{x}$, define $\mathbf{e} = \alpha\mathbf{x} - (-\mathbf{y}) = \alpha\mathbf{x} + \mathbf{y}$ as the state error, here α is a constant. The chaos projective anti-synchronization is accomplished in the sense that [59]:

$$\lim_{t \rightarrow \infty} \mathbf{e} = \lim_{t \rightarrow \infty} (\alpha\mathbf{x} + \mathbf{y}) = 0 \quad (6.3)$$

where

$$\mathbf{e} = [e_1, \dots, e_n]^T = \alpha\mathbf{x} + \mathbf{y} \quad (6.4)$$

From Eq. (6-4) we have the following error dynamics:

$$\dot{\mathbf{e}} = \alpha \dot{\mathbf{x}} + \dot{\mathbf{y}} = \alpha [A + \Delta A] \mathbf{x} + f(\mathbf{x}) - [B] \mathbf{y} + g(\mathbf{y}) \quad (6.5)$$

According to Lyapunov direct method, we have the following Lyapunov function to derive the fuzzy logic controller for projective anti-synchronization:

$$V = f(e_1, \dots, e_m, \dots, e_n) = \frac{1}{2} (e_1^2 + \dots + e_m^2 + \dots + e_n^2) > 0 \quad (6.6)$$

The derivative of the Lyapunov function in Eq. (6.6) is:

$$\dot{V} = e_1 \dot{e}_1 + \dots + e_m \dot{e}_m + \dots + e_n \dot{e}_n \quad (6.7)$$

If the vector controller in Eq. (6.5) can be suitably designed to achieve $\dot{V} < 0$, then the zero solution $\mathbf{e} = 0$ of Eq.(6.5) are asymptotically stable i.e the projective anti-synchronization is accomplished. Next, the design process of FLCC is introduced.

We use the error derivative $\dot{\mathbf{e}}(\mathbf{t}) = [\dot{e}_1, \dot{e}_2, \dots, \dot{e}_m, \dots, \dot{e}_n]^T$, as the antecedent part of the proposed FLCC to design the control input \mathbf{u} which is used in the consequent part of the proposed FLCC:

$$\mathbf{u} = [u_1, u_2, \dots, u_m, \dots, u_n]^T \quad (6.8)$$

where \mathbf{u} is a constant column vector and accomplishes the objective to stabilize the error dynamics in Eq. (6.5).

The strategy of the FLCC designed is proposed as follow and the configuration of the strategy is shown in Fig. 6.1.

Assume the upper bound and lower bound of \dot{e}_m are Z_m and $-Z_m$, then the FLCC can be design step by step:

(1) If e_m is detected as positive ($e_m > 0$), we design a controller for $\dot{e}_m < 0$ for the purpose $\dot{V} = e_m \dot{e}_m < 0$. Therefore we have the following ith($i=1,2,3$) if-then fuzzy rule as:

$$\text{Rule 1 : If } \dot{e}_m \text{ is } M_1 \text{ Then } u_{m1} = -Z_m \quad (6.9)$$

$$\text{Rule 2 : If } \dot{e}_m \text{ is } M_2 \text{ Then } u_{m2} = -Z_m \quad (6.10)$$

$$\text{Rule 3 : If } \dot{e}_m \text{ is } M_3 \text{ Then } u_{m3} = e_m \quad (6.11)$$

(2) If e_m is detected as negative ($e_m < 0$), we design a controller for $\dot{e}_m > 0$, for the purpose $\dot{V} = e_m \dot{e}_m < 0$. Therefore we have the following ith if-then fuzzy rule as:

$$\text{Rule 1 : If } \dot{e}_m \text{ is } M_1 \text{ Then } u_{m1} = Z_m \quad (6.12)$$

$$\text{Rule 2 : If } \dot{e}_m \text{ is } M_2 \text{ Then } u_{m2} = Z_m \quad (6.13)$$

$$\text{Rule 3 : If } \dot{e}_m \text{ is } M_3 \text{ Then } u_{m3} = e_m \quad (6.14)$$

(3) If e_m approaches to zero, then the synchronization is nearly achieved.

Therefore we have the following ith if-then fuzzy rule as:

$$\text{Rule 1 : If } \dot{e}_m \text{ is } M_1 \text{ Then } u_{m1} = e_m \approx 0 \quad (6.15)$$

$$\text{Rule 2 : If } \dot{e}_m \text{ is } M_2 \text{ Then } u_{m2} = e_m \approx 0 \quad (6.16)$$

$$\text{Rule 3 : If } \dot{e}_m \text{ is } M_3 \text{ Then } u_{m3} = e_m \approx 0 \quad (6.17)$$

where $M_1 = \frac{|\dot{e}_m|}{Z_m}$, $M_2 = \frac{|\dot{e}_m|}{Z_m}$ and $M_3 = \text{sgn}\left(\frac{Z_m - \dot{e}_m}{Z_m}\right) + \text{sgn}\left(\frac{\dot{e}_m - Z_m}{Z_m}\right)$,

M_1, M_2 and M_3 refer to the membership functions of positive (P), negative (N) and zero (Z) separately which are presented in Fig. 6.2. For each case, u_{mi} , $i= 1\sim 3$ is the i -th output of \dot{e}_m , which is a constant controller. The centroid defuzzifier evaluates the output of all rules as follows:

$$u_m = \frac{\sum_{i=1}^3 M_i \times u_{mi}}{\sum_{i=1}^3 M_i} \quad (6.18)$$

The fuzzy rule base is listed in Table 1, in which the input variables in the antecedent part of the rules are \dot{e}_m and the output variable in the consequent part is u_{mi} .

Table 1 Rule-table of FLCC

Rule	Antecedent	Consequent Part
	\dot{e}_m	u_{mi}
1	Negative (N)	u_{m1}
2	Positive (P)	u_{m2}
3	Zero (Z)	u_{m3}

With appropriate fuzzy logic constant controllers in Eq. (6.7), a negative definite derivatives of Lyapunov function \dot{V} can be obtained and the asymptotical stability of Lyapunov theorem can be achieved.

Consequently, the processes of FLCC designed to control a system following the trajectory of a master system are getting the upper bound and lower bound of the error derivatives of the goal and control systems without any controller, i.e. $-Z_m \leq \dot{e}_m \leq Z_m$. Through the fuzzy logic system which follows the rules of Eq. (6.9) ~ Eq. (6.17), a negative definite derivatives of Lyapunov function \dot{V} can be

obtained and the asymptotically stability of Lyapunov theorem can be achieved.

6.3 Simulation Results

There are two examples in this Section. Each example is divided into two parts, projective anti-synchronization by FLCC and that by traditional method. In the end of each example, we give the simulation results of two controllers and list the tables and figures to show the effectiveness and robustness of our method.

Case 1

6.1 Projective Anti-Synchronization of Sprott Systems by New FLCC

The Sprott 19 system [60] is:

$$\begin{cases} \dot{x}_1 = x_2 \\ \dot{x}_2 = x_3 \\ \dot{x}_3 = ax_3 + bx_2 - x_2^3 - x_1 \end{cases} \quad (6.19)$$

When initial condition $(x_{10}, x_{20}, x_{30}) = (0, 1, 0)$ and parameters $a = -0.6, b = 2.75$, chaos of the Sprott 19 system appears. The chaotic behavior of Eq. (6.19) is shown in Fig. 6.3.

6.1.1 Projective Anti-Synchronization of Nonautonomous Sprott 19 System by New FLCC

The nonautonomous Sprott 19 system is:

$$\begin{cases} \frac{dx_1(t)}{dt} = x_2(t) \\ \frac{dx_2(t)}{dt} = x_3(t) \\ \frac{dx_3(t)}{dt} = a(1 + \Delta_1)x_3(t) + bx_2(t) - x_2^3 - x_1 \end{cases} \quad (6.20)$$

When initial condition $(x_{10}, x_{20}, x_{30}) = (0, 1, 0)$, parameters $a = -0.6, b = 2.75$, and $\Delta_1 = \text{pulse generator}$ is an nonautonomous term as shown in Fig. 6.4. Chaos of the nonautonomous Sprott 19 system appears in Fig. 6.5.

The Sprott 22 system [60] is:

$$\begin{cases} \dot{x}_1 = x_2 \\ \dot{x}_2 = x_3 \\ \dot{x}_3 = cx_3 - x_2 - \sin x_1 \end{cases} \quad (6.21)$$

When initial condition $(x_{10}, x_{20}, x_{30}) = (0.01, 1, 0.01)$ and parameters $c = 0.2$, chaos of the Sprott 22 system is shown in Fig. 6.6.

The slave Sprott 22 system with controllers is:

$$\begin{cases} \frac{dy_1(t)}{dt} = y_2(t) + u_1 \\ \frac{dy_2(t)}{dt} = y_3(t) + u_2 \\ \frac{dy_3(t)}{dt} = cy_3(t) - y_2(t) - \sin y_1 + u_3 \end{cases} \quad (6.22)$$

For initial condition $(y_{10}, y_{20}, y_{30}) = (0.01, 1, 0.01)$ and parameters $c = 0.25$, chaos of the slave Sprott 22 system in Eq.(6.21) appears as well. u_1, u_2 and u_3 are FLCC to anti-synchronize the slave Sprott 22 system to master Sprott 19 system.

The error vector for projective anti-synchronization is

$$\mathbf{e} = \begin{bmatrix} e_1(t) \\ e_2(t) \\ e_3(t) \end{bmatrix} = \alpha \begin{bmatrix} x_1(t) \\ x_2(t) \\ x_3(t) \end{bmatrix} + \begin{bmatrix} y_1(t) \\ y_2(t) \\ y_3(t) \end{bmatrix} \quad (6.23)$$

Here α is the projective constant.

Our aim is

$$\lim_{t \rightarrow \infty} \mathbf{e} = 0 \quad (6.24)$$

From Eqs. (6.20), (6.22), (6.23), we have the following error dynamics:

$$\begin{cases} \dot{e}_1 = \alpha[x_2(t)] + (y_2(t) + u_1) \\ \dot{e}_2 = \alpha[x_3(t)] + (y_3(t) + u_2) \\ \dot{e}_3 = \alpha[a(1 + \Delta_1)x_3(t) + bx_2(t) - x_2^3 - x_1] + (cy_3(t) - y_2(t) - \sin y_1 + u_3) \end{cases} \quad (6.25)$$

Choosing Lyapunov function as:

$$V = \frac{1}{2}(e_1^2 + e_2^2 + e_3^2) \quad (6.26)$$

Its time derivative is:

$$\begin{aligned}
\dot{V} &= e_1 \dot{e}_1 + e_2 \dot{e}_2 + e_3 \dot{e}_3 \\
&= e_1 \{ \alpha[x_2(t)] + (y_2(t) + u_1) \} \\
&\quad + e_2 \{ \alpha[x_3(t)] + (y_3(t) + u_2) \} \\
&\quad + e_3 \{ \alpha[a(1 + \Delta_1)x_3(t) + bx_2(t) - x_2^3 - x_1] + (cy_3(t) - y_2(t) - \sin y_1 + u_3) \}
\end{aligned} \tag{6.27}$$

In order to design FLCC, we divide Eq. (6.27) into three parts as follows:

Assume $V = \frac{1}{2}(e_1^2 + e_2^2 + e_3^2) = V_1 + V_2 + V_3$, then $\dot{V} = e_1 \dot{e}_1 + e_2 \dot{e}_2 + e_3 \dot{e}_3 = \dot{V}_1 + \dot{V}_2 + \dot{V}_3$,

where $V_1 = \frac{1}{2}e_1^2$, $V_2 = \frac{1}{2}e_2^2$ and $V_3 = \frac{1}{2}e_3^2$.

$$\text{Part 1: } \dot{V}_1 = e_1 \dot{e}_1 = e_1 \{ \alpha[x_2(t)] + (y_2(t) + u_1) \}$$

$$\text{Part 2: } \dot{V}_2 = e_2 \dot{e}_2 = e_2 \{ \alpha[x_3(t)] + (y_3(t) + u_2) \}$$

$$\text{Part 3: } \dot{V}_3 = e_3 \dot{e}_3 = e_3 \{ \alpha[a(1 + \Delta_2)x_3(t) + bx_2(t) - x_2^3 - x_1] \\ + (cy_3(t) - y_2(t) - \sin y_1 + u_3) \}$$

FLCC in *Part 1*, *2* and *3* can be obtained via the fuzzy rules in Table 1. The maximum value and minimum value can be observed in time histories of error derivatives without any controllers shown in Fig. 6.7.

FLCC are proposed in *Part 1*, *2* and *3* to make $\dot{V}_1 = e_1 \dot{e}_1 < 0$, $\dot{V}_2 = e_2 \dot{e}_2 < 0$ and $\dot{V}_3 = e_3 \dot{e}_3 < 0$. Hence we have $\dot{V} = \dot{V}_1 + \dot{V}_2 + \dot{V}_3 < 0$. It is clear that all of the rules in FLCC can lead that the Lyapunov function satisfies the asymptotical stability theorem. The simulation results are shown in Fig. 6.8 and Fig. 6.9. The projection of phase portraits of system (6.22) with chaotic behaviors is shown in Fig. 6.6.

6.1.2 Robust Projective Anti-Synchronization of Nonautonomous Sprott System with Stochastic Disturbance by FLCC

The master nonautonomous Sprott 19 system with stochastic disturbance is:

$$\begin{cases} \frac{dx_1(t)}{dt} = x_2(t) + \Delta_2 \\ \frac{dx_2(t)}{dt} = x_3(t) + \Delta_2 \\ \frac{dx_3(t)}{dt} = a(1 + \Delta_1)x_3(t) + bx_2(t) - x_2^3 - x_1 + \Delta_2 \end{cases} \quad (6.28)$$

For initial condition $(x_{10}, x_{20}, x_{30}) = (0, 1, 0)$. The pulse generator Δ_1 is a nonautonomous term in Fig. 6.4, Δ_2 is band-limited white noise (PSD=0.1) in Fig. 6.10, and parameters are $a=-0.6$, $b=2.75$. Chaos of Eq. (6.28), the nonautonomous Sprott 19 system with stochastic disturbance appears in Fig. 6.11.

The slave system is the same as Eq. (6.22) and Lyapunov function derived through Eq. (6.23)~(6.27).

Let $\alpha = 2$, we have the following error dynamics:

$$\begin{cases} \dot{e}_1 = \alpha[x_2(t) + \Delta_2] + (y_2(t) + u_1) \\ \dot{e}_2 = \alpha[x_3(t) + \Delta_2] + (y_3(t) + u_2) \\ \dot{e}_3 = \alpha[a(1 + \Delta_1)x_3(t) + bx_2(t) - x_2^3 - x_1 + \Delta_2] + (cy_3(t) - y_2(t) - \sin y_1 + u_3) \end{cases} \quad (6.29)$$

And time derivative of Lyapunov function is:

$$\begin{aligned} \dot{V} &= e_1\dot{e}_1 + e_2\dot{e}_2 + e_3\dot{e}_3 \\ &= e_1\{\alpha[x_2(t) + \Delta_2] + (y_2(t) + u_1)\} \\ &\quad + e_2\{\alpha[x_3(t) + \Delta_2] + (y_3(t) + u_2)\} \\ &\quad + e_3\{\alpha[a(1 + \Delta_1)x_3(t) + bx_2(t) - x_2^3 - x_1 + \Delta_2] \\ &\quad + (cy_3(t) - y_2(t) - \sin y_1 + u_3)\} \end{aligned} \quad (6.30)$$

The maximum value and minimum value without any controller can be observed by time histories of error derivatives shown in Fig 6.12. The robust projective anti-synchronization scheme to make $\dot{V} = e_1\dot{e}_1 + e_2\dot{e}_2 + e_3\dot{e}_3 < 0$. It is clear that all of the rules in FLCC can lead that the Lyapunov function satisfies the asymptotical

stability theorem. The simulation results are shown in Fig. 6.13 and Fig. 6.14.

6.1.3 Robust Projective Anti-Synchronization of Nonautonomous Sprott System with Stochastic Disturbance by Traditional Method

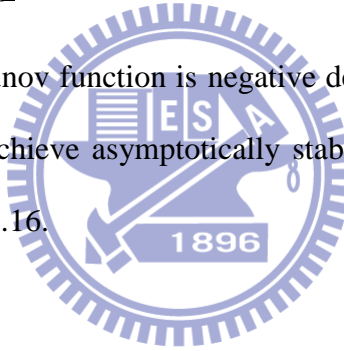
In order to lead the derivative of Lyapunov function in Eq. (6.30) to negative definite, we choose robust traditional nonlinear controllers as:

$$\begin{cases} u_1 = -[\alpha(x_2 + \Delta_2) + y_2 + e_1] \\ u_2 = -[\alpha(x_3 + \Delta_2) + y_3 + e_2] \\ u_3 = -\{\alpha[a(1 + \Delta_1)x_3 + bx_2 - x_2^3 - x_1 + \Delta_2] + cy_3 - y_2 - \sin y_1 + e_3\} \end{cases} \quad (6.31)$$

And we can obtain

$$\dot{V} = -\dot{e}_1 e_1 - \dot{e}_2 e_2 - \dot{e}_3 e_3 \quad (6.32)$$

The derivative of Lyapunov function is negative definite and the error dynamics in Eq. (6.29) are going to achieve asymptotically stable. The simulation results are shown in Fig. 6.15 and Fig. 6.16.



6.1.4 FLCC Compared to Traditional Method

In this subsection, the controllers and numerical simulation results in subsection 6.1.2 and subsection 6.1.3 are listed in Tables 2 and 3 for comparison. Comparing two kinds of controller in Table 2 and two kinds of errors in Table 3, it is clear to find out that (1) The controllers in FLCC designing are much simpler than traditional ones; (2) The performance of the error convergence of states by FLCC is much better than that by traditional method.

Consequently, even the system contains noise and parameter uncertainty, the FLCC can still remain the high performance to synchronize the two chaotic systems with uncertainty and stochastic signals exactly and efficiently.

Table 2 The controllers of FLCC and of traditional method.

Controller	FLCC	Traditional method
u_1	$Z_{m1} = 10$	$-[\alpha(x_2 + \Delta_2) + y_2 + e_1]$
u_2	$Z_{m2} = 20$	$-[\alpha(x_3 + \Delta_2) + y_3 + e_2]$
u_3	$Z_{m3} = 50$	$-\{a[a(1 + \Delta_1)x_3 + bx_2 - x_2^3 - x_1 + \Delta_2] + cy_3 - y_2 - \sin y_1 + e_3\}$



Table 3 Errors data after the action of controllers.

Time	FLCC	Traditional method
after the action		
of controllers	e_1	e_1
35.97 s	0.000000000000000177636	-0.00054576536205530601
35.98 s	0.000000000000000088818	-0.00054033490596872014
35.99 s	0.000000000000000088819	-0.00053495848382301148
36.0 s	0.000000000000000088818	-0.00052963555797180817
36.01 s	-0.0000000000000000355271	-0.00052436559611734879
	e_2	e_2
35.97 s	0.000000000000000133227	-0.00656173798135295527
35.98 s	0.000000000000000133227	-0.00649644759754419709
35.99 s	0.000000000000000133227	-0.00643180686390909528
36.0 s	0.000000000000000133227	-0.00636780931631975022
36.01 s	-0.0000000000000000355271	-0.00630444855496925527
	e_3	e_3
36.05 s	0.000000000000000799361	0.02132987975686884141
36.06 s	0.000000000000000799361	0.02111764390717763007
36.07 s	0.000000000000000799361	0.02090751983947569670
36.08 s	0.000000000000000710543	0.02069948654118025644
36.09 s	0.000000000000000710543	0.02049352320878927713

Case 2

6.2 Projective Anti-Synchronization of Sprott System and Ge-Ku-Mathieu Systems

6.2.1 Chaos Projective Anti-Synchronization of Nonautonomous Sprott 19 System and Ge-Ku-Mathieu (GKM) System by New FLCC

The nonautonomous Sprott 19 system is:

$$\begin{cases} \frac{dx_1(t)}{dt} = x_2(t) \\ \frac{dx_2(t)}{dt} = x_3(t) \\ \frac{dx_3(t)}{dt} = a(1 + \Delta_1)x_3(t) + b(1 + \Delta_1\Delta_2)x_2(t) - x_2^3 - x_1 \end{cases} \quad (6.33)$$

When initial condition $(x_{10}, x_{20}, x_{30}) = (0, 1, 0)$, parameters $a = -0.6, b = 2.75$, pulse generator Δ_1 in Fig. 6.4, band-limited white noise Δ_2 in Fig. 6.10, chaos of the nonautonomous Sprott 19 system with stochastic disturbance appears in Fig. 6.17.

The slave GKM system is:

$$\begin{cases} \frac{dy_1(t)}{dt} = y_2(t) + u_1 \\ \frac{dy_2(t)}{dt} = -my_2(t) - y_1(t)\{n[c - y_1^2(t)] + dy_2(t)y_3(t)\} + u_2 \\ \frac{dy_3(t)}{dt} = -[g + hy_1(t)]y_3(t) + ly_2(t) + py_1(t)y_3(t) + u_3 \end{cases} \quad (6.34)$$

When initial condition $(y_{10}, y_{20}, y_{30}) = (0.01, 0.01, 0.01)$ and parameters $m = -0.6, n = 5, c = 11, d = 0.3, g = 8, h = 10, l = 0.5, p = 0.2$, chaos of the GKM system appears as well. u_1, u_2 and u_3 are FLCC to anti-synchronize projectively the slave GKM system to the master one.

Our aim is

$$\lim_{t \rightarrow \infty} \mathbf{e} = 0 \quad (6.35)$$

where the error vector

$$[e] = \begin{bmatrix} e_1(t) \\ e_2(t) \\ e_3(t) \end{bmatrix} = \alpha \begin{bmatrix} x_1(t) \\ x_2(t) \\ x_3(t) \end{bmatrix} + \begin{bmatrix} y_1(t) \\ y_2(t) \\ y_3(t) \end{bmatrix} \quad (6.36)$$

Here α is constant

From Eq. (6.36), we have the following error dynamics:

$$\begin{cases} \dot{e}_1 = \alpha[x_2(t)] + (y_2(t) + u_1) \\ \dot{e}_2 = \alpha[x_3(t)] + \{-my_2(t) - y_1(t) \\ \quad \times [n(c - y_1^2(t)) + dy_2(t)y_3(t)] + u_2\} \\ \dot{e}_3 = \alpha[a(1 + \Delta_1)x_3(t) + b(1 + \Delta_1\Delta_2)x_2(t) - x_2^3 - x_1] \\ \quad + [-(g + hy_1(t))y_3(t) + ly_2(t) + py_1(t)y_3(t) + u_3] \end{cases} \quad (6.37)$$

Choosing Lyapunov function as:

$$V = \frac{1}{2}(e_1^2 + e_2^2 + e_3^2) \quad (6.38)$$

Its time derivative is:

$$\begin{aligned} \dot{V} &= e_1\dot{e}_1 + e_2\dot{e}_2 + e_3\dot{e}_3 \\ &= e_1\{\alpha[x_2(t)] + (y_2(t) + u_1)\} \\ &\quad + e_2\{\alpha[x_3(t)] + \{-my_2(t) - y_1(t) \\ &\quad \times [n(c - y_1^2(t)) + dy_2(t)y_3(t)] + u_2\} \\ &\quad + e_3\{\alpha[a(1 + \Delta_1)x_3(t) + b(1 + \Delta_1\Delta_2)x_2(t) - x_2^3 - x_1] \\ &\quad + [-(g + hy_1(t))y_3(t) + ly_2(t) + py_1(t)y_3(t) + u_3]\} \end{aligned} \quad (6.39)$$

In order to design FLCC, we divide Eq. (6.39) into three parts as follows:

Assume $V = \frac{1}{2}(e_1^2 + e_2^2 + e_3^2) = V_1 + V_2 + V_3$, then $\dot{V} = e_1\dot{e}_1 + e_2\dot{e}_2 + e_3\dot{e}_3 = \dot{V}_1 + \dot{V}_2 + \dot{V}_3$,

where $V_1 = \frac{1}{2}e_1^2$, $V_2 = \frac{1}{2}e_2^2$ and $V_3 = \frac{1}{2}e_3^2$.

$$\text{Part 1: } \dot{V}_1 = e_1\dot{e}_1 = e_1\{\alpha[x_2(t)] + (y_2(t) + u_1)\}$$

$$\text{Part 2: } \dot{V}_2 = e_2\dot{e}_2 = e_2\{\alpha[x_3(t)] + \{-my_2(t) - y_1(t) \\ \quad \times [n(c - y_1^2(t)) + dy_2(t)y_3(t)] + u_2\}$$

$$\text{Part 3: } \dot{V}_3 = e_3 \dot{e}_3 = e_3 \{ \alpha [a(1 + \Delta_1)x_3(t) + b(1 + \Delta_1\Delta_2)x_2(t) - x_2^3 - x_1] \\ + [-(g + hy_1(t))y_3(t) + ly_2(t) + py_1(t)y_3(t) + u_3] \}$$

FLCC in *Part 1*, *2* and *3* can be obtained via the fuzzy rules in Table 1. The maximum value and minimum value can be observed in time histories of error derivatives without any controller shown in Fig. 6.18.

FLCC are proposed in *Part 1*, *2* and *3* and make $\dot{V}_1 = e_1 \dot{e}_1 < 0$, $\dot{V}_2 = e_2 \dot{e}_2 < 0$ and $\dot{V}_3 = e_3 \dot{e}_3 < 0$. Hence, we have $\dot{V} = \dot{V}_1 + \dot{V}_2 + \dot{V}_3 < 0$. It is clear that all of the rules in our FLCC can lead that the Lyapunov function satisfies the asymptotical stability theorem. The simulation results are shown in Fig. 6.19 and Fig. 6.20.

6.2.2 Robust Projective Anti-Synchronization of Nonautonomous Sprott System with Stochastic Disturbance and GKM System by FLCC

The master nonautonomous Sprott 19 system with stochastic disturbance is:

$$\begin{cases} \frac{dx_1(t)}{dt} = x_2(t) + \Delta_1 \\ \frac{dx_2(t)}{dt} = x_3(t) \\ \frac{dx_3(t)}{dt} = a(1 + \Delta_2)x_3(t) + b(1 + \Delta_1\Delta_2)x_2(t) - x_2^3 - x_1 \end{cases} \quad (6.40)$$

For initial condition $(x_{10}, x_{20}, x_{30}) = (0, 1, 0)$, pulse generator Δ_1 in Fig. 6.4, band-limited white noise disturbance Δ_2 (PSD=0.1) in Fig. 6.10, and parameters $a=-0.6$, $b=2.75$, chaos of the nonautonomous Sprott 19 system with stochastic signal appears. The chaotic behavior of Eq. (6.40) is shown in Fig. 6.21.

The slave system was same as Eq. (6.34) and Lyapunov function derived through Eqs. (6.35) ~ (6.39).

Let $\alpha = 2$, we have the following error dynamics:

$$\begin{cases} \dot{e}_1 = \alpha[x_2(t) + \Delta_2] + (y_2(t) + u_1) \\ \dot{e}_2 = \alpha[x_3(t)] + \{-my_2(t) - y_1(t) \\ \quad \times [n(c - y_1^2(t)) + dy_2(t)y_3(t)] + u_2\} \\ \dot{e}_3 = \alpha[a(1 + \Delta_1)x_3(t) + b(1 + \Delta_1\Delta_2)x_2(t) - x_2^3 - x_1] \\ \quad + [-(g + hy_1(t))y_3(t) + ly_2(t) + py_1(t)y_3(t) + u_3] \end{cases} \quad (6.41)$$

Time derivative of Lyapunov function is:

$$\begin{aligned} \dot{V} &= e_1\dot{e}_1 + e_2\dot{e}_2 + e_3\dot{e}_3 \\ &= e_1\{\alpha[x_2(t) + \Delta_2] + (y_2(t) + u_1)\} \\ &\quad + e_2\{\alpha[x_3(t)] + \{-my_2(t) - y_1(t) \\ &\quad \times [n(c - y_1^2(t)) + dy_2(t)y_3(t)] + u_2\}\} \\ &\quad + e_3\{\alpha[a(1 + \Delta_1)x_3(t) + b(1 + \Delta_1\Delta_2)x_2(t) - x_2^3 - x_1] \\ &\quad + [-(g + hy_1(t))y_3(t) + ly_2(t) + py_1(t)y_3(t) + u_3]\} \end{aligned} \quad (6.42)$$

The maximum value and minimum value without any controller can be observed in time histories of error derivatives shown in Fig 6.22. The projective anti-synchronization scheme to make $\dot{V} = e_1\dot{e}_1 + e_2\dot{e}_2 + e_3\dot{e}_3 < 0$. It is clear that all of the rules in FLCC can lead that the Lyapunov function satisfies the asymptotical stability theorem. The simulation results are shown in Fig. 6.23 and Fig. 6.24.

6.2.3 Robust Projective Anti-Synchronization of Nonautonomous Sprott 19 System with Stochastic Disturbance and GKM System by Traditional Method

According to Eq. (6.42), we design complicated controllers to anti-synchronize projectively chaotic systems in subsection 6.2.2 by traditional method.

We choose controllers are

$$\begin{cases} u_1 = -[\alpha(x_2 + \Delta_2) + y_2 + e_1] \\ u_2 = -\{\alpha x_3(t) + [-my_2(t) - y_1(t) \\ \quad \times [n(c - y_1^2(t)) + dy_2(t)y_3(t)]] + e_2\} \\ u_3 = -\{\alpha[a(1 + \Delta_1)x_3(t) + b(1 + \Delta_1\Delta_2)x_2(t) - x_2^3 - x_1] \\ \quad + [-(g + hy_1(t))y_3(t) + ly_2(t) + py_1(t)y_3(t)] + e_3\} \end{cases} \quad (6.43)$$

And we can obtain

$$\dot{V} = -\dot{e}_1 e_1 - \dot{e}_2 e_2 - \dot{e}_3 e_3 \quad (6.44)$$

The derivative of Lyapunov function is negative definite and the error dynamics in Eq. (6.41) achieves asymptotical stability. The simulation results are shown in Fig. 6.25 and Fig. 6.26.

6.2.4 FLCC Compared to Traditional Method

In this case, the controllers and numerical simulation results of subsection 6.2.2 and subsection 6.2.3 are listed in Table 4 and Table 5 for comparison. The master and slave systems are more complex than Case 1, but the good-robustness and high performance can be still achieved through FLCC. The two main superiorities are still existed: (1) The controllers in FLCC designing are much simpler than traditional ones; (2) The performance of the convergence of error states by FLCC is much better than by traditional method.

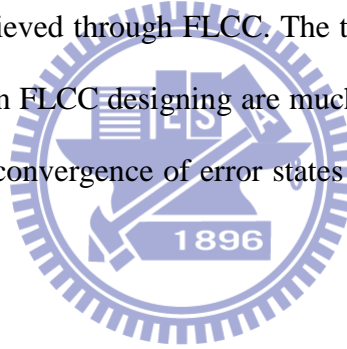


Table 4 The controller of FLCC and of traditional method.

Controller	FLCC	Traditional method
u_1	$Z_{m1} = 20$	$-\{\alpha(x_2 + \Delta_2) + y_2 + e_1\}$
u_2	$Z_{m2} = 100$	$-\{\alpha x_3(t) + [-my_2(t) - y_1(t) \times [n(c - y_1^2(t)) + dy_2(t)y_3(t)]] + e_2\}$
u_3	$Z_{m3} = 200$	$-\{\alpha[a(1 + \Delta_1)x_3(t) + b(1 + \Delta_1\Delta_2)x_2(t) - x_2^3 - \dots + [-(g + hy_1(t))y_3(t) + ly_2(t) + py_1(t)y_3(t)]\}$

Table 5 Errors data after the action of controllers.

Time after the action of controllers	FLCC	Traditional
	e_1	e_1
38.15 s	0.000000000000000001388	0.00032496190090512689
38.16 s	-0.0000000000000000258127	0.00032172847596594056
38.17 s	0.0000000000000000646705	0.00031852722414243972
38.18 s	0.0000000000000000641154	0.00031535782530682510
38.19 s	0.0000000000000000634215	0.00031221996251651341
	e_2	e_2
38.15 s	0.00000000000000003373603	0.00204273347495999638
38.16 s	0.00000000000000003341424	0.00202240793727799430
38.17 s	0.00000000000000003309332	0.00200228464207508148
38.18 s	0.00000000000000003276893	0.00198236157700495399
38.19 s	0.00000000000000003245841	0.00196263674974449503
	e_3	e_3
38.15 s	0.00000000000000003749778	-0.00101150580259323775
38.16 s	0.00000000000000003713696	-0.00100144115169376047
38.17 s	0.00000000000000003677614	-0.00099147664574397720
38.18 s	0.00000000000000003638756	-0.00098161128828502808
38.19 s	0.0000000000000000360267	-0.00097184409277292771

6.4 Summary

A simplest fuzzy controller (FLCC) is introduced to projective anti-synchronization of non-autonomous chaotic systems with stochastic disturbance. Three main contributions can be concluded: (1) High performance of the convergence of error states in synchronization; (2) Good robustness in projective anti-synchronization of the chaotic systems with stochastic disturbance; (3) Simple constant controllers are used, which can be easily obtained.



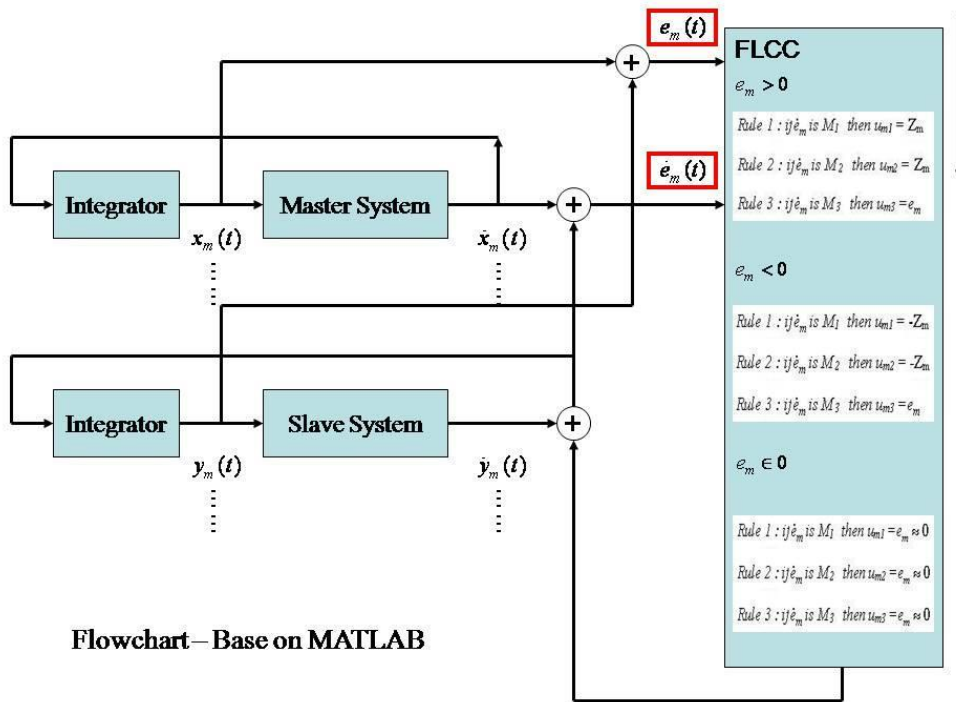


Fig. 6.1. The configuration of fuzzy logic controller.

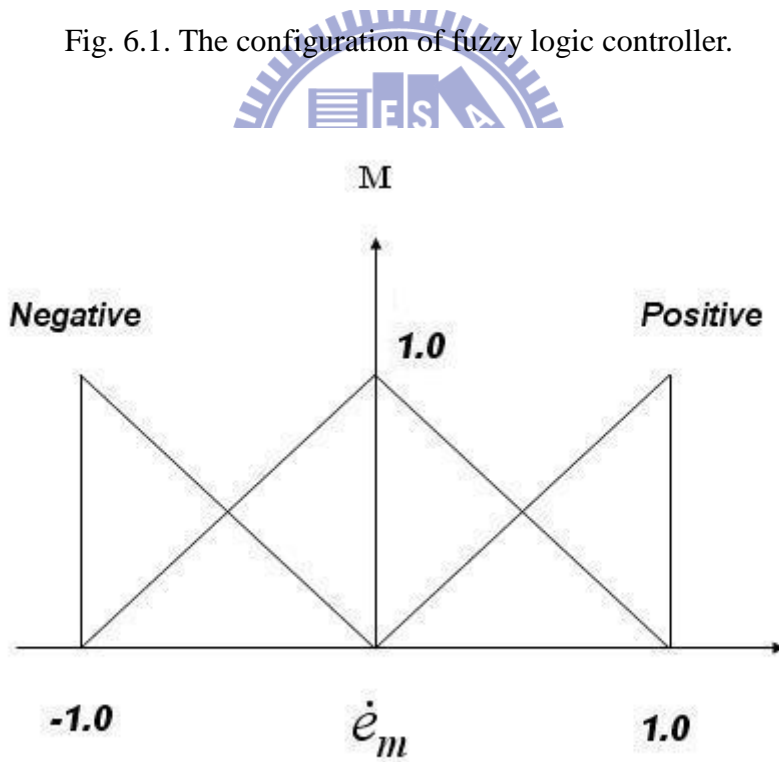


Fig. 6.2. Membership function.

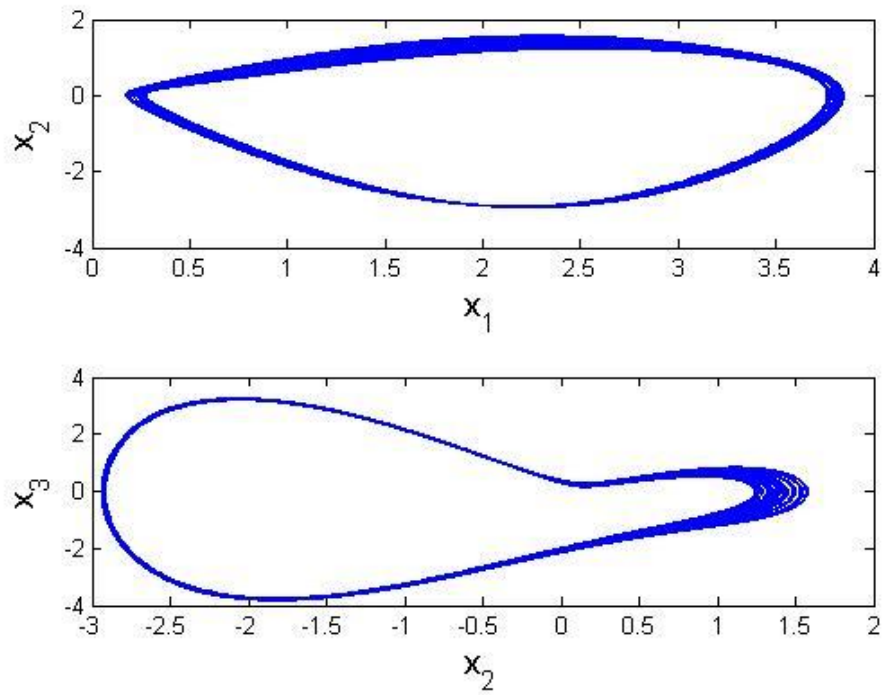


Fig. 6.3. Projections of phase portrait of chaotic Sprott No.19 system with $a=-0.6$,

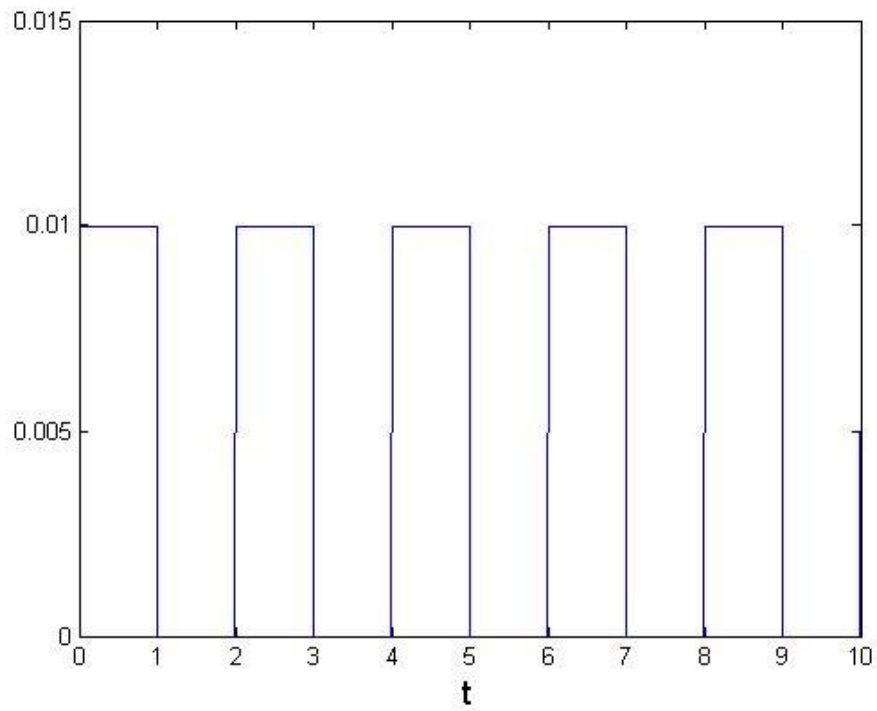


Fig. 6.4. Δ_1 is pulse generator.

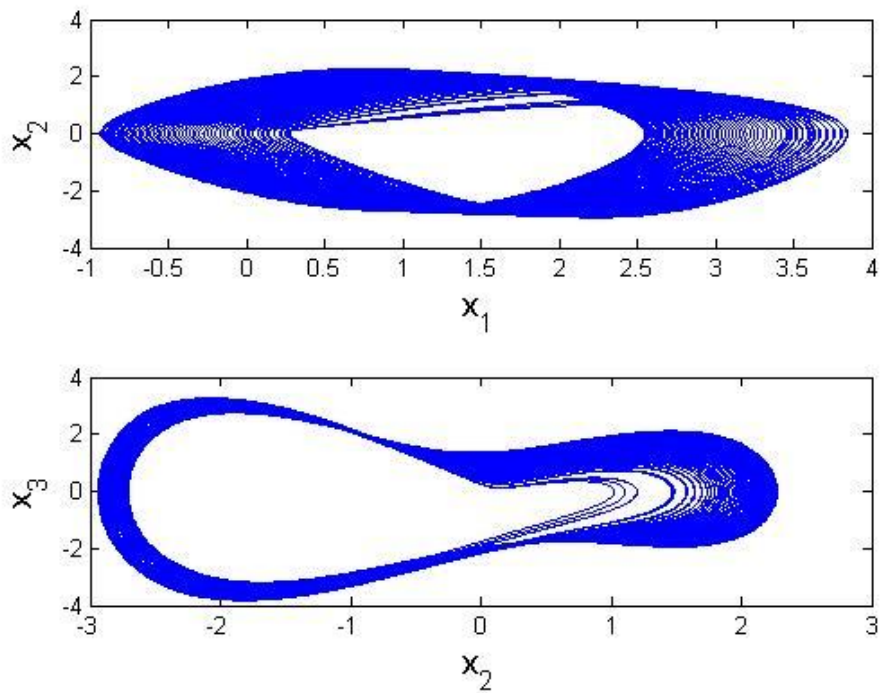


Fig. 6.5. Projections of phase portrait of nonautonomous chaotic Sprott 19 system and

$$a=-0.6, b=2.75.$$

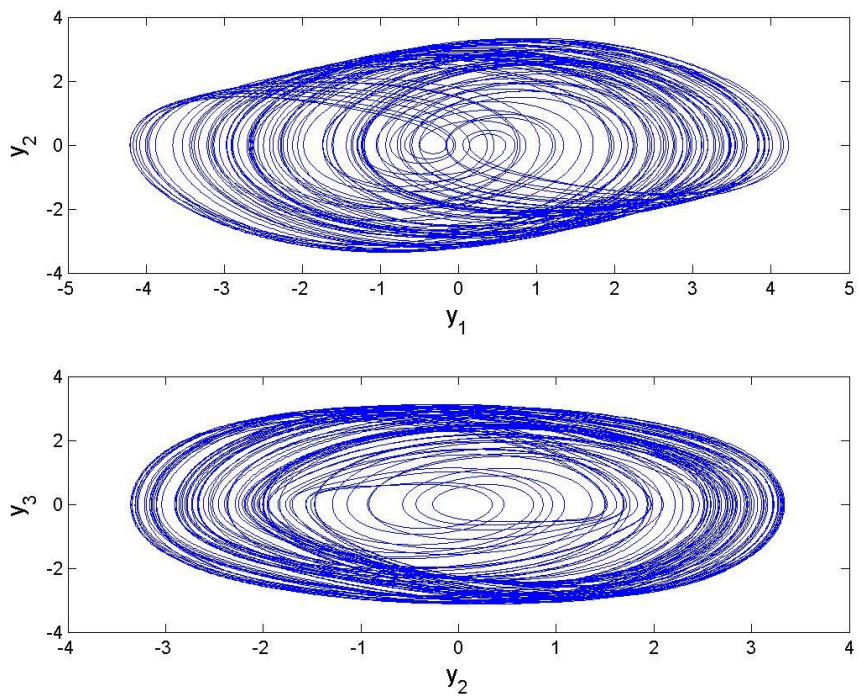


Fig. 6.6. Projections of phase portrait of chaotic Sprott 22 system with controllers.

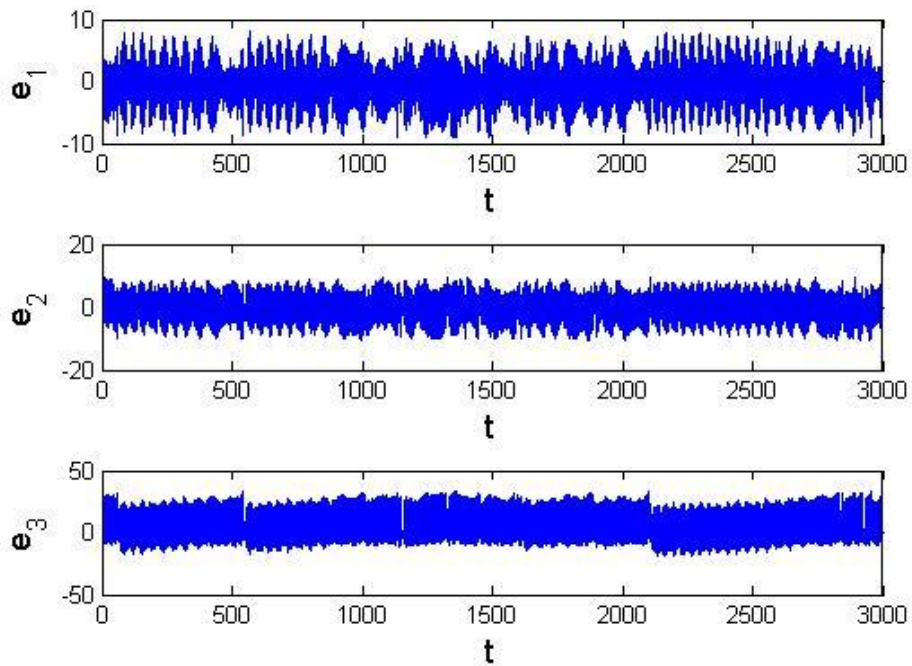


Fig. 6.7. Time histories of error derivatives for master and slave Sprott nonautonomous chaotic systems without controllers.

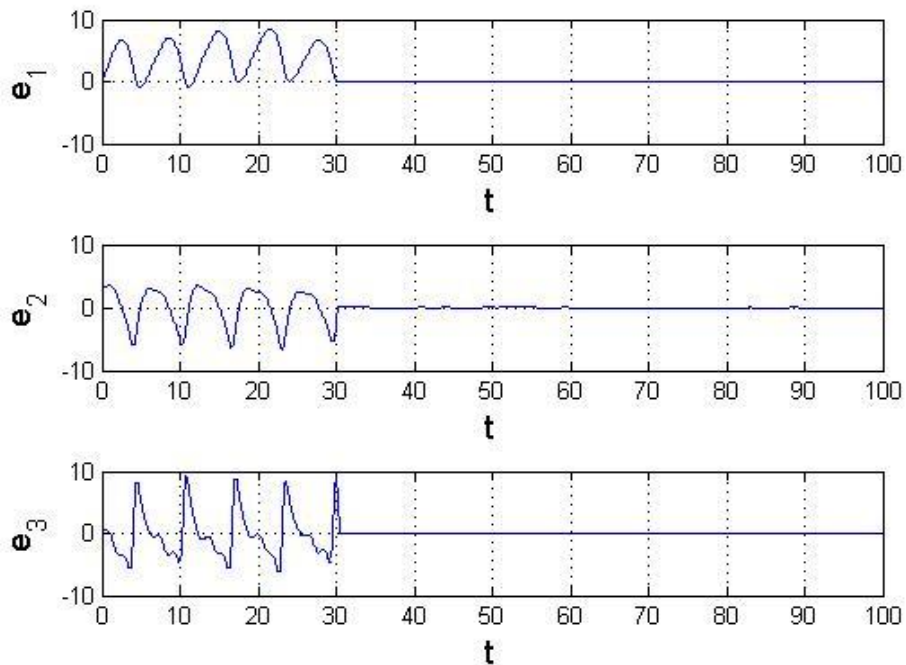


Fig. 6.8. Time histories of errors for Case1 (nonautonomous system) the FLCC is added after 30s.

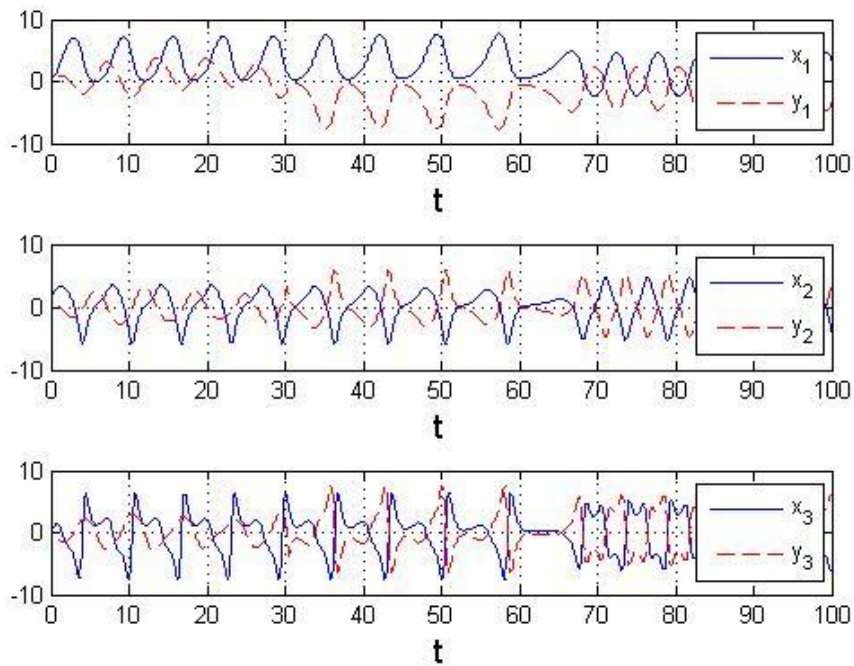


Fig. 6.9. Time histories of states for Case1 (nonautonomous system) the FLCC is added after 30s.

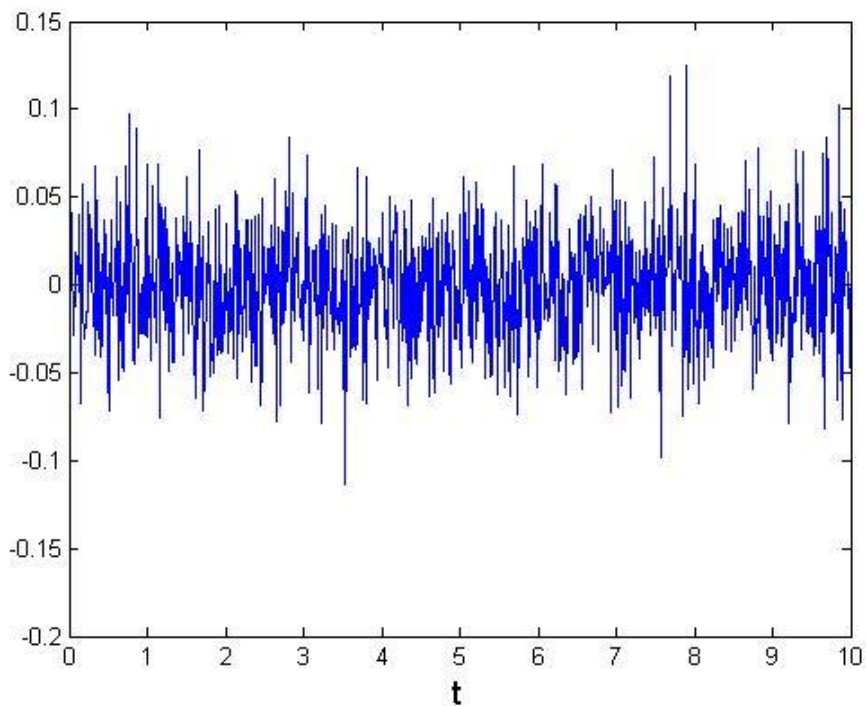


Fig. 6.10. The stochastic signal of Δ_2 is band-limited white noise(PSD=0.1).

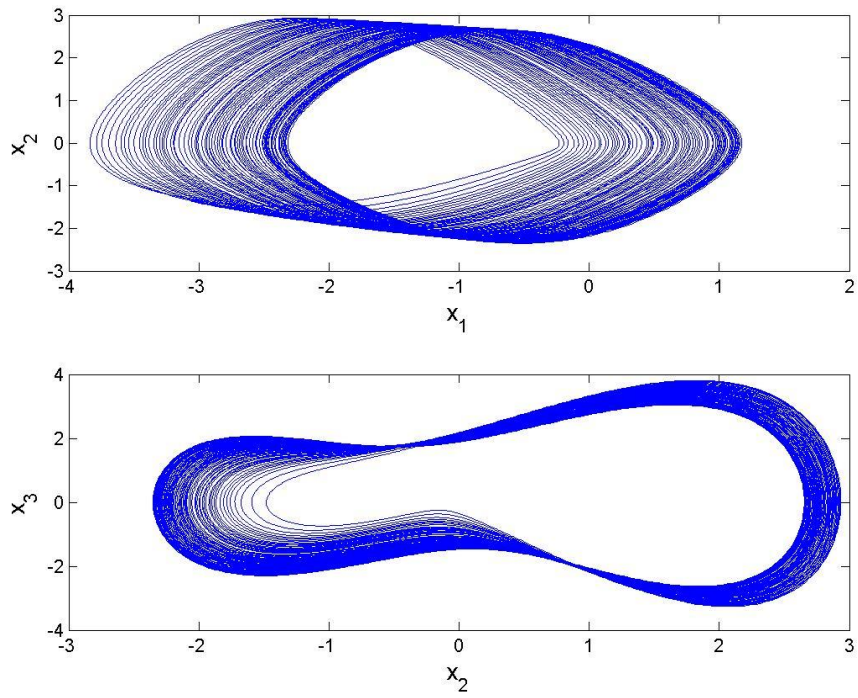


Fig. 6.11. Projections of phase portrait of nonautonomous chaotic Sprott 19 system with stochastic disturbance Δ_2 , $a=-0.6$ and $b=2.75$.

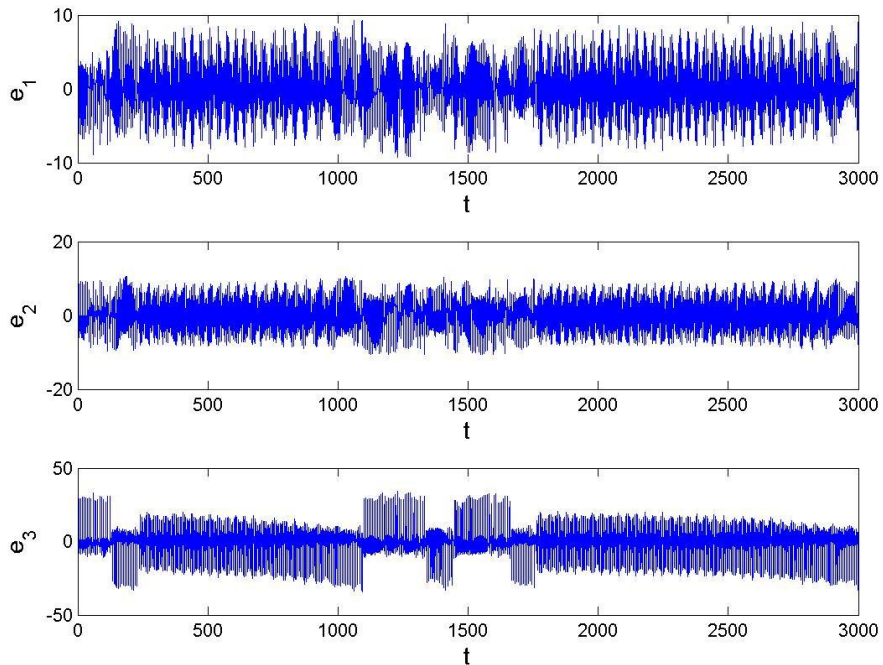


Fig. 6.12. Time histories of error derivatives for master and slave Sprott chaotic systems without controllers.

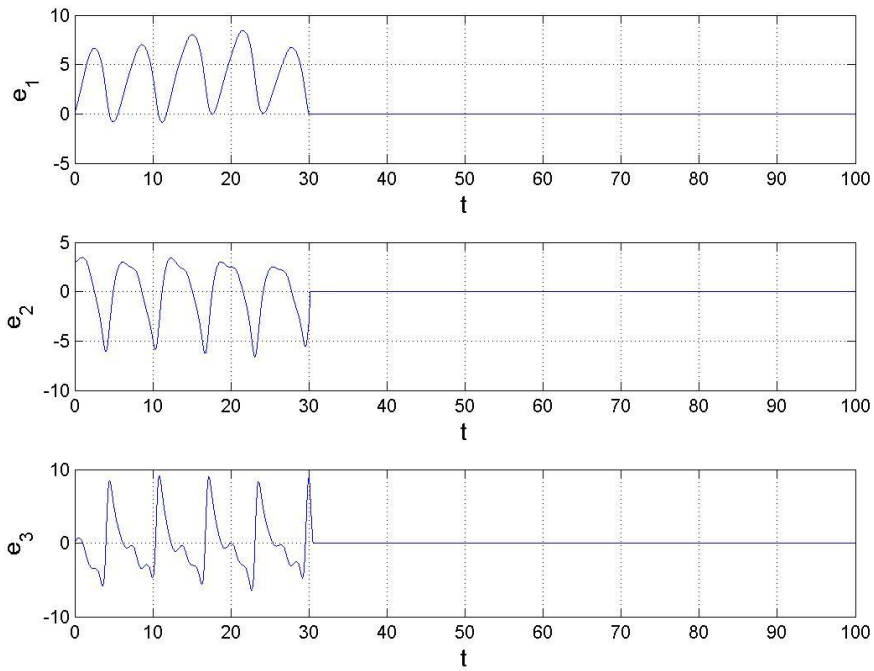


Fig. 6.13. Time histories of errors for subsection 3.1.2, the FLCC is applied after 30s.

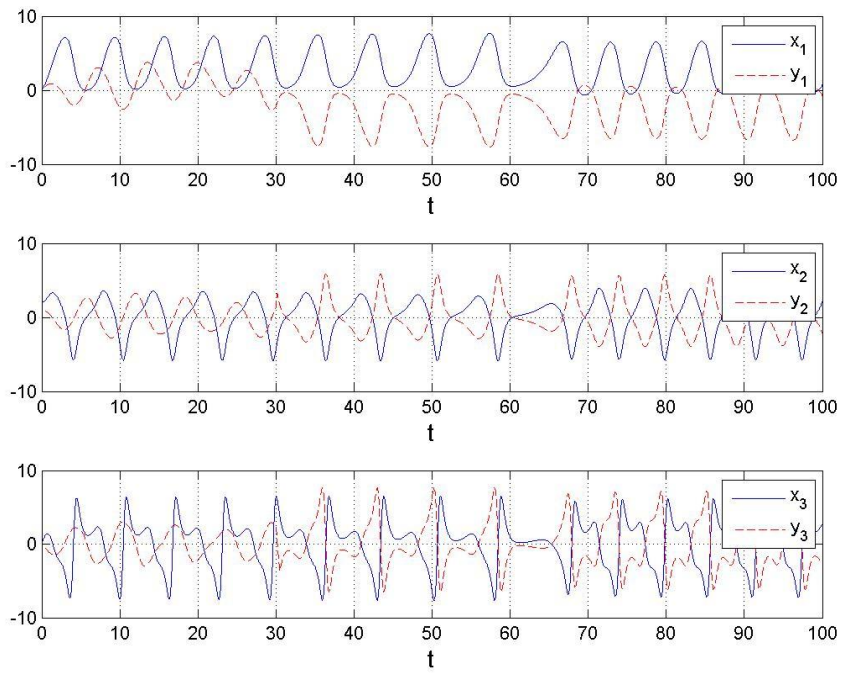


Fig. 6.14. Time histories of states for subsection 3.1.2, the FLCC is applied after 30s.

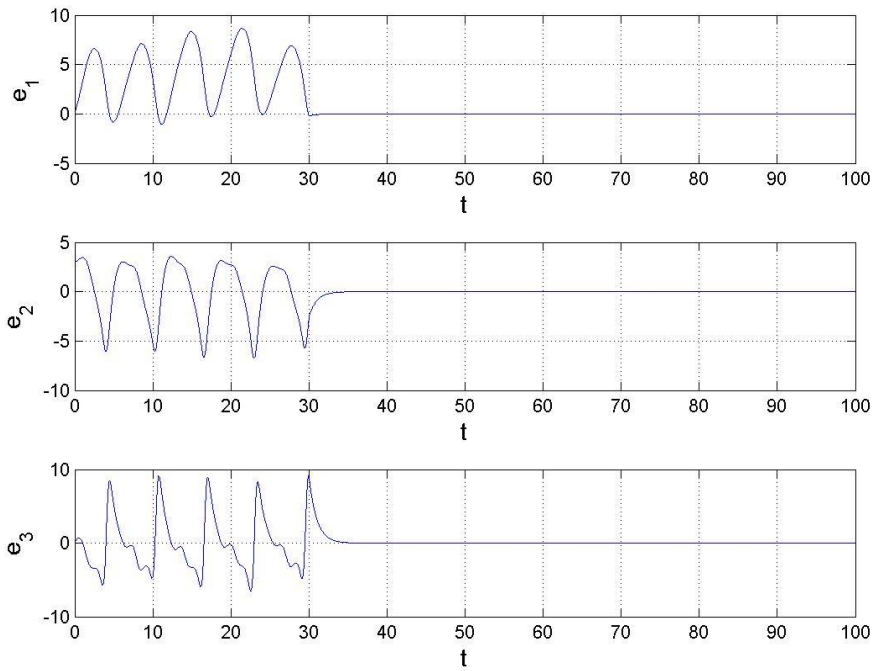


Fig. 6.15. Time histories of errors for subsection 3.1.3 the traditional nonlinear controller is applied after 30s.

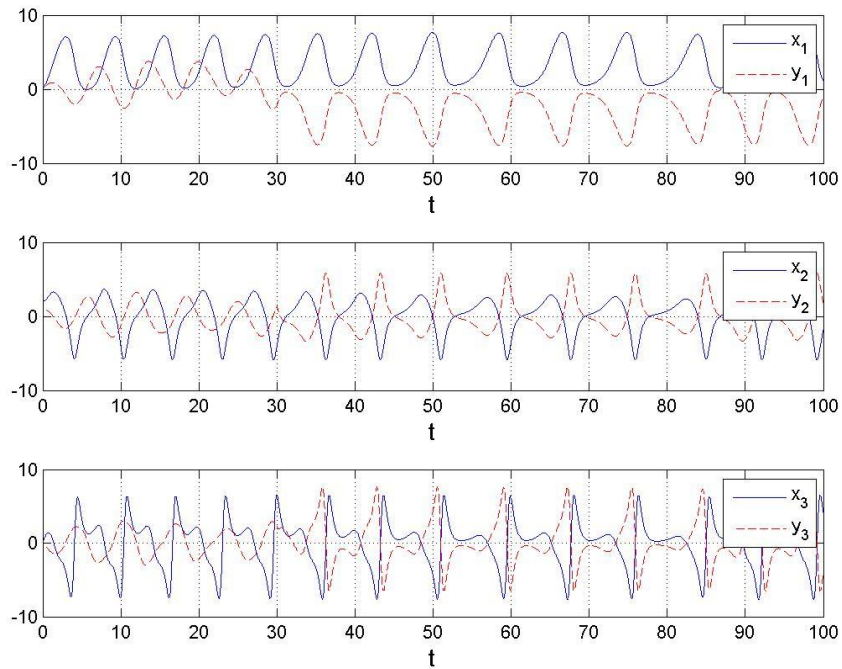


Fig. 6.16. Time histories of states for subsection 3.1.3 the traditional nonlinear controller is applied after 30s.

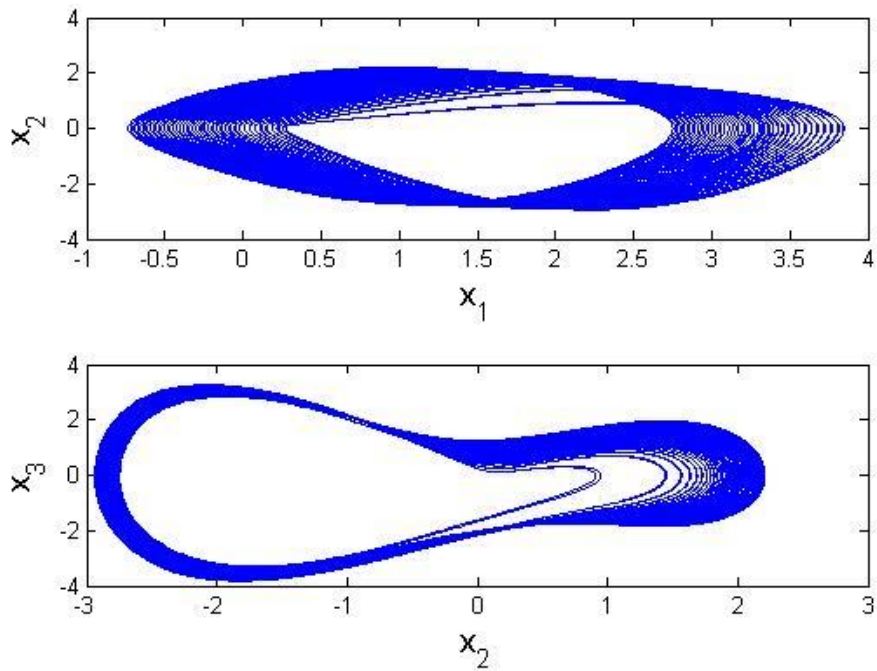


Fig. 6.17. Projections of phase portrait of nonautonomous chaotic Sprott 19 system with stochastic disturbance where $a=-0.6$, $b=2.75$.

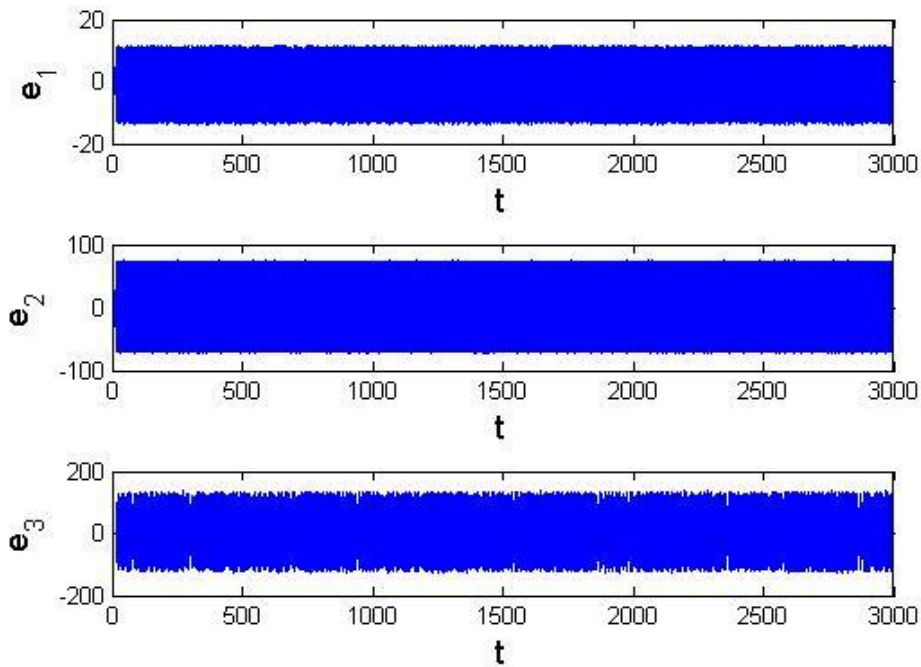


Fig. 6.18. Time histories of error derivatives for subsection 3.2.1.

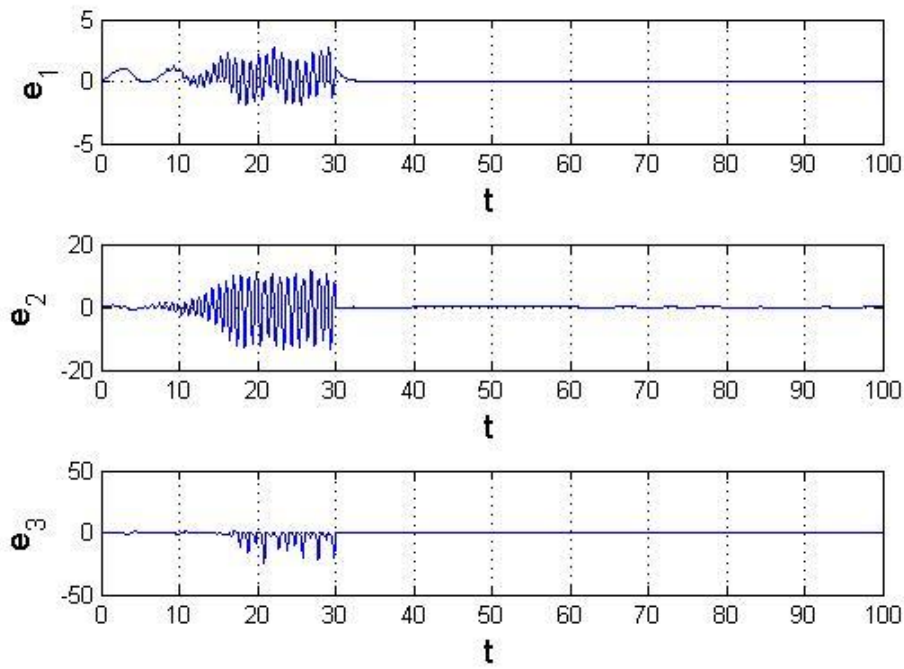


Fig. 6.19. Time histories of errors for section 3.2 where FLCC is added after 30s.

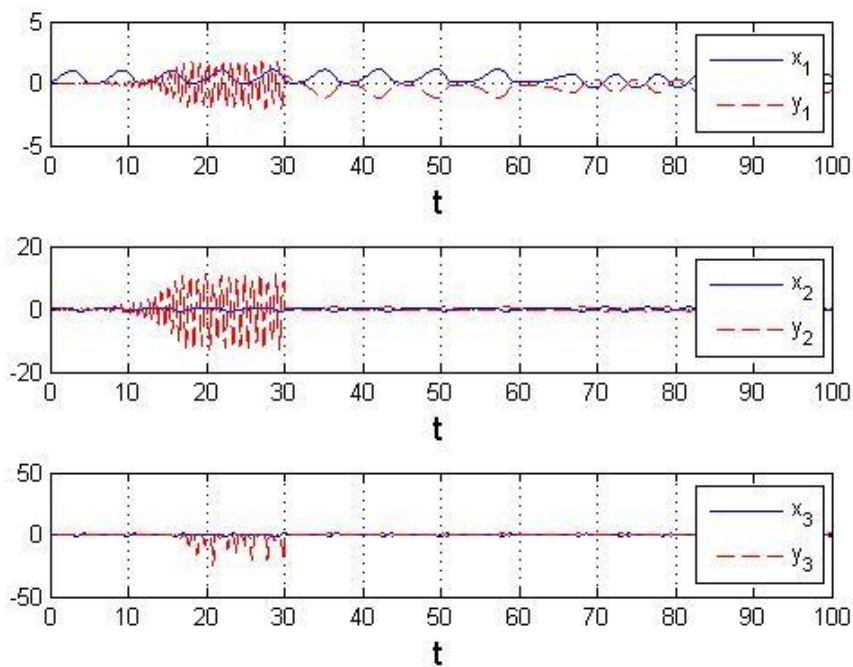
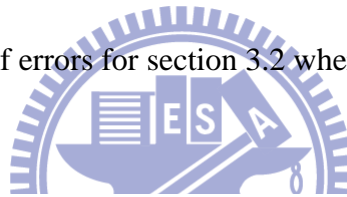


Fig. 6.20. Time histories of states for subsection 2-3.2 the FLCC is coming into after

30s.

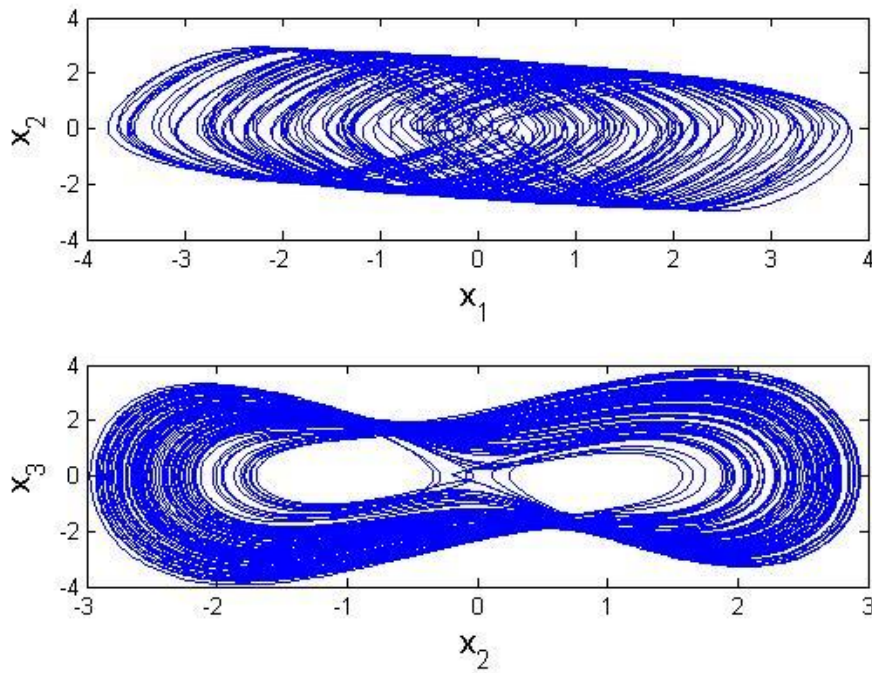


Fig. 6.21. Projections of phase portrait of nonautonomous chaotic Sprott 19 system with stochastic disturbance where $a=-0.6$, $b=2.75$.

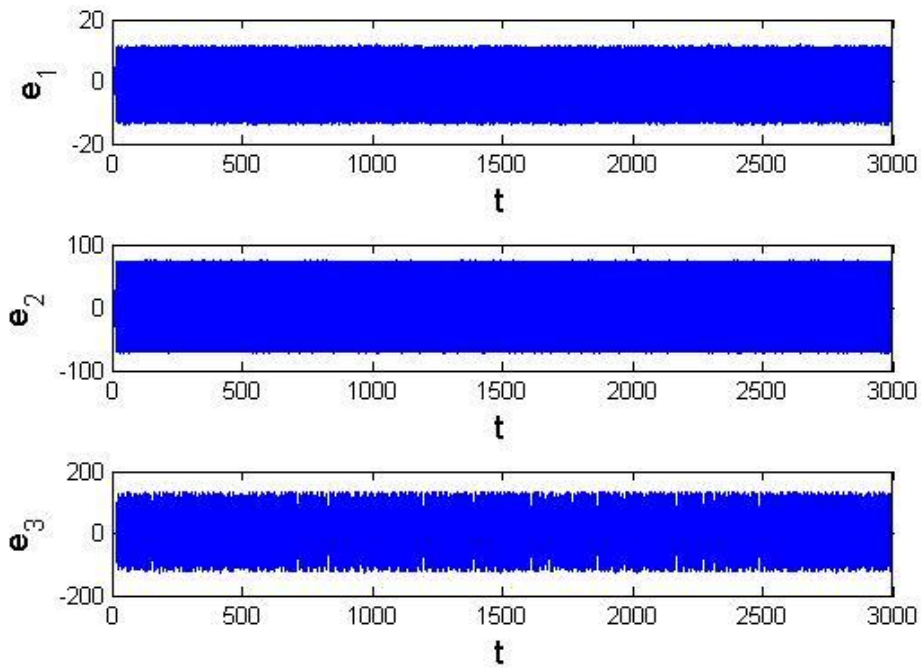


Fig. 6.22. Time histories of error derivatives for Sprott chaotic systems without controllers.

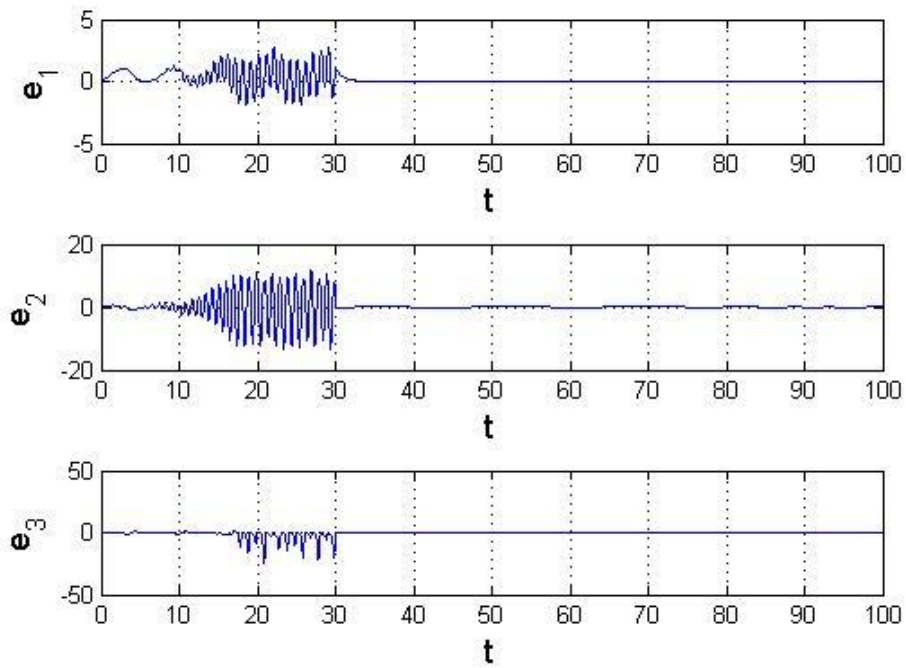


Fig. 6.23. Time histories of errors for subsection 3.2.2 where FLCC are added after

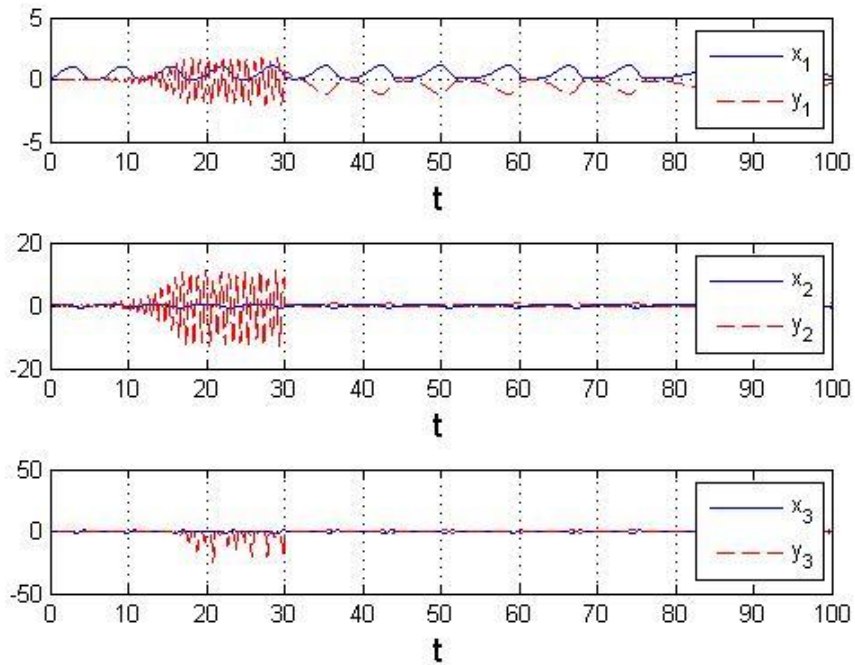


Fig. 6.24. Time histories of states for subsection 3.2.2 where the FLCC are added after

30s.

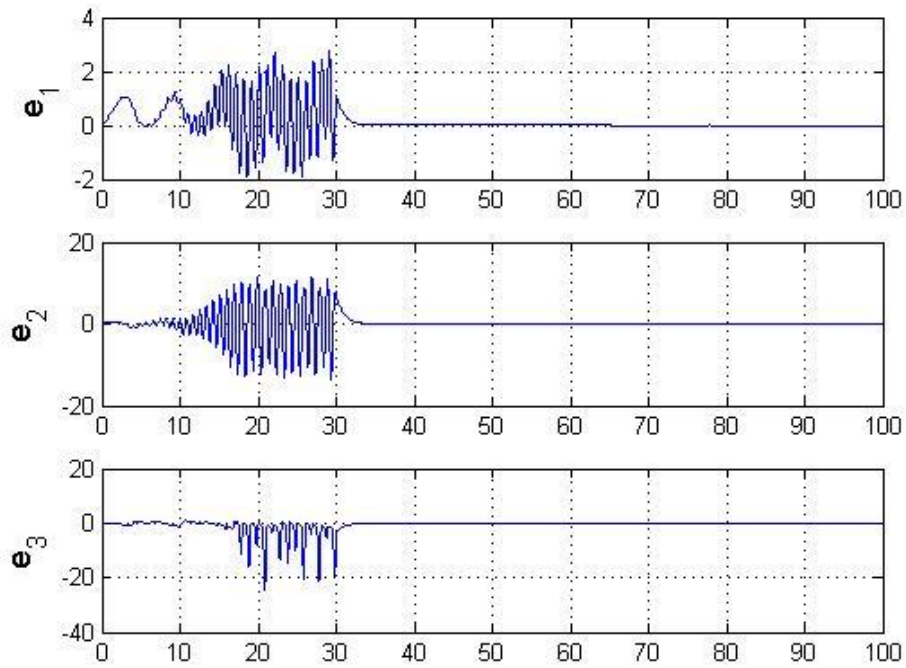


Fig. 6.25. Time histories of errors for subsection 3.2.3 where the traditional controllers are added into after 30s.

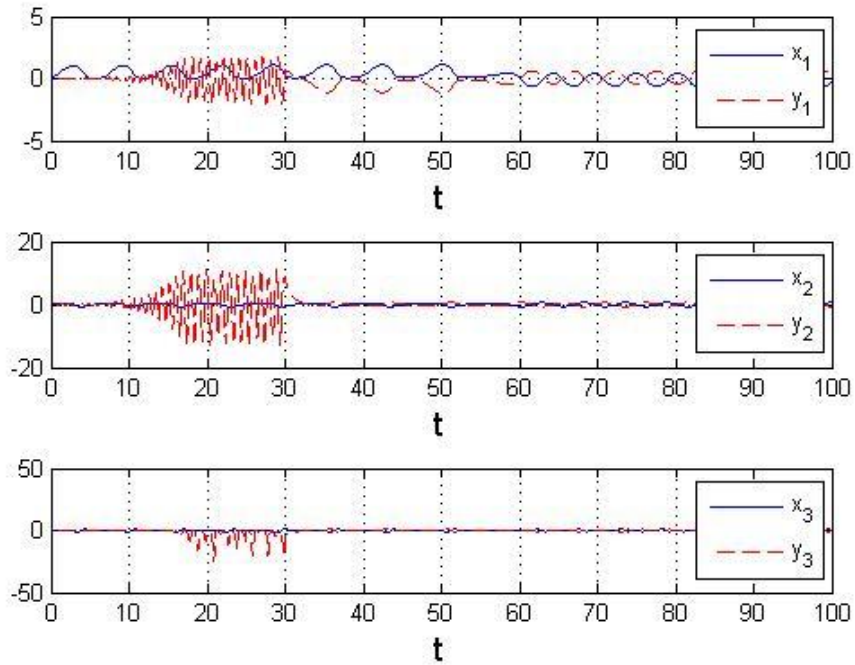


Fig. 6.26. Time histories of states for subsection 3.2.3 where the traditional controllers are added into after 30s.

Chapter 7

Fuzzy Modeling and Synchronization of Chaotic

Systems by a New Fuzzy Model

7.1 Preliminary

In this Chapter, a new fuzzy model [61] is used to simulate and synchronize two different chaotic systems. Via the new fuzzy model, a complicated nonlinear system is linearized to a simple form – linear coupling of only two linear subsystems and the numbers of fuzzy rules can be reduced from 2^N to $2 \times N$ (where N is the number of nonlinear terms). The fuzzy equations become much simpler.

7.2 New Fuzzy Model Theory

In system analysis and design, it is important to select an appropriate model representing a real system. As an expression model of a real plant, the fuzzy implications and the fuzzy reasoning method suggested by Takagi and Sugeno are traditionally used. The new fuzzy model is also described by fuzzy IF-THEN rules. The core of the new fuzzy model is that we express each nonlinear equation into two linear sub-equations by fuzzy IF-THEN rules and take all the first linear sub-equations to form one linear subsystem and all the second linear sub-equations to form another linear subsystem. The overall fuzzy model of the system is achieved by fuzzy blending of this two linear subsystem models. Consider a continuous-time nonlinear dynamic system as follows:

Equation i:

rule 1:

IF $z_i(t)$ is M_{i1}

THEN $\dot{x}_i(t) = A_{i1}x(t) + B_{i1}u(t)$,

rule 2:

$$\begin{aligned} \text{IF } z_i(t) \text{ is } M_{i2} \\ \text{THEN } \dot{x}_i(t) = A_{i2}x(t) + B_{i2}u(t), \end{aligned} \quad (7.1)$$

where

$$x(t) = [x_1(t), x_2(t), \dots, x_n(t)]^T,$$

$$u(t) = [u_1(t), u_2(t), \dots, u_n(t)]^T,$$

$i=1,2,\dots,n$, where n is the number of nonlinear terms. M_{i1}, M_{i2} are fuzzy sets, A_i, B_i are column vectors and $\dot{x}_i(t) = A_{ij}x(t) + B_{ij}u(t)$, $j=1,2$, is the output from the first and the second IF-THEN rules. Given a pair of $(\mathbf{x}(t), \mathbf{u}(t))$ and take all the first linear sub-equations to form one linear subsystem and all the second linear sub-equations to form another linear subsystem, the final output of the fuzzy system is inferred as follows:

$$\dot{x}(t) = M_1 \begin{bmatrix} A_{11}x(t) + B_{11}u(t) \\ A_{21}x(t) + B_{21}u(t) \\ \vdots \\ A_{i1}x(t) + B_{i1}u(t) \end{bmatrix} + M_2 \begin{bmatrix} A_{12}x(t) + B_{12}u(t) \\ A_{22}x(t) + B_{22}u(t) \\ \vdots \\ A_{i2}x(t) + B_{i2}u(t) \end{bmatrix} \quad (7.2)$$

where M_1 and M_2 are diagonal matrices as following:

$$\text{dia}(M_1) = [M_{11} \quad M_{21} \quad \dots \quad M_{i1}], \quad \text{dia}(M_2) = [M_{12} \quad M_{22} \quad \dots \quad M_{i2}]$$

Note that for each equation i :

$$\sum_{j=1}^2 M_{ij}(z_i(t)) = 1,$$

$$M_{ij}(z_i(t)) \geq 0, \quad i = 1, 2, \dots, n \text{ and } j=1,2.$$

Via the new fuzzy model, the final form of the fuzzy model becomes very simple. The new model provides a much more convenient approach for fuzzy model research and fuzzy application. The simulation results of chaotic systems are discussed in next Section.

7.3 New Fuzzy Model of Chaotic Systems

In this Section, the new fuzzy models of three chaotic systems, Sprott 19 system, Sprott 22 system and Lorenz system, are given for Model 1, Model 2 and Model 3.

Model system:

$$\begin{cases} \dot{x}_1 = x_2 \\ \dot{x}_2 = x_3 \\ \dot{x}_3 = ax_3 + bx_2 - x_2^3 - x_1 \end{cases} \quad (7.3)$$

When initial condition $(x_{10}, x_{20}, x_{30}) = (0, 1, 0)$ and parameters $a = -0.6, b = 2.75$, chaos of the Sprott 19 system appears. The chaotic behavior of Eq. (7.3) is shown in Fig. 7.1.

Model 1: New Fuzzy Model of Sprott 19 System with Uncertainty

The Sprott 19 system with uncertainty is:

$$\begin{cases} \dot{x}_1 = x_2 + \Delta_1 \\ \dot{x}_2 = x_3 + \Delta_2 \\ \dot{x}_3 = ax_3 + bx_2 - x_2^3 - x_1 \end{cases} \quad (7.4)$$

with initial condition $(x_{10}, x_{20}, x_{30}) = (0, 1, 0)$. Uncertain terms are Δ_1 is white noise in Fig. 7.2 and Δ_2 is pulse generator in Fig. 7.3 with parameters are $a = -0.6, b = 2.75$, chaos of the Sprott 19 system with uncertainty appears. The chaotic behavior of Eq. (7.4) is shown in Fig. 7.4.

If T-S fuzzy model is used for representing local linear models of Sprott 19 system with uncertainty, $N = 3$, $2^N = 2^3 = 8$, 8 fuzzy rules and 8 linear subsystems are need. The process of modeling is shown as follows:

T-S fuzzy model:

Assume that:

- (1) $\Delta_1 \in [-Z_1, Z_1]$ and $Z_1 > 0$
- (2) $\Delta_2 \in [-Z_2, Z_2]$ and $Z_2 > 0$

(3) $x_2^2 \in [-Z_3, Z_3]$ and $Z_3 > 0$

Then we have the following T-S fuzzy rules:

Rule 1: IF Δ_1 is M_{11} , Δ_2 is M_{21} and x_2^2 is M_{31} THEN $\dot{X} = A_1 X$,

Rule 2: IF Δ_1 is M_{11} , Δ_2 is M_{21} and x_2^2 is M_{32} THEN $\dot{X} = A_2 X$,

Rule 3: IF Δ_1 is M_{11} , Δ_2 is M_{22} and x_2^2 is M_{31} THEN $\dot{X} = A_3 X$,

Rule 4: IF Δ_1 is M_{11} , Δ_2 is M_{22} and x_2^2 is M_{32} THEN $\dot{X} = A_4 X$,

Rule 5: IF Δ_1 is M_{12} , Δ_2 is M_{21} and x_2^2 is M_{31} THEN $\dot{X} = A_5 X$,

Rule 6: IF Δ_1 is M_{12} , Δ_2 is M_{21} and x_2^2 is M_{32} THEN $\dot{X} = A_6 X$,

Rule 7: IF Δ_1 is M_{12} , Δ_2 is M_{22} and x_2^2 is M_{31} THEN $\dot{X} = A_7 X$,

Rule 8: IF Δ_1 is M_{12} , Δ_2 is M_{22} and x_2^2 is M_{32} THEN $\dot{X} = A_8 X$,

Then the final output of the Sprott 19 system with uncertainty can be composed by fuzzy linear subsystems mentioned above. It is obviously an inefficient and complicated work.

New fuzzy model:

By using the new fuzzy model, Sprott 19 system with uncertainty can be linearized as simple linear equations. The steps of fuzzy modeling are shown as follows:

Steps of fuzzy modeling:

Step 1:

Assume that $\Delta_1 \in [-Z_1, Z_1]$ and $Z_1 > 0$, then the first equation of (7.4) can be exactly represented by new fuzzy model as following:

$$\text{Rule 1: IF } \Delta_1 \text{ is } M_{11}, \text{ THEN } \dot{x}_1 = x_2 + Z_1, \quad (7.5)$$

$$\text{Rule 2: IF } \Delta_1 \text{ is } M_{12}, \text{ THEN } \dot{x}_1 = x_2 - Z_1, \quad (7.6)$$

where

$$M_{11} = \frac{1}{2} \left(1 + \frac{\Delta_1}{Z_1}\right), \quad M_{12} = \frac{1}{2} \left(1 - \frac{\Delta_1}{Z_1}\right),$$

and $Z_1 = 2$. M_{11} and M_{12} are fuzzy sets of the first equation of (7.4) and

$$M_{11} + M_{12} = 1.$$

Step 2:

Assume that $\Delta_2 \in [-Z_2, Z_2]$ and $Z_2 > 0$, then the second equation of (7.4) can be exactly represented by new fuzzy model as following:

$$\text{Rule 1: IF } \Delta_2 \text{ is } M_{21}, \text{ THEN } \dot{x}_2 = x_3 + Z_2, \quad (7.7)$$

$$\text{Rule 2: IF } \Delta_2 \text{ is } M_{22}, \text{ THEN } \dot{x}_2 = x_3 - Z_2, \quad (7.8)$$

where

$$M_{21} = \frac{1}{2} \left(1 + \frac{\Delta_2}{Z_2}\right), \quad M_{22} = \frac{1}{2} \left(1 - \frac{\Delta_2}{Z_2}\right),$$

and $Z_2 = 0.001$. M_{21} and M_{22} are fuzzy sets of the second equation of (7.4) and

$$M_{21} + M_{22} = 1.$$

Step 3:

Assume that $x_2^2 \in [-Z_3, Z_3]$ and $Z_3 > 0$, then the third equation of (7.4) can be exactly represented by new fuzzy model as following:

$$\text{Rule 1: IF } x_2^2 \text{ is } M_{31}, \text{ THEN } \dot{x}_3 = ax_3 + bx_2 - Z_3x_2 - x_1, \quad (7.9)$$

$$\text{Rule 2: IF } x_2^2 \text{ is } M_{32}, \text{ THEN } \dot{x}_3 = ax_3 + bx_2 + Z_3x_2 - x_1, \quad (7.10)$$

where

$$M_{31} = \frac{1}{2} \left(1 + \frac{x_2^2}{Z_3}\right), \quad M_{32} = \frac{1}{2} \left(1 - \frac{x_2^2}{Z_3}\right),$$

and $Z_3 = 10$. M_{31} and M_{32} are fuzzy sets of the third equation of (7.4) and

$$M_{31} + M_{32} = 1.$$

Here, we call Eqs.(7.5), (7.7) and (7.9) the first linear subsystem under the fuzzy rules, and Eqs.(7.6), (7.8) and (7.10) the second linear subsystem under the fuzzy rules.

The first linear subsystem is

$$\begin{cases} \dot{x}_1 = x_2 + Z_1 \\ \dot{x}_2 = x_3 + Z_2 \\ \dot{x}_3 = ax_3 + bx_2 - Z_3x_2 - x_1 \end{cases} \quad (7.11)$$

The second linear subsystem is

$$\begin{cases} \dot{x}_1 = x_2 - Z_1 \\ \dot{x}_2 = x_3 - Z_2 \\ \dot{x}_3 = ax_3 + bx_2 + Z_3x_2 - x_1 \end{cases} \quad (7.12)$$

The final output of the fuzzy Sprott 19 system with uncertainty is inferred as follows and the chaotic behavior of fuzzy system is shown in Fig. 7.5. Now we have:

$$\begin{aligned} \begin{bmatrix} \dot{x}_1 \\ \dot{x}_2 \\ \dot{x}_3 \end{bmatrix} &= \begin{bmatrix} M_{11} & 0 & 0 \\ 0 & M_{21} & 0 \\ 0 & 0 & M_{31} \end{bmatrix} \begin{bmatrix} x_2 + Z_1 \\ x_3 + Z_2 \\ ax_3 + bx_2 - Z_3x_2 - x_1 \end{bmatrix} \\ &+ \begin{bmatrix} M_{12} & 0 & 0 \\ 0 & M_{22} & 0 \\ 0 & 0 & M_{32} \end{bmatrix} \begin{bmatrix} x_2 - Z_1 \\ x_3 - Z_2 \\ ax_3 + bx_2 + Z_3x_2 - x_1 \end{bmatrix} \end{aligned} \quad (7.13)$$

Eq. (7.13) can be rewritten as a simple mathematical expression:

$$\dot{X}(t) = \sum_{i=1}^2 \Psi_i (A_i X(t) + \tilde{b}_i) \quad (7.14)$$

where Ψ_i are diagonal matrices as follows:

$$dia(\Psi_1) = [M_{11} \quad M_{21} \quad M_{31}], \quad dia(\Psi_2) = [M_{12} \quad M_{22} \quad M_{32}]$$

$$A_1 = \begin{bmatrix} 0 & 1 & \bar{0} \\ 0 & 0 & 1 \\ -1 & b - Z_3 & a \end{bmatrix}, \quad \tilde{b}_1 = \begin{bmatrix} Z_1 \\ Z_2 \\ 0 \end{bmatrix}$$

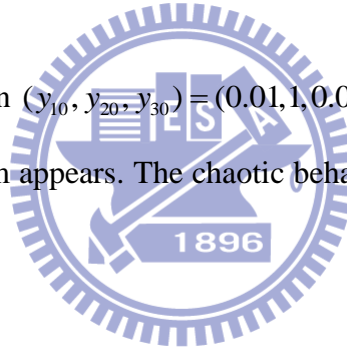
$$A_2 = \begin{bmatrix} 0 & 1 & 0 \\ 0 & 0 & 1 \\ -1 & b + Z_3 & d \end{bmatrix}, \tilde{b}_2 = \begin{bmatrix} -Z_1 \\ -Z_2 \\ 0 \end{bmatrix}$$

Via new fuzzy model, the number of fuzzy rules can be greatly reduced. Just two linear subsystems are enough to express such complex chaotic behaviors. The simulation results are similar the original chaotic behavior of the Sprott 19 system with uncertainty as show in Fig. 7.5.

Model system:

$$\begin{cases} \dot{y}_1 = y_2 \\ \dot{y}_2 = y_3 \\ \dot{y}_3 = -cy_3 - y_2 - \sin y_1 \end{cases} \quad (7.15)$$

When initial condition $(y_{10}, y_{20}, y_{30}) = (0.01, 1, 0.01)$ and parameter $c = 0.25$, chaos of the Sprott 22 system appears. The chaotic behavior of Eq. (7.15) is shown in Fig. 7.6.



Model 2: New Fuzzy Model of Sprott 22 System with Uncertainty

The Sprott 22 system with uncertainty is:

$$\begin{cases} \dot{y}_1 = y_2 + \Delta_1 \\ \dot{y}_2 = y_3 + \Delta_2 \\ \dot{y}_3 = -cy_3 - y_2 - \sin y_1 \end{cases} \quad (7.16)$$

where uncertainty Δ_1 is pulse generator show in Fig. 7.3, Δ_2 is white noise (PSD=0.01) show in Fig. 7.2, $c = 0.25$, and initial conditions are chosen as $(0.01, 1, 0.01)$, the Sprott 22 model with uncertainty exhibits chaotic motion which is shown in Fig. 7.7

New fuzzy model:

Assume that:

- (1) $\Delta_1 \in [-Z_4, Z_4]$ and $Z_4 > 0$,
- (2) $\Delta_2 \in [-Z_5, Z_5]$ and $Z_5 > 0$,
- (3) $\sin y_1 \in [-Z_6, Z_6]$ and $Z_6 > 0$,

then we have the following new fuzzy rules:

$$\text{Rule 1: IF } \Delta_1 \text{ is } N_{11}, \text{ THEN } \dot{y}_1 = y_2 + Z_4, \quad (7.17)$$

$$\text{Rule 2: IF } \Delta_1 \text{ is } N_{12}, \text{ THEN } \dot{y}_1 = y_2 - Z_4, \quad (7.18)$$

where

$$N_{11} = \frac{1}{2} \left(1 + \frac{\Delta_1}{Z_4}\right), \quad N_{12} = \frac{1}{2} \left(1 - \frac{\Delta_1}{Z_4}\right).$$

and

$$\text{Rule 1: IF } \Delta_2 \text{ is } N_{21}, \text{ THEN } \dot{y}_2 = y_3 + Z_5, \quad (7.19)$$

$$\text{Rule 2: IF } \Delta_2 \text{ is } N_{22}, \text{ THEN } \dot{y}_2 = y_3 - Z_5, \quad (7.20)$$

where

$$N_{21} = \frac{1}{2} \left(1 + \frac{\Delta_2}{Z_5}\right), \quad N_{22} = \frac{1}{2} \left(1 - \frac{\Delta_2}{Z_5}\right).$$

and

$$\text{Rule 1: IF } \sin y_1 \text{ is } N_{31}, \text{ THEN } \dot{y}_3 = -cy_3 - y_2 - Z_6, \quad (7.21)$$

$$\text{Rule 2: IF } \sin y_1 \text{ is } N_{32}, \text{ THEN } \dot{y}_3 = -cy_3 - y_2 + Z_6, \quad (7.22)$$

where

$$N_{31} = \frac{1}{2} \left(1 + \frac{\sin y_1}{Z_6}\right), \quad N_{32} = \frac{1}{2} \left(1 - \frac{\sin y_1}{Z_6}\right).$$

in Eqs. (7.17)~(7.22), $Z_4 = 0.00015$, $Z_5 = 0.05$ and $Z_6 = 1$.

N_{11} , N_{12} , N_{21} , N_{22} , N_{31} and N_{32} are fuzzy sets of Eq.(7.16)

and $N_{11} + N_{12} = 1$, $N_{21} + N_{22} = 1$ and $N_{31} + N_{32} = 1$

Here, we call (7.17) ,(7.19) and (7.21) the first liner subsystem under the fuzzy rules and (7.18) , (7.20) and (7.22) the second liner subsystem under the fuzzy rules.

The first linear subsystem is

$$\begin{cases} \dot{y}_1 = y_2 + Z_4 \\ \dot{y}_2 = y_3 + Z_5 \\ \dot{y}_3 = -cy_3 - y_2 - Z_6 \end{cases} \quad (7.23)$$

The second linear subsystem is

$$\begin{cases} \dot{y}_1 = y_2 - Z_4 \\ \dot{y}_2 = y_3 - Z_5 \\ \dot{y}_3 = -cy_3 - y_2 + Z_6 \end{cases} \quad (7.24)$$

The final output of the fuzzy Sprott 22 system with uncertainty is inferred as follows and the chaotic behavior of fuzzy system is shown in Fig. 7.8.

$$\begin{aligned} \begin{bmatrix} \dot{y}_1 \\ \dot{y}_2 \\ \dot{y}_3 \end{bmatrix} &= \begin{bmatrix} N_{11} & 0 & 0 \\ 0 & N_{21} & 0 \\ 0 & 0 & N_{31} \end{bmatrix}^T \begin{bmatrix} y_2 + Z_4 \\ y_3 + Z_5 \\ -cy_3 - y_2 - Z_6 \end{bmatrix} \\ &+ \begin{bmatrix} N_{12} & 0 & 0 \\ 0 & N_{22} & 0 \\ 0 & 0 & N_{32} \end{bmatrix}^T \begin{bmatrix} y_2 - Z_4 \\ y_3 - Z_5 \\ -cy_3 - y_2 + Z_6 \end{bmatrix} \end{aligned} \quad (7.25)$$

Eq. (7.25) can be rewritten as a simple mathematical expression:

$$\dot{Y}(t) = \sum_{i=1}^2 \Gamma_i (C_i Y(t) + \tilde{c}_i) \quad (7.26)$$

where

$$\text{dia}(\Gamma_1) = [N_{11} \quad N_{21} \quad N_{31}], \quad \text{dia}(\Gamma_2) = [N_{12} \quad N_{22} \quad N_{32}]$$

$$C_1 = \begin{bmatrix} 0 & 1 & 0 \\ 0 & 0 & 1 \\ 0 & -1 & -c \end{bmatrix}, \quad \tilde{c}_1 = \begin{bmatrix} Z_4 \\ Z_5 \\ -Z_6 \end{bmatrix}$$

$$C_2 = \begin{bmatrix} 0 & 1 & 0 \\ 0 & 0 & 1 \\ 0 & -1 & -c \end{bmatrix}, \quad \tilde{c}_2 = \begin{bmatrix} -Z_4 \\ -Z_5 \\ Z_6 \end{bmatrix}$$

Via new fuzzy model, two linear subsystems are enough to express such complex chaotic behaviors. The simulation results are similar the original chaotic behavior of

the Sprott 22 system with uncertainty in Fig. 7.8.

Model system:

$$\begin{cases} \dot{x}_1 = -g(x_1 - x_2) \\ \dot{x}_2 = -x_1 x_3 + h x_1 - x_2 \\ \dot{x}_3 = x_1 x_2 - l x_3 \end{cases}$$

When initial condition $(x_{10}, x_{20}, x_{30}) = (6, 5, 10)$ and parameters $g = 10$, $h = 27.43$ and $l = 8/3$, chaos of the Lorenz system appears.

Model 3: New Fuzzy Model of Lorenz System

The Lorenz system is:

$$\begin{cases} \dot{x}_1 = -g(x_1 - x_2) \\ \dot{x}_2 = -x_1 x_3 + h x_1 - x_2 \\ \dot{x}_3 = x_1 x_2 - l x_3 \end{cases} \quad (7.27)$$

With $g = 10$, $h = 27.43$, $l = 8/3$, and initial conditions are chosen as $(6, 5, 10)$, the Lorenz model exhibits chaotic motion which is shown in Fig. 7.9.

New fuzzy model:

Assume that:

- (1) $x_3 \in [-Z_7, Z_7]$ and $Z_7 > 0$,
- (2) $x_2 \in [-Z_8, Z_8]$ and $Z_8 > 0$,

then we have the following new fuzzy rules:

\dot{x}_1 is a linear term, so it doesn't need to linearize

$$\text{Rule 1: } Q_{11} = 0.5, \text{ THEN } \dot{x}_1 = -g(x_1 - x_2), \quad (7.28)$$

$$\text{Rule 2: } Q_{12} = 0.5, \text{ THEN } \dot{x}_1 = -g(x_1 - x_2), \quad (7.29)$$

and

$$\text{Rule 1: IF } x_3 \text{ is } Q_{21}, \text{ THEN } \dot{x}_2 = -x_1 Z_7 + h x_1 - x_2, \quad (7.30)$$

$$\text{Rule 2: IF } x_3 \text{ is } Q_{22}, \text{ THEN } \dot{x}_2 = x_1 Z_7 + h x_1 - x_2, \quad (7.31)$$

where

$$Q_{21} = \frac{1}{2} \left(1 + \frac{x_3}{Z_7}\right), \quad Q_{22} = \frac{1}{2} \left(1 - \frac{x_3}{Z_7}\right).$$

and

$$\text{Rule 1: IF } x_2 \text{ is } Q_{31}, \text{ THEN } \dot{x}_3 = x_1 Z_8 - l x_3, \quad (7.32)$$

$$\text{Rule 2: IF } x_2 \text{ is } Q_{32}, \text{ THEN } \dot{x}_3 = -x_1 Z_8 - l x_3, \quad (7.33)$$

where

$$Q_{31} = \frac{1}{2} \left(1 + \frac{x_2}{Z_8}\right), \quad Q_{32} = \frac{1}{2} \left(1 - \frac{x_2}{Z_8}\right).$$

in Eqs. (7.30)~(7.33), $Z_7 = 50$ and $Z_8 = 30$. $Q_{11}, Q_{12}, Q_{21}, Q_{22}, Q_{31}$ and Q_{32} are fuzzy sets of Eq.(7-12) and $Q_{11} + Q_{12} = 1, Q_{21} + Q_{22} = 1$ and $Q_{31} + Q_{32} = 1$

Here, we call (7.28) ,(7.30) and (7.32) the first liner subsystem under the fuzzy rules and (7.29) , (7.31) and (7.33) the second liner subsystem under the fuzzy rules.

The first linear subsystem is

$$\begin{cases} \dot{x}_1 = -g(x_1 - x_2) \\ \dot{x}_2 = -x_1 Z_7 + h x_1 - x_2 \\ \dot{x}_3 = x_1 Z_8 - l x_3 \end{cases} \quad (7.34)$$

The second linear subsystem is

$$\begin{cases} \dot{x}_1 = -g(x_1 - x_2) \\ \dot{x}_2 = x_1 Z_7 + h x_1 - x_2 \\ \dot{x}_3 = -x_1 Z_8 - l x_3 \end{cases} \quad (7.35)$$

The final output of the fuzzy Lorenz system is inferred as follows and the chaotic behavior of fuzzy system is shown in Fig. 7.10.

$$\begin{aligned} \begin{bmatrix} \dot{x}_1 \\ \dot{x}_2 \\ \dot{x}_3 \end{bmatrix} &= \begin{bmatrix} Q_{11} & 0 & 0 \\ 0 & Q_{21} & 0 \\ 0 & 0 & Q_{31} \end{bmatrix}^T \begin{bmatrix} -g(x_1 - x_2) \\ -x_1 Z_7 + h x_1 - x_2 \\ x_1 Z_8 - l x_3 \end{bmatrix} \\ &+ \begin{bmatrix} Q_{12} & 0 & 0 \\ 0 & Q_{22} & 0 \\ 0 & 0 & Q_{32} \end{bmatrix}^T \begin{bmatrix} -g(x_1 - x_2) \\ x_1 Z_7 + h x_1 - x_2 \\ -x_1 Z_8 - l x_3 \end{bmatrix} \end{aligned} \quad (7.36)$$

Eq. (7.36) can be rewritten as a simple mathematical expression:

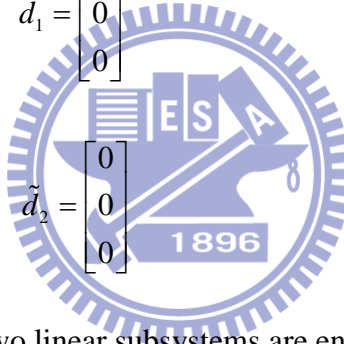
$$\dot{X}(t) = \sum_{i=1}^2 \Gamma_i (D_i X(t) + \tilde{d}_i) \quad (7.37)$$

where

$$\text{dia}(\Gamma_1) = [Q_{11} \quad Q_{21} \quad Q_{31}], \quad \text{dia}(\Gamma_2) = [Q_{12} \quad Q_{22} \quad Q_{32}]$$

$$D_1 = \begin{bmatrix} -g & g & 0 \\ h - Z_7 & -1 & 0 \\ Z_8 & 0 & -l \end{bmatrix}, \quad \tilde{d}_1 = \begin{bmatrix} 0 \\ 0 \\ 0 \end{bmatrix}$$

$$D_2 = \begin{bmatrix} -g & g & 0 \\ h + Z_7 & -1 & 0 \\ -Z_8 & 0 & -l \end{bmatrix}, \quad \tilde{d}_2 = \begin{bmatrix} 0 \\ 0 \\ 0 \end{bmatrix}$$



Via new fuzzy model, two linear subsystems are enough to express such complex chaotic behaviors. The simulation results are similar the original chaotic behavior of the Lorenz system in Fig. 7.10.

7.4 Fuzzy Synchronization Scheme

In this Section, we derive the new fuzzy synchronization scheme based on our new fuzzy model to synchronize two totally different fuzzy chaotic systems. The following fuzzy systems as the master and slave systems are given:

master system:

$$\dot{X}(t) = \sum_{i=1}^2 \Psi_i (A_i X(t) + \tilde{b}_i) \quad (7.38)$$

slave system:

$$\dot{Y}(t) = \sum_{i=1}^2 \Gamma_i (C_i Y(t) + \tilde{c}_i) + BU(t) \quad (7.39)$$

Eq. (7.38) and Eq. (7.39) represent the two different chaotic systems, and in Eq. (7.39) there is control input $U(t)$. Define the error signal as $e(t) = X(t) - Y(t)$, we have:

$$\dot{e}(t) = \dot{X}(t) - \dot{Y}(t) = \sum_{i=1}^2 \Psi_i (A_i X(t) + \tilde{b}_i) - \sum_{i=1}^2 \Gamma_i (C_i Y(t) + \tilde{c}_i) - BU(t) \quad (7.40)$$

The fuzzy controllers are designed as follows:

$$U(t) = u_1(t) + u_2(t) \quad (7.41)$$

where

$$u_1(t) = \sum_{i=1}^2 \Psi_i F_i X(t) - \sum_{i=1}^2 \Gamma_i P_i Y(t),$$

$$u_2(t) = \sum_{i=1}^2 \Psi_i \tilde{b}_i - \sum_{i=1}^2 \Gamma_i \tilde{c}_i$$

such that $\|e(t)\| \rightarrow 0$ as $t \rightarrow \infty$. Our design is to determine the feedback gains F_i and P_i .

By substituting $U(t)$ into Eq.(7.40), we obtain:

$$\dot{e}(t) = \sum_{i=1}^2 \Psi_i \{(A_i - BF_i)X(t)\} - \sum_{i=1}^2 \Gamma_i \{(C_i - BP_i)Y(t)\} \quad (7.42)$$

Theorem 1: The error system in Eq. (7.42) is asymptotically stable and the slave system in Eq. (7.39) can synchronize the master system in Eq. (7.38) under the fuzzy controller in Eq. (7.41) if the following conditions below can be satisfied:

$$G = (A_1 - BF_1) = (A_2 - BF_2) = (C_1 - BP_1) < 0, i=1 \sim 2. \quad (7.43)$$

Proof:

The errors in Eq. (7.42) can be exactly linearized via the fuzzy controllers in Eq. (7.41) if there exist the feedback gains F_i such that

$$(A_1 - BF_1) = (A_2 - BF_2) = (C_1 - BP_1) = (C_2 - BP_2) < 0. \quad (7.44)$$

Then the overall control system is linearized as

$$\dot{e}(t) = Ge(t), \quad (7.45)$$

where $G = (A_1 - BF_1) = (A_2 - BF_2) = (C_1 - BP_1) = (C_2 - BP_2) < 0$.

As a consequence, the zero solution of the error system (7.45) linearized via the

fuzzy controller (7.41) is asymptotically stable.

7.5 Simulation Result

There are two examples in this Section to investigate the effectiveness and feasibility of our new fuzzy model.

Example 1: Synchronization of Sprott 19 System and Sprott 22 System

The fuzzy Sprott 19 system with uncertainty in Eq. (7.4) is chosen as the master system and the fuzzy slave Sprott 22 system with uncertainty in Eq. (7.16), with fuzzy controllers is as follows:

$$\dot{Y}(t) = \sum_{i=1}^2 \Gamma_i (C_i Y(t) + \tilde{c}_i) + BU(t) \quad (7.46)$$

where Γ_i are diagonal matrices

$$\text{dia}(\Gamma_1) = [N_{11} \quad N_{21} \quad N_{31}], \quad \text{dia}(\Gamma_2) = [N_{12} \quad N_{22} \quad N_{32}]$$

and

$$C_1 = \begin{bmatrix} 0 & 1 & 0 \\ 0 & 0 & 1 \\ 0 & -1 & -c \end{bmatrix}, \quad \tilde{c}_1 = \begin{bmatrix} Z_4 \\ Z_5 \\ -Z_6 \end{bmatrix}$$

$$C_2 = \begin{bmatrix} 0 & 1 & 0 \\ 0 & 0 & 1 \\ 0 & -1 & -c \end{bmatrix}, \quad \tilde{c}_2 = \begin{bmatrix} -Z_4 \\ -Z_5 \\ Z_6 \end{bmatrix}.$$

Therefore, the error and error dynamics are:

$$\begin{bmatrix} e_1 \\ e_2 \\ e_3 \end{bmatrix} = \begin{bmatrix} x_1 - y_1 \\ x_2 - y_2 \\ x_3 - y_3 \end{bmatrix},$$

$$\begin{bmatrix} \dot{e}_1 \\ \dot{e}_2 \\ \dot{e}_3 \end{bmatrix} = \begin{bmatrix} \dot{x}_1 - \dot{y}_1 \\ \dot{x}_2 - \dot{y}_2 \\ \dot{x}_3 - \dot{y}_3 \end{bmatrix} = \sum_{i=1}^2 \Psi_i (A_i X(t) + \tilde{b}_i) - \dot{Y}(t) = \sum_{i=1}^2 \Gamma_i (C_i Y(t) + \tilde{c}_i) - BU(t) \quad (7.47)$$

B is chosen as an identity matrix and the fuzzy controllers in Eq. (7.41) are used:

$$\begin{bmatrix} \dot{e}_1 \\ \dot{e}_2 \\ \dot{e}_3 \end{bmatrix} = \Psi_1 [A_1 - BF_1]_{3 \times 3} \begin{bmatrix} x_1 \\ x_2 \\ x_3 \end{bmatrix} + \Psi_2 [A_2 - BF_2]_{3 \times 3} \begin{bmatrix} x_1 \\ x_2 \\ x_3 \end{bmatrix} \\ - \Gamma_1 [C_1 - BF_1]_{3 \times 3} \begin{bmatrix} y_1 \\ y_2 \\ y_3 \end{bmatrix} - \Gamma_2 [C_2 - BF_2]_{3 \times 3} \begin{bmatrix} y_1 \\ y_2 \\ y_3 \end{bmatrix} \quad (7.48)$$

According to Eq.(7.43) , we have $G = [A_1 - BF_1] = [A_2 - BF_2] = [C_1 - BF_1] = [C_2 - BF_2] < 0$. G is chosen as:

$$G = \begin{bmatrix} -1 & 0 & 0 \\ 0 & -1 & 0 \\ 0 & 0 & -1 \end{bmatrix} \quad (7.49)$$

Thus, the feedback gains F_1 , F_2 , P_1 and P_2 can be determined by the following equation:

$$F_1 = B^{-1} [A_1 - G] = \begin{bmatrix} 1 & 1 & 0 \\ 0 & 1 & 1 \\ -1 & b - Z_3 & a + 1 \end{bmatrix} \\ F_2 = B^{-1} [A_2 - G] = \begin{bmatrix} 1 & 1 & 0 \\ 0 & 1 & 1 \\ -1 & b + Z_3 & a + 1 \end{bmatrix} \quad (7.50)$$

$$P_1 = B^{-1} [C_1 - G] = \begin{bmatrix} 1 & 1 & 0 \\ 0 & 1 & 1 \\ 0 & -1 & 1 - c \end{bmatrix}$$

$$P_2 = B^{-1} [C_2 - G] = \begin{bmatrix} 1 & 1 & 0 \\ 0 & 1 & 1 \\ 0 & -1 & 1 - c \end{bmatrix}$$

The synchronization errors are shown in Fig. 7.11.

Example 2: Synchronization of Lorenz System and Sprott 22 System.

The fuzzy Lorenz system in Eq. (7.27) is chosen as the master system and the

fuzzy slave Sprott 22 system with uncertainty in Eq. (7.16), with fuzzy controllers is as follows:

$$\dot{Y}(t) = \sum_{i=1}^2 \Gamma_i (C_i Y(t) + \tilde{c}_i) + BU(t) \quad (7.51)$$

where Γ_i are diagonal matrices

$$\text{dia}(\Gamma_1) = [N_{11} \quad N_{21} \quad N_{31}], \quad \text{dia}(\Gamma_2) = [N_{12} \quad N_{22} \quad N_{32}]$$

and

$$C_1 = \begin{bmatrix} 0 & 1 & 0 \\ 0 & 0 & 1 \\ 0 & -1 & -c \end{bmatrix}, \quad \tilde{c}_1 = \begin{bmatrix} Z_4 \\ Z_5 \\ -Z_6 \end{bmatrix}$$

$$C_2 = \begin{bmatrix} 0 & 1 & 0 \\ 0 & 0 & 1 \\ 0 & -1 & -c \end{bmatrix}, \quad \tilde{c}_2 = \begin{bmatrix} 0 \\ 0 \\ 1 - Z_6 \end{bmatrix}$$

Therefore, the error and error dynamics are:

$$\begin{bmatrix} e_1 \\ e_2 \\ e_3 \end{bmatrix} = \begin{bmatrix} x_1 - y_1 \\ x_2 - y_2 \\ x_3 - y_3 \end{bmatrix},$$

$$\begin{bmatrix} \dot{e}_1 \\ \dot{e}_2 \\ \dot{e}_3 \end{bmatrix} = \begin{bmatrix} \dot{x}_1 - \dot{y}_1 \\ \dot{x}_2 - \dot{y}_2 \\ \dot{x}_3 - \dot{y}_3 \end{bmatrix} = \sum_{i=1}^2 \Psi_i (D_i X(t) + \tilde{d}_i) - \dot{Y}(t) = \sum_{i=1}^2 \Gamma_i (C_i Y(t) + \tilde{c}_i) - BU(t) \quad (7.52)$$

B is chosen as an identity matrix and the fuzzy controllers in Eq. (7.41) are used:

$$\begin{bmatrix} \dot{e}_1 \\ \dot{e}_2 \\ \dot{e}_3 \end{bmatrix} = \Psi_1 [D_1 - BF_1]_{3 \times 3} \begin{bmatrix} x_1 \\ x_2 \\ x_3 \end{bmatrix} + \Psi_2 [D_2 - BF_2]_{3 \times 3} \begin{bmatrix} x_1 \\ x_2 \\ x_3 \end{bmatrix} \\ - \Gamma_1 [C_1 - BF_1]_{3 \times 3} \begin{bmatrix} y_1 \\ y_2 \\ y_3 \end{bmatrix} - \Gamma_2 [C_2 - BF_2]_{3 \times 3} \begin{bmatrix} y_1 \\ y_2 \\ y_3 \end{bmatrix} \quad (7.53)$$

According to Eq. (7.43), we have $G = [D_1 - BF_1] = [D_2 - BF_2] = [C_1 - BF_1]$

$= [C_2 - BF_2] < 0$. G is chosen as:

$$G = \begin{bmatrix} -1 & 0 & 0 \\ 0 & -1 & 0 \\ 0 & 0 & -1 \end{bmatrix} \quad (7.54)$$

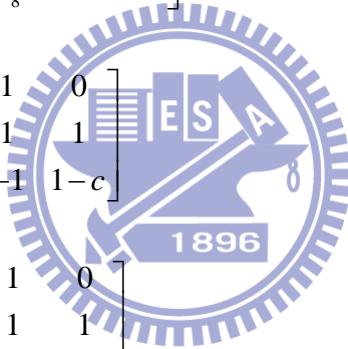
Thus, the feedback gains F_1 , F_2 , P_1 and P_2 can be determined by the following equation:

$$F_1 = B^{-1} [D_1 - G] = \begin{bmatrix} 1-g & g & 0 \\ h-Z_7 & 0 & 0 \\ Z_8 & 0 & 1-l \end{bmatrix}$$

$$F_2 = B^{-1} [D_2 - G] = \begin{bmatrix} 1-g & g & 0 \\ h+Z_7 & 0 & 0 \\ -Z_8 & 0 & 1-l \end{bmatrix} \quad (7.55)$$

$$P_1 = B^{-1} [C_1 - G] = \begin{bmatrix} 1 & 1 & 0 \\ 0 & 1 & 1 \\ 0 & -1 & 1-c \end{bmatrix}$$

$$P_2 = B^{-1} [C_2 - G] = \begin{bmatrix} 1 & 1 & 0 \\ 0 & 1 & 1 \\ 0 & -1 & 1-c \end{bmatrix}$$



The synchronization errors are shown in Fig. 7.12.

7.6 Summary

In this Chapter, a new strategy to achieve chaos synchronization via the new fuzzy model is proposed. By using the new fuzzy model, not only a complicated nonlinear system can be linearized to a simple form, linear coupling of only two linear subsystems and the numbers of fuzzy rules can be reduced from 2^N to $2 \times N$, but also the idea of PDC and LMI-based method can be applied to synchronize two totally different fuzzy systems.

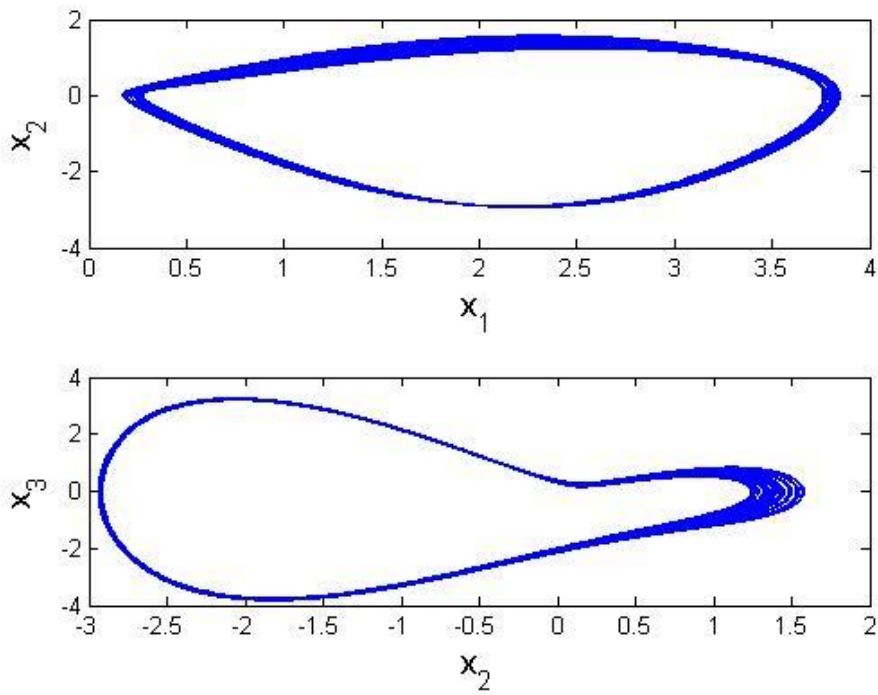


Fig. 7.1 Chaotic behavior of Sprott 19 system.

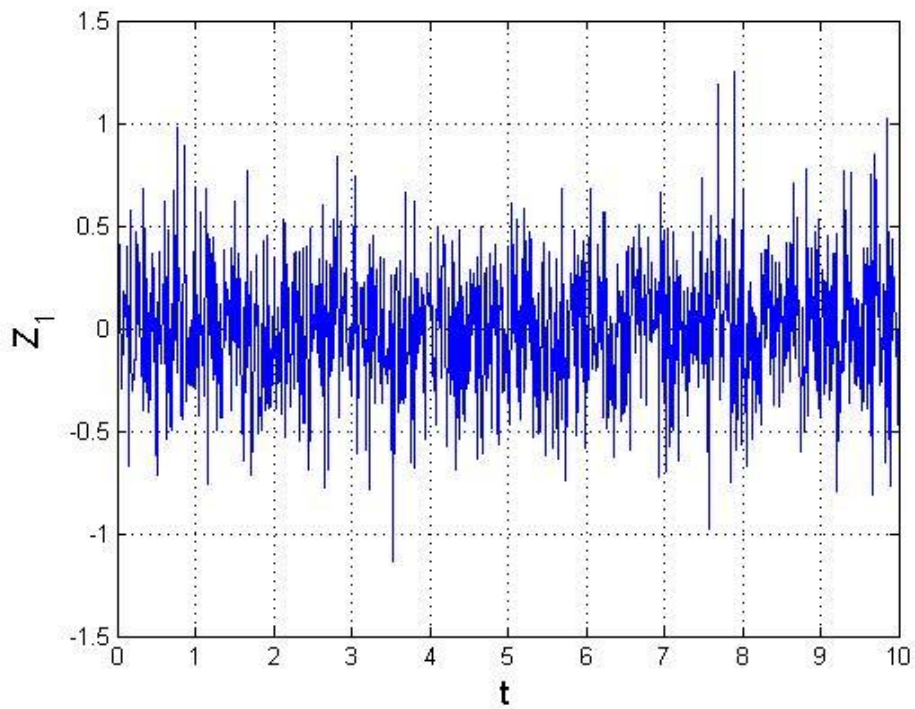


Fig. 7.2 The uncertainty signal of Δ_1 is band-limited white noise(PSD=0.001).

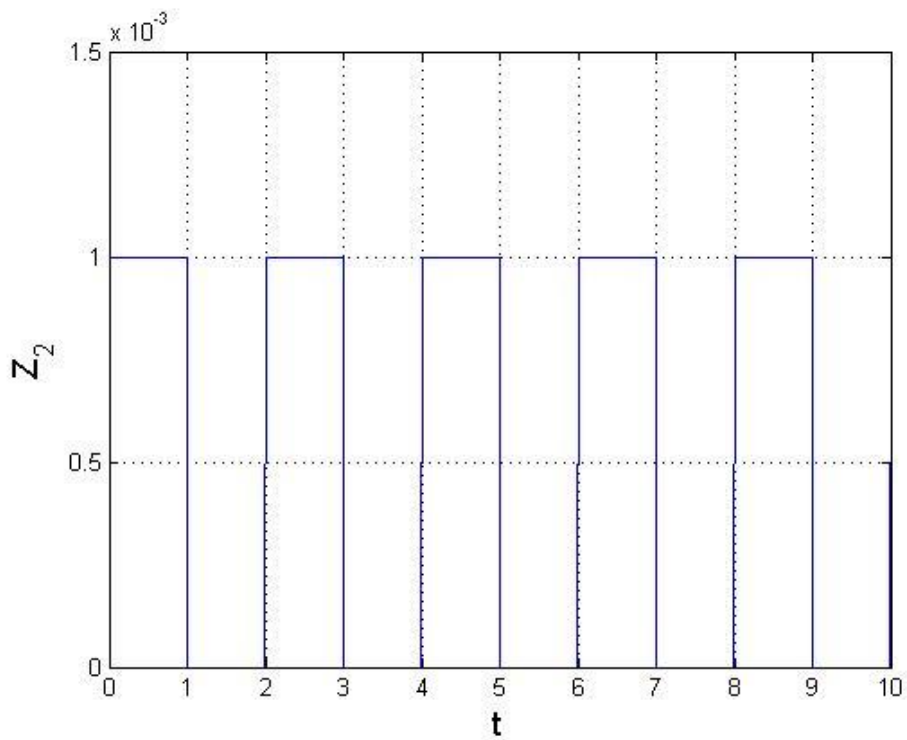


Fig. 7.3 Δ_2 is pulse generator.

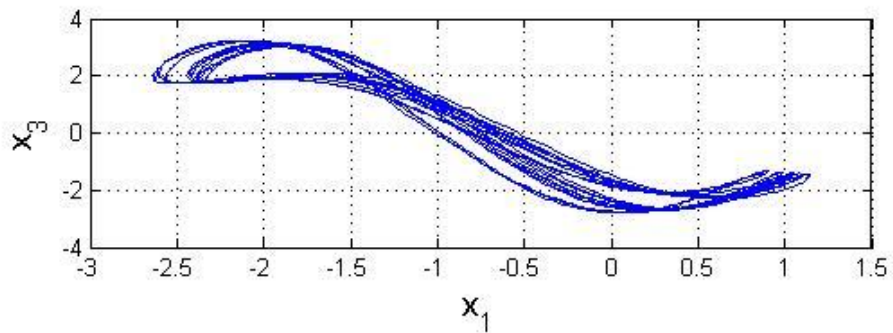
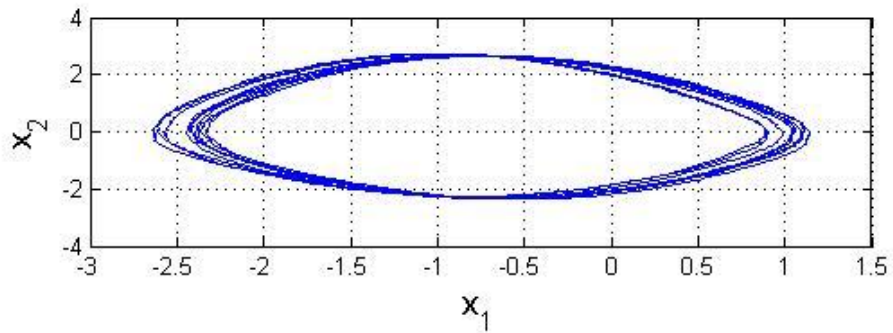


Fig. 7.4 Chaotic behavior of Sprott 19 system with uncertainty.

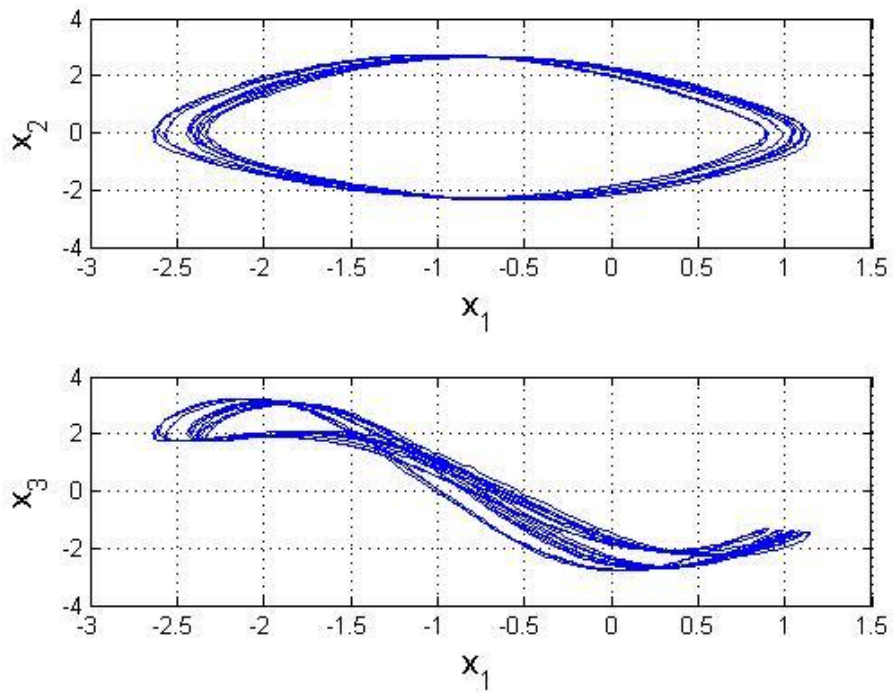


Fig. 7.5 Chaotic behavior of new fuzzy Sprott 19 system with uncertainty.

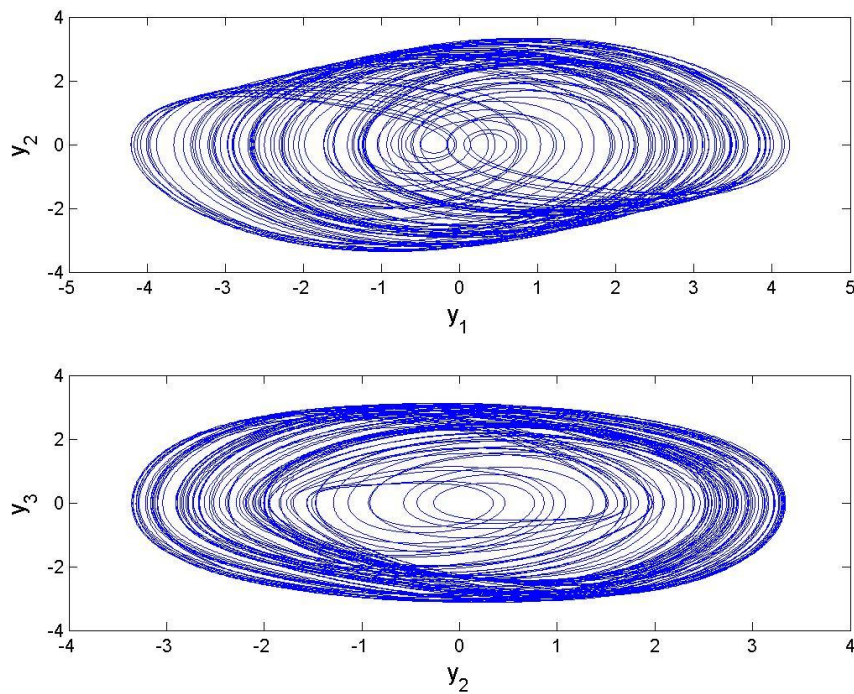


Fig. 7.6. Chaotic behavior of Sprott 22 system.

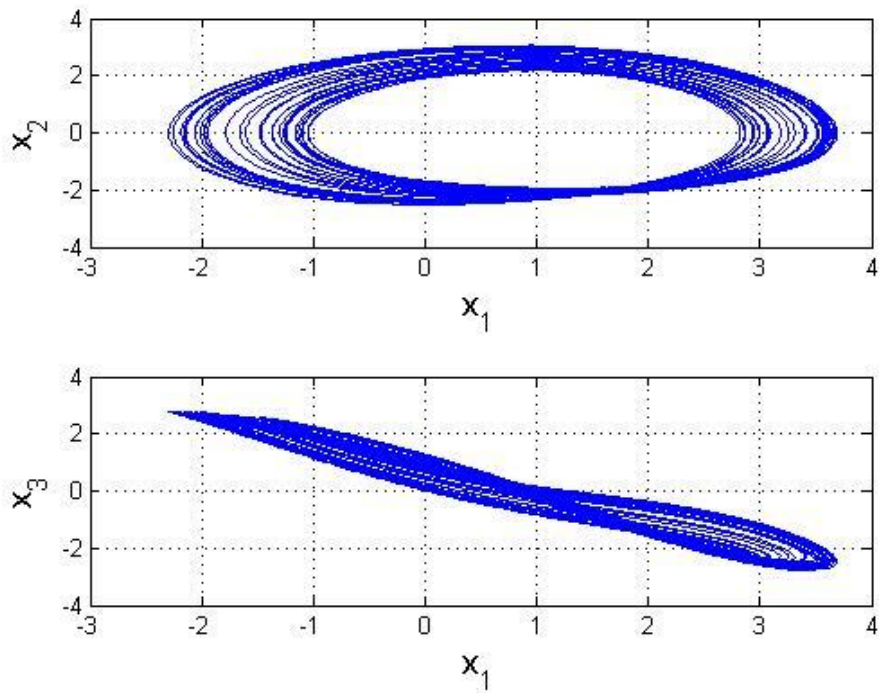


Fig. 7.7 Chaotic behavior of Sprott 22 system with uncertainty.

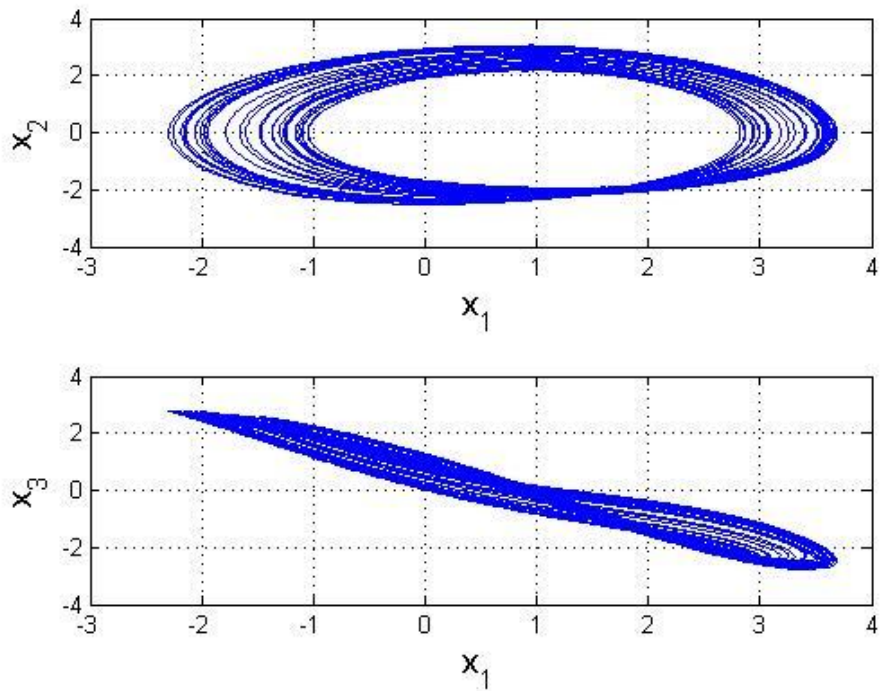


Fig. 7.8 Chaotic behavior of new fuzzy Sprott 22 system with uncertainty.

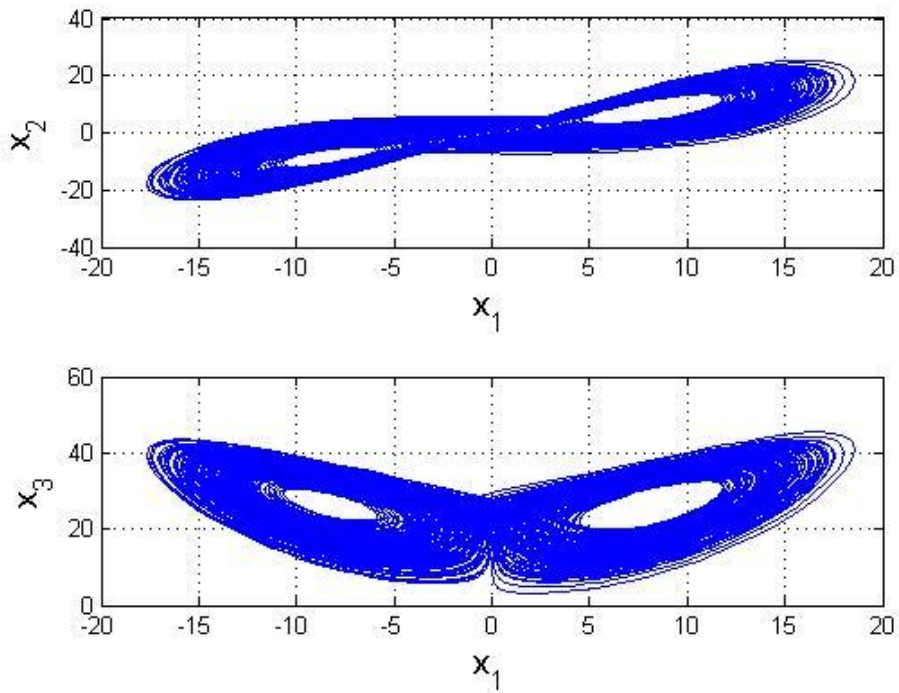


Fig. 7.9 Chaotic behavior of Lorenz system.

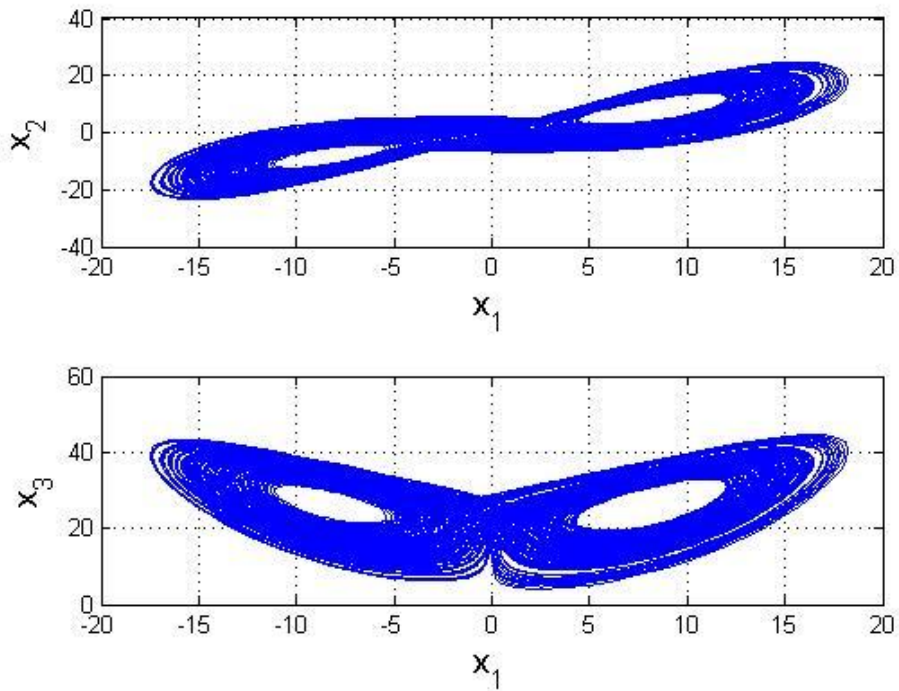


Fig. 7.10 Chaotic behavior of new fuzzy Lorenz system.

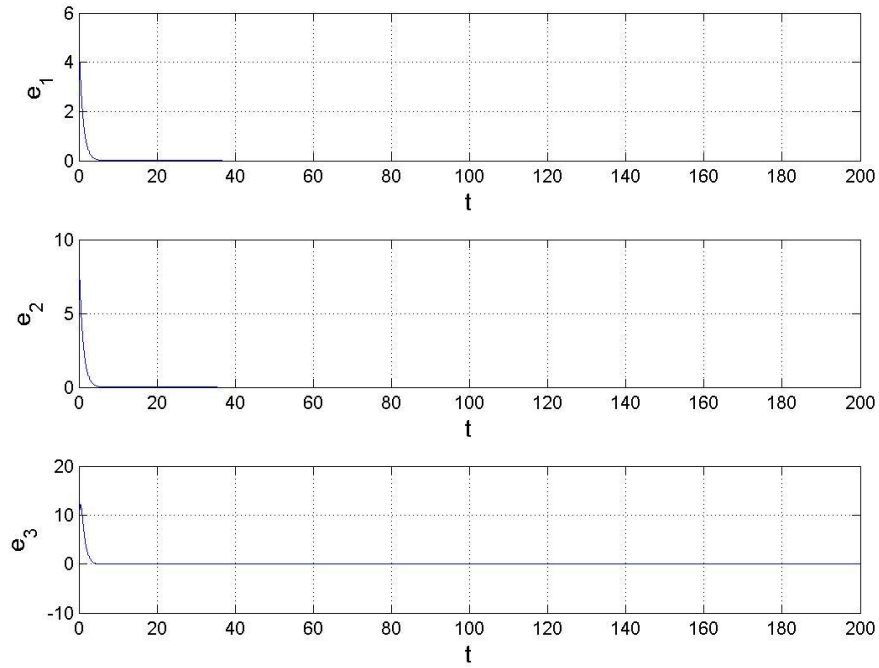


Fig. 7.11. Time histories of errors for Example 1.

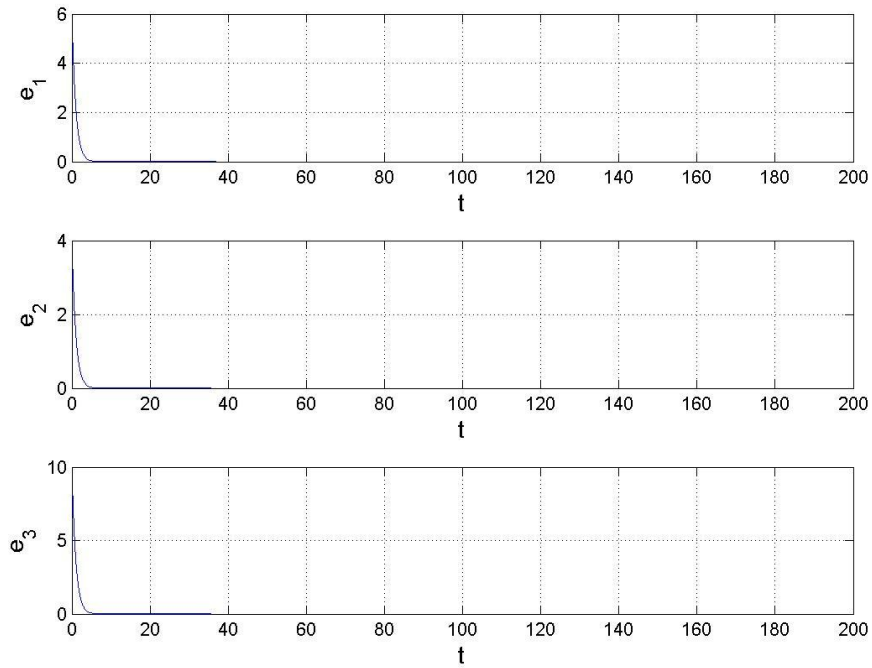


Fig. 7.12. Time histories of errors for Example 2.

Chapter 8

Conclusions

In this thesis, chaos and various chaos synchronizations of Ge-Ku-Mathieu system and Sprott 19, 22 systems are studied. In Chapter 2, the chaotic behavior of new Ge-Ku-Mathieu system is studied by phase portraits, time history, Poincaré maps, Lyapunov exponent and bifurcation diagrams.

In Chapter 3, a new symplectic synchronization problem of chaotic systems are investigated based on Barbalat's Lemma. Traditional generalized synchronization is a special case for the double symplectic synchronization. By applying active control, the double symplectic synchronization is achieved. Furthermore, the double symplectic synchronization could be applied to the design of secret communication with more security than generalized synchronization due to the complexity of its synchronization form.

In Chapter 4, a new strategy to achieve chaos synchronization by the different translation pragmatismal synchronization using stability theory of partial region is proposed. The conditions of the Lyapunov function for pragmatismal asymptotical stability are lower than that for traditional asymptotical stability. By using the different translation pragmatismal synchronization by stability theory of partial region, with the same conditions for Lyapunov function, $V > 0$, $\dot{V} \leq 0$, as that in current scheme of adaptive synchronization, we not only obtain the generalized synchronization of chaotic systems but also prove strictly that the estimated parameters approach the uncertain values. The Lyapunov function is simple linear homogeneous function for error states, the controllers are more simple and have less simulation error because they are in lower degree than that of traditional controllers.

In Chapter 5, a new type of synchronization, multiple symplectic synchronization, is studied. It is an extension of double symplectic synchronization. By applying active control, the multiple symplectic synchronization is achieved. Furthermore, the multiple symplectic synchronization of chaotic systems can be used to increase the

security of secret communication.

In Chapter 6, a simplest fuzzy controller (FLCC) is introduced to projective anti-synchronization of non-autonomous chaotic systems with stochastic disturbance. Three main contributions can be concluded: (1) High performance of the convergence of error states in synchronization; (2) Good robustness in projective anti-synchronization of the chaotic systems with stochastic disturbance; (3) Simple constant controllers are used, which can be easily obtained.

In Chapter 7, a new strategy to achieve chaos synchronization via the new fuzzy model is proposed. By using the new fuzzy model, a complicated nonlinear system can be linearized to a simple form, linear coupling of only two linear subsystems and the numbers of fuzzy rules can be reduced from 2^N to $2 \times N$.



Appendix A

GYC Partial Region Stability Theory

A.1 Definition of the Stability on Partial Region

Consider the differential equations of disturbed motion of a nonautonomous system in the normal form

$$\frac{dx_s}{dt} = X_s(t, x_1, \dots, x_n), \quad (s = 1, \dots, n) \quad (\text{A.1})$$

where the function X_s is defined on the intersection of the partial region Ω (shown in Fig. A1) and

$$\sum_s x_s^2 \leq H \quad (\text{A.2})$$

and $t > t_0$, where t_0 and H are certain positive constants. X_s which vanishes when the variables x_s are all zero, is a real valued function of t, x_1, \dots, x_n . It is assumed that X_s is smooth enough to ensure the existence, uniqueness of the solution of the initial value problem. When X_s does not contain t explicitly, the system is autonomous.

Obviously, $x_s = 0$ ($s = 1, \dots, n$) is a solution of Eq.(A.1). We are interested to the asymptotical stability of this zero solution on partial region Ω (including the boundary) of the neighborhood of the origin which in general may consist of several subregions (Fig. A1).

Definition 1:

For any given number $\varepsilon > 0$, if there exists a $\delta > 0$, such that on the closed given partial region Ω when

$$\sum_s x_{s0}^2 \leq \delta, \quad (s = 1, \dots, n) \quad (\text{A.3})$$

for all $t \geq t_0$, the inequality

$$\sum_s x_s^2 < \varepsilon, \quad (s=1, \dots, n) \quad (\text{A.4})$$

is satisfied for the solutions of Eq.(A.1) on Ω , then the disturbed motion $x_s = 0$ ($s=1, \dots, n$) is stable on the partial region Ω .

Definition 2:

If the undisturbed motion is stable on the partial region Ω , and there exists a $\delta' > 0$, so that on the given partial region Ω when

$$\sum_s x_{s0}^2 \leq \delta', \quad (s=1, \dots, n) \quad (\text{A.5})$$

The equality

$$\lim_{t \rightarrow \infty} \left(\sum_s x_s^2 \right) = 0 \quad (\text{A.6})$$

is satisfied for the solutions of Eq.(A.1) on Ω , then the undisturbed motion $x_s = 0$ ($s=1, \dots, n$) is asymptotically stable on the partial region Ω .

The intersection of Ω and region defined by Eq.(A.5) is called the region of attraction.

Definition of Functions $V(t, x_1, \dots, x_n)$:

Let us consider the functions $V(t, x_1, \dots, x_n)$ given on the intersection Ω_1 of the partial region Ω and the region

$$\sum_s x_s^2 \leq h, \quad (s=1, \dots, n) \quad (\text{A.7})$$

for $t \geq t_0 > 0$, where t_0 and h are positive constants. We suppose that the functions are single-valued and have continuous partial derivatives and become zero when $x_1 = \dots = x_n = 0$.

Definition 3:

If there exists $t_0 > 0$ and a sufficiently small $h > 0$, so that on partial region Ω_1 and $t \geq t_0$, $V \geq 0$ (or ≤ 0), then V is a positive (or negative) semidefinite, in general semidefinite, function on the Ω_1 and $t \geq t_0$.

Definition 4:

If there exists a positive (negative) definitive function $W(x_1 \dots x_n)$ on Ω_1 , so that on the partial region Ω_1 and $t \geq t_0$

$$V - W \geq 0 \text{ (or } -V - W \geq 0), \quad (\text{A.8})$$

then $V(t, x_1, \dots, x_n)$ is a positive definite function on the partial region Ω_1 and $t \geq t_0$.

Definition 5:

If $V(t, x_1, \dots, x_n)$ is neither definite nor semidefinite on Ω_1 and $t \geq t_0$, then $V(t, x_1, \dots, x_n)$ is an indefinite function on partial region Ω_1 and $t \geq t_0$. That is, for any small $h > 0$ and any large $t_0 > 0$, $V(t, x_1, \dots, x_n)$ can take either positive or negative value on the partial region Ω_1 and $t \geq t_0$.

Definition 6: Bounded function V

If there exist $t_0 > 0$, $h > 0$, so that on the partial region Ω_1 , we have

$$|V(t, x_1, \dots, x_n)| < L$$

where L is a positive constant, then V is said to be bounded on Ω_1 .

Definition 7: Function with infinitesimal upper bound

If V is bounded, and for any $\lambda > 0$, there exists $\mu > 0$, so that on Ω_1 when $\sum_s x_s^2 \leq \mu$, and $t \geq t_0$, we have

$$|V(t, x_1, \dots, x_n)| \leq \lambda$$

then V admits an infinitesimal upper bound on Ω_1 .

*A.2 GYC Theorem of Stability and of Asymptotical Stability on Partial Region***Theorem 1**

If there can be found a definite function $V(t, x_1, \dots, x_n)$ on the partial region for Eq. (A.1), and the derivative with respect to time based on these equations are:

$$\frac{dV}{dt} = \frac{\partial V}{\partial t} + \sum_{s=1}^n \frac{\partial V}{\partial x_s} X_s \quad (\text{A.9})$$

Then, it is a semidefinite function on the partial region whose sense is opposite to that of V , or if it becomes zero identically, then the undisturbed motion is stable on the partial region.

Proof:

Let us assume for the sake of definiteness that V is a positive definite function. Consequently, there exists a sufficiently large number t_0 and a sufficiently small number $h < H$, such that on the intersection Ω_1 of partial region Ω and

$$\sum_s x_s^2 \leq h, \quad (s=1, \dots, n)$$

and $t \geq t_0$, the following inequality is satisfied

$$V(t, x_1, \dots, x_n) \geq W(x_1, \dots, x_n),$$

where W is a certain positive definite function which does not depend on t . Besides that, Eq. (A.9) may assume only negative or zero value in this region.

Let ε be an arbitrarily small positive number. We shall suppose that in any case $\varepsilon < h$. Let us consider the aggregation of all possible values of the quantities x_1, \dots, x_n , which are on the intersection ω_2 of Ω_1 and

$$\sum_s x_s^2 = \varepsilon, \quad (\text{A.10})$$

and let us designate by $l > 0$ the precise lower limit of the function W under this condition. By virtue of Eq. (A.8), we shall have

$$V(t, x_1, \dots, x_n) \geq l \quad \text{for } (x_1, \dots, x_n) \text{ on } \omega_2. \quad (\text{A.11})$$

We shall now consider the quantities x_s as functions of time which satisfy the differential equations of disturbed motion. We shall assume that the initial values x_{s0} of these functions for $t = t_0$ lie on the intersection Ω_2 of Ω_1 and the region

$$\sum_s x_s^2 \leq \delta, \quad (\text{A.12})$$

where δ is so small that

$$V(t_0, x_{10}, \dots, x_{n0}) < l \quad (\text{A.13})$$

By virtue of the fact that $V(t_0, 0, \dots, 0) = 0$, such a selection of the number δ is obviously possible. We shall suppose that in any case the number δ is smaller than ε . Then the inequality

$$\sum_s x_s^2 < \varepsilon, \quad (\text{A.14})$$

being satisfied at the initial instant will be satisfied, in the very least, for a sufficiently small $t - t_0$, since the functions $x_s(t)$ vary continuously with time. We shall show that these inequalities will be satisfied for all values $t > t_0$. Indeed, if these inequalities were not satisfied at some time, there would have to exist such an instant $t = T$ for which this inequality would become an equality. In other words, we would have

$$\sum_s x_s^2(T) = \varepsilon,$$

and consequently, on the basis of Eq. (A.11)

$$V(T, x_1(T), \dots, x_n(T)) \geq l \quad (\text{A.15})$$

On the other hand, since $\varepsilon < h$, the inequality (Eq.(A.7)) is satisfied in the entire interval of time $[t_0, T]$, and consequently, in this entire time interval $\frac{dV}{dt} \leq 0$. This yields

$$V(T, x_1(T), \dots, x_n(T)) \leq V(t_0, x_{10}, \dots, x_{n0}),$$

which contradicts Eq. (A.14) on the basis of Eq. (A.13). Thus, the inequality (Eq.(A.4)) must be satisfied for all values of $t > t_0$, hence follows that the motion is stable.

Finally, we must point out that from the view-point of mathematics, the stability on partial region in general does not be related logically to the stability on whole region. If an undisturbed solution is stable on a partial region, it may be either stable

or unstable on the whole region and vice versa. In specific practical problems, we do not study the solution starting within Ω_2 and running out of Ω .

Theorem 2

If in satisfying the conditions of Theorem 1, the derivative $\frac{dV}{dt}$ is a definite function on the partial region with opposite sign to that of V and the function V itself permits an infinitesimal upper limit, then the undisturbed motion is asymptotically stable on the partial region.

Proof:

Let us suppose that V is a positive definite function on the partial region and that consequently, $\frac{dV}{dt}$ is negative definite. Thus on the intersection Ω_1 of Ω and the region defined by Eq. (A.7) and $t \geq t_0$ there will be satisfied not only the inequality (Eq.(A.8)), but the following inequality as well:

$$\frac{dV}{dt} \leq -W_1(x_1, \dots, x_n), \quad (\text{A.16})$$

where W_1 is a positive definite function on the partial region independent of t .

Let us consider the quantities x_s as functions of time which satisfy the differential equations of disturbed motion assuming that the initial values $x_{s0} = x_s(t_0)$ of these quantities satisfy the inequalities (Eq. (A.12)). Since the undisturbed motion is stable in any case, the magnitude δ may be selected so small that for all values of $t \geq t_0$ the quantities x_s remain within Ω_1 . Then, on the basis of Eq. (A.16) the derivative of function $V(t, x_1(t), \dots, x_n(t))$ will be negative at all times and, consequently, this function will approach a certain limit, as t increases without limit, remaining larger than this limit at all times. We shall show that this limit is equal to some positive quantity different from zero. Then for all values of $t \geq t_0$ the following inequality will be satisfied:

$$V(t, x_1(t), \dots, x_n(t)) > \alpha \quad (\text{A.17})$$

where $\alpha > 0$.

Since V permits an infinitesimal upper limit, it follows from this inequality that

$$\sum_s x_s^2(t) \geq \lambda, \quad (s = 1, \dots, n), \quad (\text{A.18})$$

where λ is a certain sufficiently small positive number. Indeed, if such a number λ did not exist, that is, if the quantity $\sum_s x_s(t)$ were smaller than any preassigned number no matter how small, then the magnitude $V(t, x_1(t), \dots, x_n(t))$, as follows from the definition of an infinitesimal upper limit, would also be arbitrarily small, which contradicts Eq. (A.17).

If for all values of $t \geq t_0$ the inequality (Eq. (A.18)) is satisfied, then Eq. (A.16) shows that the following inequality will be satisfied at all times:

$$\frac{dV}{dt} \leq -l_1,$$

where l_1 is positive number different from zero which constitutes the precise lower limit of the function $W_1(t, x_1(t), \dots, x_n(t))$ under condition (Eq. (A.18)). Consequently, for all values of $t \geq t_0$ we shall have:

$$V(t, x_1(t), \dots, x_n(t)) = V(t_0, x_{10}, \dots, x_{n0}) + \int_{t_0}^t \frac{dV}{dt} dt \leq V(t_0, x_{10}, \dots, x_{n0}) - l_1(t - t_0),$$

which is, obviously, in contradiction with Eq.(A.17). The contradiction thus obtained shows that the function $V(t, x_1(t), \dots, x_n(t))$ approached zero as t increase without limit. Consequently, the same will be true for the function $W(x_1(t), \dots, x_n(t))$ as well, from which it follows directly that

$$\lim_{t \rightarrow \infty} x_s(t) = 0, \quad (s = 1, \dots, n),$$

which proves the theorem.

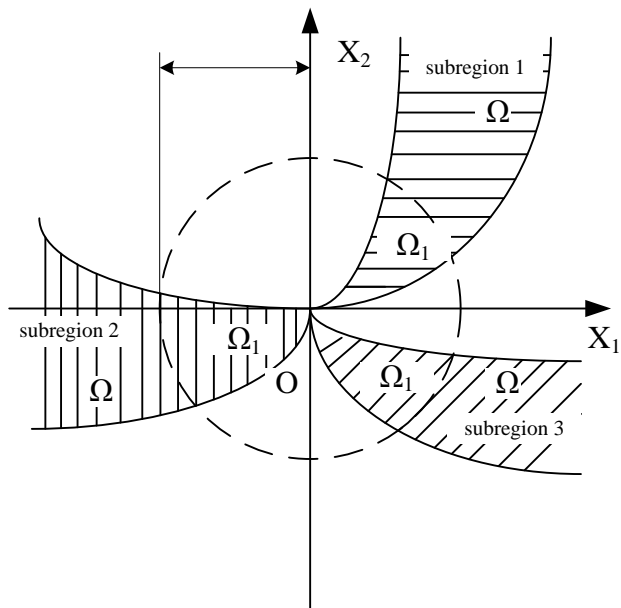


Fig. A.1. Partial regions Ω and Ω_1



Appendix B

Pragmatical Asymptotical Stability Theory

The stability for many problems in real dynamical systems is actual asymptotical stability, although may not be mathematical asymptotical stability. The mathematical asymptotical stability demands that trajectories from all initial states in the neighborhood of zero solution must approach the origin as $t \rightarrow \infty$. If there are only a small part or even a few of the initial states from which the trajectories do not approach the origin as $t \rightarrow \infty$, the zero solution is not mathematically asymptotically stable. However, when the probability of occurrence of an event is zero, it means the event does not occur actually. If the probability of occurrence of the event that the trajectories from the initial states are that they do not approach zero when $t \rightarrow \infty$, is zero, the stability of zero solution is actual asymptotical stability though it is not mathematical asymptotical stability. In order to analyze the asymptotical stability of the equilibrium point of such systems, the pragmatical asymptotical stability theorem is used.

Let X and Y be two manifolds of dimensions m and n ($m < n$), respectively, and φ be a differentiable map from X to Y , then $\varphi(X)$ is subset of Lebesgue measure 0 of Y [62]. For an autonomous system

$$\frac{dx}{dt} = f(x_1, \dots, x_n) \tag{B-1}$$

where $x = [x_1, \dots, x_n]^T$ is a state vector, the function $f = [f_1, \dots, f_n]^T$ is defined on $D \subset R^n$ and $\|x\| \leq H > 0$. Let $x=0$ be an equilibrium point for the system (B-1).

Then

$$f(0) = 0 \tag{B-2}$$

For a nonautonomous systems,

$$\dot{x} = f(x_1, \dots, x_{n+1}) \quad (\text{B-3})$$

where $x = [x_1, \dots, x_{n+1}]^T$, the function $f = [f_1, \dots, f_n]^T$ is define on

$D \subset R^n \times R_+$, here $t = x_{n+1} \in R_+$. The equilibrium point is

$$f(0, x_{n+1}) \ni 0. \quad (\text{B-4})$$

Definition The equilibrium point for the system (B-1) is pragmatically asymptotically stable provided that with initial points on C which is a subset of Lebesgue measure 0 of D, the behaviors of the corresponding trajectories cannot be determined, while with initial points on D-C, the corresponding trajectories behave as that agree with traditional asymptotical stability [63,64].

Theorem Let $V = [x_1, \dots, x_n]^T: D \rightarrow R_+$ be positive definite and analytic on D, where x_1, x_2, \dots, x_n are all space coordinates such that the derivative of V through Eq. (A-1) or (A-3), \dot{V} , is negative semi-definite of $[x_1, x_2, \dots, x_n]^T$.

For autonomous system, Let X be the m-manifold consisted of point set for which $\forall x \neq 0, \dot{V}(x) = 0$ and D is a n-manifold. If $m+1 < n$, then the equilibrium point of the system is pragmatically asymptotically stable.

For nonautonomous system, let X be the $m+1$ -manifold consisting of point set of which $\forall x \neq 0, \dot{V}(x_1, x_2, \dots, x_n) = 0$ and D is $n+1$ -manifold. If $m+1+1 < n+1$, i.e. $m+1 < n$ then the equilibrium point of the system is pragmatically asymptotically stable. Therefore, for both autonomous and nonautonomous system the formula $m+1 < n$ is universal. So the following proof is only for autonomous system. The proof for nonautonomous system is similar.

Proof Since every point of X can be passed by a trajectory of Eq. (B-1), which is one-dimensional, the collection of these trajectories, A, is a $(m+1)$ -manifold [65,

66].

If $m+1 < n$, then the collection C is a subset of Lebesgue measure 0 of D . By the above definition, the equilibrium point of the system is pragmatically asymptotically stable.

If an initial point is ergodically chosen in D , the probability of that the initial point falls on the collection C is zero. Here, equal probability is assumed for every point chosen as an initial point in the neighborhood of the equilibrium point. Hence, the event that the initial point is chosen from collection C does not occur actually. Therefore, under the equal probability assumption, pragmatical asymptotical stability becomes actual asymptotical stability. When the initial point falls on $D-C$, $\dot{V}(x) < 0$, the corresponding trajectories behave as that agree with traditional asymptotical stability because by the existence and uniqueness of the solution of initial-value problem, these trajectories never meet C .

In Eq. (2-7) V is a positive definite function of n variables, i.e. p error state variables and $n-p=m$ differences between unknown and estimated parameters, while $\dot{V} = e^T C e$ is a negative semi-definite function of n variables. Since the number of error state variables is always more than one, $p > 1$, $m+1 < n$ is always satisfied, by pragmatical asymptotical stability theorem we have

$$\lim_{t \rightarrow \infty} e = 0 \quad (\text{B-5})$$

and the estimated parameters approach the uncertain parameters. The pragmatical adaptive control theorem is obtained. Therefore, the equilibrium point of the system is pragmatically asymptotically stable. Under the equal probability assumption, it is actually asymptotically stable for both error state variables and parameter variables.

References

- [1] S. K. Han, C. Kerner and Y. Kuramoto, "Dephasing and bursting in coupled neural oscillators", *Phys. Rev. Lett.* 75 (1995) 3190.
- [2] B. Blasius, A. Huppert and L. Stone, "Complex dynamics and phase synchronization in spatially extended ecological systems", *Nature* 399 (1999) 354.
- [3] K. M. Cuomo and V. Oppenheim, "Circuit implementation of synchronized chaos with application to communication", *Phys. Rev. Lett.* 71 (1993) 65.
- [4] L. Kocarev and U. Parlitz, "General approach for chaotic synchronization with application to communication", *Phys. Rev. Lett.* 74 (1995) 5028.
- [5] C. Wang, and S. S. Ge, "Adaptive synchronization of uncertain chaotic systems via backstepping design", *Chaos, Solitons and Fractals*, 12 (2001) 119-1206.
- [6] R. Femat, J. A. Ramirze and G.F. Anaya "Adaptive synchronization of high-order chaotic systems: A feedback with low-order parameterization", *Physica D*, 139 (2000) 231-246.
- [7] Mei Sun, Lixin Tian and Shumin Jiang, Jun Xu, "Feedback control and adaptive control of the energy resource chaotic system", *Chaos, Solitons and Fractals*, 74 (2007) 1725-2834.
- [8] R. Femat and G. S. Perales, "On the chaotic synchronization phenomenon", *Phys. Letters A* 262 (1999) 50-60.
- [9] H. D. I. Abarbanel, N. F. Rulkov and M. M. Sushchik, "Generalized synchronization of chaos: The auxiliary systems", *Phys. Rev. E*, 53 (1996) 4528-4535.
- [10] S. S. Yang and C. K. Duan, "Generalized synchronization in chaotic systems", *Chaos, Solitons and Fractals*, 9 (1998) 1701-1703.
- [11] X. S. Yang, "Concepts of synchronization in dynamic systems", *Phys. Letters A*, 260 (1999) 340-344.
- [12] L.M. Pecora and T.L. Carroll, "Synchronization in chaotic systems", *Phys. Rev. Lett.* 64 (1990) 821-824.
- [13] M. G. Rosenblum, A. S. Pikovsky, and J. Kurths, "Phase synchronization of chaotic oscillators", *Phys. Rev. Lett.* 76 (1996) 1805.
- [14] M. G. Rosenblum, A. S. Pikovsky, and J. Kurths, "From phase to lag synchronization in coupled chaotic oscillators", *Phys. Rev. Lett.* 78 (1997) 4193.

- [15] N. F. Rulkov, M. M. Sushchik, L. S. Tsimring, and H. D. I. Abarbanel, "Generalized synchronization of chaos in directionally coupled chaotic systems", *Phys. Rev. E*, 51 (1995) 980
- [16] Z. M. Ge and C.H. Yang, "Pragmatical generalized synchronization of chaotic systems with uncertain parameters by adaptive control." *Physica D: Nonlinear Phenomena* 231(2007) 87-94.
- [17] Krawiecki A, Sukiennicki A. "Generalizations of the concept of marginal synchronization of chaos." *Chaos, Solitons & Fractals* 11(2000) 1445-58.
- [18] Z. M. Ge, C. H. Yang, H. H. Chen and S. C. Lee. "Non-linear dynamics and chaos control of a physical pendulum with vibrating and rotation support." *J Sound Vib* 242(2001) 247-64.
- [19] M. Y. Chen, Z. Z. Han, Y. Shang "General synchronization of Genesio–Tesi system." *Int J Bifurcat Chaos* 14(2004) 347-54.
- [20] Z. M. Ge and C. H. Yan. "The generalized synchronization of a Quantum-CNN chaotic oscillator with different order systems." *Chaos, Solutions & Fractals* 35 (2008) 980-90.
- [21] Z. M. Ge and C. H. Yang. "Symplectic synchronization of different chaotic systems" *Chaos, Solitons & Fractals*, 40(2009) 2532-2543.
- [22] X. Wu and Z. H. Guan, Z. Wu and Tao. Li, "Chaos synchronization between Chen system and Genesio system", *Phys., letters A* 364 (2007) 484-87.
- [23] M. Hu, Z. Xu, Rong. Zhang and A. Hu, "Adaptive full state hybrid projective synchronization of chaotic systems with the same and different order", *Phys., letters A* 365 (2007) 315-327.
- [24] Park Ju H., "Adaptive synchronization of hyperchaotic chen system with uncertain parameters", *Chaos, Solitons and Fractals* 26 (2005) 959-964.
- [25] Park Ju H., "Adaptive synchronization of rossler system with uncertain parameters", *Chaos, Solitons and Fractals* 25 (2005) 333-338.
- [26] E. M. Elabbasy, H. N. Agiza and M. M. El-Desoky, "Adaptive synchronization of a hyperchaotic system with uncertain parameters", *Chaos, Solitons and Fractals* 30 (2006) 1133-1142.
- [27] L.A. Zadeh, "Fuzzy logic", *IEEE Comput.* 21 (1998) 83-93.
- [28] H. T. Yau, C. L. Kuo and J. J. Yan, "Fuzzy sliding mode control for chaos", *Int. J. Nonlin. Sci. Numer. simulat.* 17 (2006) 333-338.
- [29] A. Shahraz and R. Bozorbmeahry Boozarjomehry, "A fuzzy sliding mode control

- approach for nonlinear chemical processes”, *Control Engineering Practice* 17 (2009) 541-550.
- [30] C. Y. Chen, T. H. S. Li, Y. C. Yeh, “EP-based kinematic control and adaptive fuzzy sliding-mode dynamic control for wheeled mobile robots”, *Information Science* 179 (2009) 180-195.
- [31] Y. W. Wang, Z. H. Guan and H. O. Wang, “LMI-based fuzzy stability and synchronization of Chen’s system”, *Physics Letter A* 320 (2003) 154-159.
- [32] Guang Li and Amir Khajepour, “Robust control of a hydraulically driven flexible arm using backstepping technique”, *Journal of Sound and Vibration* 280 (2005) 759-779.
- [33] T. H. S. Li, C. L. Kuo and N. R. Guo, “Design of an EP-based fuzzy sliding-mode control for a magnetic ball suspension system”, *Chaos, Solitons & Fractals* 33 (2007) 1523-1531.
- [34] H. T. Yau and C. S. Shieh, “Chaos synchronization using fuzzy logic controller”, *Nonlinear Analysis: Real World Applications* 9 (2008) 1800-1810.
- [35] S. Y. Li and Z. M. Ge, “Generalized synchronization of chaotic systems with different orders by fuzzy logic constant controller” submitted to *Expert Systems with Application* (2010).
- [36] L. A. Zadeh, “Fuzzy logic”, *IEEE Comput.* 21 (1988) 83-93.
- [37] T. Takagi and M. Sugeno, “Fuzzy identification of systems and its applications to modelling and control,” *IEEE Trans. Syst., Man., Cybern.*, 15 (1985) 116-132.
- [38] L. Luoh, “New stability analysis of T–S fuzzy system with robust approach”, *Math Comput Simul*, 59 (2002) 335-340.
- [39] X. j. Wu, X. j. Zhu, G. y. Cao and H. y. Tu, “Dynamic modeling of SOFC based on a T–S fuzzy model”, *Simul Model Prac Theory*, 16 (2008) 494-504.
- [40] X. Liu and S. Zhong, “T – S fuzzy model-based impulsive control of chaotic systems with exponential decay rate”, *Phys Lett A*, 370 (2007) 260-264.
- [41] J. H. Kim, C. W. Park, E. Kim and M. Park, “Adaptive synchronization of T–S fuzzy chaotic systems with unknown parameters”, *Chaos Solitons & Fractals*, 24 (2005) 1353-1361.
- [42] C. S. Chiu and T. S. Chiang, “Robust output regulation of T-S fuzzy systems with multiple time-varying state and input delays”, *IEEE Trans. Fuzzy Syst.*, 17 (2009) 962 -975.

- [43] B. Yoo and W. Ham, “Adaptive fuzzy sliding mode control of nonlinear system”, *IEEE Trans. Fuzzy Syst.*, 6 (1998) 315 -321.
- [44] H. X. Li and S. Tong, “A hybrid adaptive fuzzy control for a class of nonlinear MIMO systems”, *IEEE Trans. Fuzzy Syst.*, 11 (2003) 24 - 34.
- [45] C. L. Hwang, “A novel Takagi-Sugeno-based robust adaptive fuzzy sliding-mode controller”, *IEEE Trans. Fuzzy Syst.*, 12, (2004) 676 – 687.
- [46] J. Wang, X. Xiong, M. Zhao and Y. Zhang, “Fuzzy stability and synchronization of hyperchaos systems”, *Chaos Solitons & Fractals*, 35 (2008) 922-930.
- [47] Y. W. Wang, Z. H. Guan and H. O. Wang, “LMI-based fuzzy stability and synchronization of Chen's system”, *Phys Lett A*, 320 (2003) 154-159.
- [48] H. Zhang, X. Liao and J. Yu, “Fuzzy modeling and synchronization of hyperchaotic systems”, *Chaos Solitons & Fractals*, 26 (2005) 835-843.
- [49] S. W. Kau, H. J. Lee, C. M. Yang, C. H. Lee, L. Hong and C. H. Fang, “Robust H_{∞} fuzzy static output feedback control of T-S fuzzy systems with parametric uncertainties”, *Fuzzy Sets Syste*, 158 (2007) 135-146.
- [50] Garfinkel A, Spano ML, Ditto WL, Weiss JN. “Controlling cardiac chaos. *Science*” 257 (1992)1230-1235.
- [51] Z. M. Ge, C. W. Yao and H.K.Chen, “Stability on partial region in dynamics.” *Journal of Chinese Society of Mechanical Engineer* 115 (1994)140-151.
- [52] Z. M. Ge and H. K. Chen, “Three asymptotical stability theorems on partial region with application.” *Japanese Journal of Applied Physics* 37 (1998) 2762-2773.
- [53] Z. M. Ge and F. N. Ku, “Stability, bifurcation and chaos of a pendulum on a rotating arm”, *Jpn. J. Appl. Phys.* 36 (1997) Part 1.
- [54] Z. M. Ge, and C. H. Yang, “Symplectic synchronization of different chaotic systems”, *Chaos, Solitons & Fractals*, 2007, doi: 10.1016/j.chaos.2007.10.055.0
- [55] H. K. Khalil, *Nonlinear systems*, 3rd edition, Prentice Hall, New Jersey, 2002.
- [56] J.-H. Park, “Adaptive synchronization of hyperchaotic chen system with uncertain parameters”, *Chaos, Solitons Fractals*, 26 (2005) 959-964.
- [57] J.-H. Park, “Adaptive synchronization of Rossler system with uncertain parameters”, *Chaos, Solitons Fractals*, 2
- [58] E.-M. Elabbasy, H.-N. Agiza and M.-M. El-Desoky, “Adaptive synchronization of a hyperchaotic system with uncertain parameter”, *Chaos, Solitons Fractals*, 30

(2006) 1133-1142.

- [59] R. Mainieri and J. Rehacek, "Projective synchronization in three-dimensional chaotic systems". *Phys. Rev. Lett.* 82 (1999) 3042.
- [60] J. C. Sprott, "Simple chaotic systems and circuits", *Am. J. Phys.*, 68 (2000) 8.
- [61] Z. M. Ge and S. Y. Li, "Fuzzy modeling and synchronization of chaotic two-cells quantum cellular neural networks nano system via a novel fuzzy model" accepted by *Journal of Computational and Theoretical Nanoscience* 2009.
- [62] Matsushima, Y., *Differentiable Manifolds*, Marcel Dekker, City, 1972
- [63] Z.M. Ge, J.K. Yu, and Y.T. Chen, "Pragmatical asymptotical stability theorem with application to satellite system", *Jpn. J. Appl. Phys.*, 38 (1999) 6178.
- [64] Z.M. Ge and J.K. Yu, "Pragmatical asymptotical stability theorem partial region and for partial variable with applications to gyroscopic systems", *the Chinese Journal of Mechanics*, 16 (2000) 179.
- [65] G.P. Jiang, G. Chen and W.K.S. Tang, "A new criterion for chaos synchronization using linear state feedback control". *Int J Bifurcat Chaos*, 13 (2003):2343-51.
- [66] Rafikov, M., Balthazar, J.M., "On a optimal control design for Rossler system". *Phys Rev Lett A* 64 (1990) 821-4.

